

Spatial and Temporal Variability in Surficial Seabed Character, Waipaoa River Margin, New Zealand

By

Joseph M. Kiker

July, 2012

Director(s) of Thesis: Drs. Reide Corbett and J.P. Walsh

Major Department: Geological Sciences

The Waipaoa River margin, located off the northeast coast of the North Island of New Zealand, provides an opportunity to examine shelf-wide sediment dynamics in a coastal setting. The region is characterized by a narrow shelf (~20 km) and ample sediment supply ( $15 \text{ Mt y}^{-1}$ ), ideal precursors to assess the fidelity of the stratigraphic record. Sediments are delivered to this margin via the Waipaoa River which drains a small mountainous catchment ( $2205 \text{ km}^2$ ) comprised of highly erodible fine-grained lithologies. As part of an NSF-funded project, a time-series of surface seabed properties were used as a foundation to evaluate spatial and temporal changes in sediment dynamics and strata formation on the adjacent margin. Samples were collected on four cruises over 13 months; January, May, and September 2010; and February 2011.

Site deposition was assessed using short-lived radionuclides, X-radiography, and through measurement of surface seabed grain-size distribution and organic content. Seabed erodibility was measured with a Gust microcosm device and presented as the total eroded mass ( $\text{kg m}^{-2}$ ) for a given experiment. Generally, sediment deposition was variable, in both space and time and dependent on pre-sampling fluvial and oceanographic conditions. Sediment erodibility also varied; generally sediments were more erodible in water depths <40 m in comparison to deeper areas. Pronounced temporal variation in sediment erodibility was evident at sites located in <40

m water depth. X-radiographs collected from these sites generally show interbedded muds and sands, whereas images of sediments collected from more distal shelf locations are more homogenous, the result of efficient biological mixing in the surface seabed.

The temporary and periodic emplacement of flood layers on the Waipaoa margin was most likely responsible for sediment erodibility variation in sites <40 m water depth. X-radiography coupled with grain-size and porosity measurements indicated fluid-mud deposition in Poverty Bay and the region immediate to the bay mouth. Radioisotope measurements suggest that recently deposited layers are more erodible than the average erodibility level calculated for the shelf. Other published research from the York River estuary, VA indicated that the seasonal emplacement of thick sediment deposits following river discharge resulted in higher measured bed erodibility. Post-depositional alteration of the seabed likely also resulted in reduced low erodibility measured on the Waipaoa margin. In summary, recently deposited sediments in the nearshore were prone to erosion and transported to more quiescent and deeper shelf regions, where high rates of modern sediment accumulation have been shown by previous researchers. These processes affected surficial seabed properties which in turn influenced subsequent sediment remobilization.



Spatial and Temporal Variability in Surficial Seabed Character, Waipaoa River Margin, New Zealand

---

A Thesis

Presented to the Faculty of the Department of Geological Sciences

East Carolina University

In Partial Fulfillment

of the Requirements for the Degree of

Master of Science

---

by

Joseph M. Kiker

July, 2012

© Joseph M. Kiker, 2012

Approval Sheet

This thesis is submitted in partial fulfillment of the  
Requirements for the degree of  
Master of Science  
July 2012  
Academic Committee Members

---

Dr. D. Reide Corbett  
Co-Advisor

---

Dr. J.P. Walsh  
Co-Advisor

---

Dr. Siddhartha Mitra

---

Dr. Alan Orpin

---

Dr. Stephen Culver  
Department of Geological Sciences, Chair

---

Paul J. Gemperline  
Dean of the Graduate School

## ACKNOWLEDGEMENTS

I would like to thank my co-advisors, Drs. Reide Corbett and J.P. Walsh for their continued support throughout my time at East Carolina University, and also my committee members, Dr. Siddhartha Mitra and Dr. Alan Orpin for their assistance with field work and their feedback on this document. I would also like to thank the captain and crew of the *R/V's Roger Revelle* and *Kaharoa* and the many individuals who assisted with field and lab work. This study was supported by funding from the National Science Foundation (Grant #OCE-0841092).

## TABLE OF CONTENTS

ACKNOWLEDGEMENTS .....	iv
TABLE OF CONTENTS .....	v
LIST OF TABLES .....	vii
LIST OF FIGURES .....	viii
LIST OF SYMBOLS .....	xiii
1 INTRODUCTION .....	1
2 Spatial and Temporal Variability in Sediment Deposition and Seabed Character on the Waipaoa Shelf, New Zealand .....	3
Abstract .....	3
2.1 Introduction .....	4
2.2 Background .....	6
2.2.1 <i>Sediment Dynamics</i> .....	6
2.2.2 <i>Waipaoa Margin</i> .....	10
2.3 Methods .....	11
2.3.1 <i>Meteorological, River, and Oceanographic Conditions</i> .....	11
2.3.2 <i>Sample Collection and Analyses</i> .....	12
2.4 Results .....	15
2.4.1 <i>Discharge, Modeled Waves, and Wind Observations</i> .....	15
2.4.2 <i>Radioisotopes</i> .....	15
2.4.3 <i>Seabed Character</i> .....	18
2.5 Discussion .....	19
2.5.1 <i>Spatial and Temporal Variation of Sediment Deposition</i> .....	19
2.5.2 <i>Change in Seabed Character with Sediment Deposition</i> .....	23
2.6 Conclusions .....	24
3 Spatial and Temporal Variation in Sediment Erodibility on the Waipaoa River Margin, New Zealand .....	37
Abstract .....	37
3.1 Introduction .....	37
3.2 Background .....	39



3.2.1 <i>Sediment Erodibility</i> .....	39
3.2.2 <i>Controls on Erodibility</i> .....	40
3.2.3 <i>Waipaoa Sedimentary System</i> .....	43
3.3 <i>Materials and Methods</i> .....	44
3.3.1 <i>Sampling Collection and Analysis</i> .....	45
3.3.2 <i>Statistical Analysis</i> .....	49
3.4 <i>Results</i> .....	50
3.4.1 <i>Data Assessment and Error Determination</i> .....	50
3.4.2 <i>Spatial and Temporal Variability in Seabed Attributes</i> .....	51
3.5 <i>Discussion</i> .....	52
3.5.1 <i>Controls on Sediment Erodibility</i> .....	52
3.5.2 <i>Influence of Depositional History on Sediment Erodibility</i> .....	55
3.5.3 <i>Erodibility Measurements in the Context of Previous Work</i> .....	57
3.5.4 <i>Considerations and Implications for Modeling</i> .....	60
3.6 <i>Conclusions</i> .....	61
4 <b>CONCLUSIONS AND FUTURE WORK</b> .....	79
References.....	82
Appendix I <i>Site Logs</i> .....	91
Appendix II <i>Radioisotope Down-core Activities and Inventories</i> .....	97
Appendix III <i>Grain Size and LOI Data</i> .....	130
Appendix IV <i>Site X-radiographs and Other Physical Data</i> .....	137

## LIST OF TABLES

Table 2-1 Summary of average fluvial, oceanographic, and meteorological conditions.....	36
Table 3-1 Power law fit parameters relating critical stress for erosion to eroded mass.....	78
Table 3-2 Power law fit parameters relating erosion rate constant to eroded mass.....	78

## LIST OF FIGURES

- Figure 2-1 Basemap showing the location of samples in relation to the Waipaoa River (WR), Poverty Bay (PB), and Lachlan and Ariel anticlines. Sites where time-series radioisotope inventories were calculated are presented as symbol indicating the shelf region (Poverty Bay, Poverty mouth, sediment depocenters, outer shelf, and other) and are numbered..... 26
- Figure 2-2 Fluvial, oceanographic, and meteorological data for the periods of time prior (A-D) to sampling during cruises (black hatched boxes). An arbitrary cutoff of 3.5 m and 20 g l<sup>-1</sup> were chosen to represent wave and high sediment discharge events (dotted lines), respectively. Data indicate temporal variability in river discharge, sediment concentration, wave height, and wind speed including several flood periods (diamonds) and wave events (circles). ..... 27
- Figure 2-3 A comparison of short-term sediment deposition (evidenced by mean <sup>7</sup>Be penetration depths) and long-term <sup>210</sup>Pb based sediment accumulation patterns (from Miller and Kuehl, 2010 using <sup>210</sup>Pb). Variability through time is shown as the variance of values using data from all sampling periods. Data show that sediment deposition is punctuated through time and does not necessarily correspond to areas of long-term accumulation. .... 28
- Figure 2-4 Total <sup>7</sup>Be inventories for each sampling period. Variability in total <sup>7</sup>Be inventories through time indicate that sediment deposition is punctuated over the course of the study. 29
- Figure 2-5 Sediment focusing inferred from <sup>234</sup>Th ratios >1 for each sampling period. Differences in sediment focusing suggest variable sediment dispersal over the duration of this study..... 30

Figure 2-6 Sediment deposition inferred from measureable new  $^7\text{Be}$  inventories at repeat sites for May and September 2010 and February 2011. Data indicate that sediment deposition is sporadic through time. .... 31

Figure 2-7 The relative influence of fluvial and marine processes on sedimentation inferred from the  $^7\text{Be}:\text{excess } ^{234}\text{Th}$  ratio for four sampling periods. Maps show temporal variability in the dominant influences on deposition. .... 32

Figure 2-8 The mean and variance of clay percent (A) and LOI percent (B) for the period of study. Note that patterns are comparable for the two datasets. .... 33

Figure 2-9 Sediment depositional interpretations for the Waipaoa shelf relating pre-sampling fluvial and oceanographic conditions to observed sediment deposition patterns, determined by spatial changes in radioisotope inventories (indicated by shaded black regions). Interpretations (1-4) are referenced in the text and suggest that pre-sampling conditions dictate the patterns of sediment deposition on the short-term. .... 34

Figure 2-10 Evidence for variability in strata thickness (X-radiographs) and deposition ( $^7\text{Be}$  down-core profiles) over a small spatial scale (sites 13-16; Figure 2-1)..... 35

Figure 3-1 The Waipaoa shelf in relation to New Zealand. Sites where erodibility measurements were taken are partitioned based on shelf region. Ariel and Lachlan Anticlines, the Waipaoa River (WR), and Poverty Bay (PB) are referenced. .... 64

Figure 3-2 Schematic of Gust Microcosm setup (single core) showing major components involved in running an experiment. Rotation of the erosion head and the rate of water throughput dictate the applied stress on the sediment surface and as sediment passes through a flow cell turbidity is measured (modified from Green Eyes, LLC, 2010). .... 65

Figure 3-3 Coefficient of variation (CV) for replicate and repeat measurements of total eroded mass. The CV of replicate samples for the entire shelf is relatively low (13%), indicated by the dashed line. The largest CVs are associated with replicate samples collected in <60 m water depth. Repeat measurements taken from the Sediment Depocenter and Outer Shelf (closed gray square) had lower CVs than the overall average CV for replicate samples..... 66

Figure 3-4 Sediment erodibility measurements taken in January 2010 (C1), May 2010 (C2), September 2010 (C3), and February 2011 (C4). The greatest temporal variability occurs seaward of 40 m water depth, in regions of ephemeral sediment deposition..... 67

Figure 3-5 Cumulative erodibility plots for all measurements taken during the 13-month period of observation. Cutoffs were determined by clustering of total eroded mass data points (i.e., at 0.6 Pa). Plot B is an expanded view of A. Variability in profiles is seen at applied stress >0.3 Pa..... 68

Figure 3-6 Representative examples of bed structure, <sup>7</sup>Be and grain-size down-core profiles, and cumulative erodibility plots for low, medium, and high erodibility sediments. X-radiographs and surface grain-size measurements suggest that erodibility may be related to depositional history. However, down-core <sup>7</sup>Be profiles are not that different in the examples presented. .... 69

Figure 3-7 A comparison of site depositional history to sediment erodibility and measured wet bulk density. New <sup>7</sup>Be inventories were used to interpret sediment deposition and erosion (see Chapter 2). Site replicates are presented as separate observations; as a result the same site wet bulk density is plotted for each. .... 70

Figure 3-8 Recent depositional events are indicated by high surface <sup>7</sup>Be and excess <sup>234</sup>Th activities. Changes in erodibility through time suggest that more recently deposited

sediments are more erodible. Porosity, <sup>7</sup>Be down-core activities and grain-size are also presented..... 71

Figure 3-9 Significant changes in surface grain-size were observed from May to February at Site 8, within Poverty Mouth, with 6 cm of deposition measured in February. Porosity, <sup>7</sup>Be, and excess <sup>234</sup>Th down-core activities are also presented. .... 72

Figure 3-10 Bioturbation of a 2 cm flood layer occurs between September and February at Site 35, on the outer Waipaoa shelf. However, little change is observed in seabed erodibility. Porosity, <sup>7</sup>Be, and excess <sup>234</sup>Th down-core activities and grain-size are also presented..... 73

Figure 3-11 Critical shear stress ( $\tau_c$ ) vs. eroded mass (m) profiles for previous research (A & B) in the York River, Baltimore Harbor and upper Chesapeake Bay and for the Waipaoa shelf (C & D). Plots B and D are expanded views of A and C, respectively. The two data sets display similar trends. YRl = York River low erodibility; YRt = York River transitional erodibility; YRh = York River high erodibility; SM01 = Sanford and Maa (2001); S06 = Sanford (2006); YRlf = fit to YRl; YRtf = fit to YRt; YRh = fit to YRh; SM01f = fit to SM01; and S06f = fit to S06 (from Dickhudt et al., 2009); L = Waipaoa shelf low erodibility; M = Waipaoa shelf Medium erodibility; and H = Waipaoa shelf high erodibility. .... 74

Figure 3-12 Plots of erosion rate constant (M) vs. eroded mass (m) for the Waipaoa shelf. Plot B is an expanded view of plot A. The data are described with a power law fit to all sites (equation presented in Table 3-2). Power law fits to data from Poverty Bay, Poverty Mouth, the Sediment (Depocenter), and the Outer Shelf are also presented in Table 3-2, but not pictured here. .... 75

Figure 3-13 Spatial distributions of sediment erodibility for the 13-month period of observation.

Gradational boundaries between sedimentary facies for the Waipaoa River margin are indicated with dotted lines, where ILMS = interbedded laminated muds and sands, MLM = mixed layers and mottles, and MM = mottled muds (from Miller and Kuehl, 2010; Rose and Kuehl, 2010). ..... 76

Figure 3-14 Potential sediment erodibility for non-event (A) and event (B) time periods. The eroded masses selected for each region are based on maximum measured bed shear stresses associated with model runs (J. Moriarty, personal communication). Sites deemed as NA are areas where observed bed shear stresses exceed the measurement capabilities of the Gust Microcosm. .... 77

## LIST OF SYMBOLS

$I$  = Inventory ( $\text{dpm cm}^{-2}$ )

$X_i$  = Subsection Thickness (cm)

$\varphi_i$  = Porosity (unitless)

$\rho_i$  = Sediment Density ( $\text{g cm}^{-3}$ )

$A_i$  = Activity ( $\text{dpm g}^{-1}$ )

$E$  = Erosion Rate ( $\text{kg m}^{-2} \text{s}^{-1}$ )

$M$  = Erosion Rate Parameter ( $\text{kg m}^{-2} \text{S}^{-1} \text{Pa}^{-1}$ )

$\tau_b$  = Applied Stress (Pa)

$\tau_c$  = Critical Stress for Erosion (Pa)

$m$  = Eroded Mass ( $\text{kg m}^{-2}$ )



# 1 INTRODUCTION

The study of sediment dynamics and strata formation and preservation provide insight into the fate of terrestrial sediment in the marine environment. The transport and deposition of sediments on continental margins is complex, with net accumulation often the result of multiple sediment movement episodes driven by wave and tidal processes. Interpretation of the sedimentary record is further limited by post-depositional biological reworking of sediment. An additional factor to consider is that suspension of surface seabed sediment facilitates exchange of chemicals (e.g., contaminants, Håkanson, 2006) and nutrients (e.g. Fanning et al., 1982) between the seabed and water column. Also, as organic matter is often associated with fine-grained sediments, the sequestration or remobilization of sediments has important implications on carbon cycling (McKee et al., 2004). Additionally, fine-grained sediments attenuate sunlight, and thereby can decrease primary productivity and affect marine dissolved oxygen concentrations (Lawrence et al., 2004).

While extensive research has focused on understanding sediment dynamics in the marine environment, there is still much knowledge to be gained from ongoing and future research efforts. This project focuses on relating fluvial and oceanographic conditions to the evolution of the seabed surface, as a better understanding of processes and qualification of characteristics can help refine modeling efforts in this and other systems. More specifically, emphasis is placed on sediment deposition and erosion and the resultant impact on both the fate of sediment in the marine environment and the character of the seabed. The initial and possibly temporary emplacement of sediment on the seabed is measured with short-lived radionuclides (e.g., Canuel et al., 1990; Giffin and Corbett, 2003, Corbett et al., 2004; Corbett et al., 2007) and referred to as sediment deposition. But, the net sediment accumulation results from multiple sediment

deposition and removal events (McKee et al., 1983). Therefore, sediment erodibility has important implications on sediment transport and the development of sedimentary strata. Generally, sediment grain-size distribution and wet bulk-density are considered the dominant properties influencing sediment erodibility (e.g., Kandiah, 1974; Jepsen et al., 1997; Roberts et al., 1998). However, in certain environmental settings, other properties may also be important (e.g., in Grabowski et al., 2011). For example, after emplacement, biological alterations to the seabed may influence the resistance of sedimentary layers to erosion (e.g., Sutherland et al., 1998; Friend et al., 2003; Fernandes et al., 2006; Lundkvist et al., 2007; Widdows et al., 2009).

This study focused on understanding sediment dynamics on the Waipaoa River margin, New Zealand, and continental-margin sedimentary dynamics in general. Ample sediment supply and a narrow shelf, and vigorous maritime climate make the Waipaoa margin an idea field area to explore sediment dynamics and develop numerical models for sediment dispersal. This work will advance our understanding of the Waipaoa Sedimentary System, building on previous research that primarily explored decadal- to millennial-scale sedimentation patterns. A multitude of samples were collected on four research cruises spanning a 13-month period to provide insight into spatial and temporal variability in seabed character through investigation of sediment erodibility, deposition and variation in grain-size distribution, and organic material in the surface seabed. The chapters that follow present the results of our detailed investigation. Chapter Two focuses on spatial and temporal variability in sediment deposition and seabed character and the impact of fluvial and oceanographic conditions on observations. Chapter Three relates seabed erodibility to site depositional processes to explain variability in time and space.

## 2 Spatial and Temporal Variability in Sediment Deposition and Seabed Character on the Waipaoa Shelf, New Zealand

### Abstract

The stratigraphic record is the manifestation of a wide range of processes, interactions and responses to environmental change. On the continental shelf, the fidelity of the stratigraphic record is a function of sediment dynamics, which may be influenced by sediment supply, shelf morphology, fluvial and oceanographic interactions, and biota. The combined effect of sediment transport, deposition and reworking continually modify seabed character to build or destroy strata. Therefore, understanding the functioning of a wide-range of sediment dispersal systems is necessary to better determine the fate of sediment in the marine environment and differentiate the key influences in the development of the stratigraphic record. Sediment cores collected over a 13-month period on the Waipaoa margin, New Zealand provide insight into spatial and temporal variability in sediment deposition and seabed character. Seabed character on the inner shelf was variable through both space and time, but mid- and outer-shelf sites had relatively consistent seabed character over the study period. Moreover, short-lived radioisotopes suggested ephemeral deposition on the inner shelf (water depths <40 m) which likely contributed to observed variation in seabed character.  $^7\text{Be}$ -rich layers were deposited in water depths > 40 m with little change in grain-size distribution and organic content (Loss on Ignition percent) of the seabed; these likely resulted from advection of fluvial material seaward. The presence (or lack) of  $^7\text{Be}$ -laden sediment was apparently linked to pre-sampling fluvial and oceanographic conditions. Data suggested that the timing of wave events in relation to sediment discharge events is potentially a critical control in the flushing of river-derived ( $^7\text{Be}$ -rich) sediment out of Poverty Bay to more distal locations. Therefore, a low-energy wave regime coupled with high river discharge likely led to ephemeral deposition and buildup in Poverty Bay, locally in the form

of fluid muds, and introduced small-scale variability on the inner shelf. Because of the considerable seabed variability noted at shallower depths, it is suggested that future research should employ geophysical observations (multibeam, sidescan, and/or chirp) in conjunction with sampling schemes in an attempt to quantify small-scale depositional variability, possibly associated with bedform mobility.

## **2.1 Introduction**

Stratigraphic techniques have been employed in many studies to answer a wide range of geologic questions in coastal systems. Some outcrop-based studies and models assume sediment deposition to operate as a linear and continual process, but the geologic record has evolved as a compilation of punctuated events and includes gaps over a variety of geologic timescales, possibly resulting from sediment erosion and/or non-deposition (Barrell, 1917). In marine environments, including areas of high river sediment input, the fidelity of the stratigraphic record is a function of sediment dynamics, which may be influenced by sediment supply, shelf morphology, fluvial and oceanic interactions, and biota. All of which control the dispersal behavior of sediment on continental margins (Nittrouer et al., 2007).

Variability in sediment dynamics between margin systems has led to the classification of different sediment dispersal regimes and shelf morphologies (Walsh and Nittrouer, 2009). This classification scheme is simple, as boundaries between end member systems are gradational. Therefore, process-oriented research geared toward understanding sediment transport will further resolve boundaries between sediment dispersal regimes (Walsh and Nittrouer, 2009), and provide greater insight into the fate of sediment in the complex and diverse range of margin systems. Additionally, understanding sediment deposition and accumulation in the marine

environment may provide greater insight into the global carbon cycle and more specifically the burial and/or redistribution of carbon in the marine environment (McKee et al., 2004).

Sediment transport models have gained popularity as a mechanism for assessing the impact of fluvial and oceanographic conditions on sediment deposition and accumulation (e.g., Friedrichs and Scully, 2007; Bever et al., 2009, 2011; Ma et al., 2010). These models often take into account a variety of factors that include the following: wave-orbital velocity amplitude, wave period, wave propagation direction, median grain diameter, mean sediment density, sediment settling velocity, and sediment load (Warner et al., 2008). Such model inputs and boundary conditions are chosen based on fluvial and oceanographic observations, and measured seabed properties. Determination of down-core radionuclide activities provides a means of identifying areas of sediment deposition and accumulation, thereby testing the validity of sediment transport models. Therefore, determination of seabed character through sample collection and analysis is a vital aspect of sediment transport model development and implementation.

On continental margins, the preservation of event layers is dependent on the sequential timing and magnitude of sediment deposition events, which dictate the residence time of event layers in the seabed surface mixed layer (e.g., those emplaced following floods; Wheatcroft and Drake, 2003). The internal layering and associated grain-size signatures of stratigraphic layers on shelves may be transient features with bioturbation occurring in as little as a few weeks after their emplacement (Wheatcroft and Drake, 2003), particularly in shallow temperate and tropical shelves. Understanding the development of sedimentary strata (permanent or ephemeral) in dynamic marine systems may be achieved through time-series observation of changes in radioisotope and surface seabed character.

This study on the Waipaoa shelf couples time-series seabed observations of  $^7\text{Be}$  and  $^{234}\text{Th}$  in surface sediments to provide insight into spatial-temporal variability in sediment deposition, together with surface grain-size and organic content. More specifically, the research is guided by the following objectives: 1) evaluate the spatial and temporal variability in sediment deposition; 2) determine how the character of the seabed surface changes with sediment deposition; and 3) relate the variability in surficial sedimentary strata to fluvial and oceanographic conditions and processes (e.g., bioturbation).

## **2.2 Background**

### *2.2.1 Sediment Dynamics*

Sediment dynamics include the deposition, resuspension, post-depositional mixing, and horizontal transport of particles, which dictate the exchange of nutrients and contaminants between the seabed and water column and ultimately determine the fate of sediment in marine environments (Waples et al., 2006). The dominant mechanisms driving sediment transport on continental margins are waves and currents, with fine sediment resuspension on the shelf mainly occurring in response to storms. Once resuspended, currents can transport sediment predominantly in an along-isobath direction. However, storms are often characterized by different fluvial and oceanographic conditions and dispersal behaviors. A large amount of river discharge (i.e., a flood) during energetic ocean conditions is known as a “wet” storm; conversely, low discharge during stormy seas can be referred to as a “dry” storm, both of which may lead to much sediment transport and the formation of fluid muds (e.g., Ogston and Sternberg, 1999; Puig et al., 2003). Fluid muds and associated sediment-gravity flows have become more appreciated for their potential role in sediment movement in the last couple decades. They are defined in the literature as having sediment concentrations  $> 10 \text{ g l}^{-1}$  (Kineke et al., 1996; Ross and Mehta, 1989) and are easily transported under the influence of gravity on continental margins with

slopes  $>0.7^\circ$  (Wright et al., 2001). However, observations of fluid muds on continental margins not meeting this criterion suggest that high energy waves (e.g., on the Eel shelf off California) and/or strong currents (e.g., on the Waiapu shelf off East Cape of New Zealand) may also be responsible for their creation and transport (Ogston et al., 2000; Ma et al., 2008, 2010).

Seabed observations coupled with the development and application of complex models has significantly advanced our understanding of sediment gravity flows. Research on the Po River system, Italy has shown that wet storms are not necessary to generate sediment gravity flows and that high wave energy can induce such flows if sediment is available (Traykovski et al., 2007). Ogston et al., (2008) show that even in the tidally dominated Fly River, Papua New Guinea is capable of generating sediment gravity flows in the Umuda Valley when the estuary turbidity maximum migrates seaward. On the Eel shelf, wet storms may generate fluid muds in close proximity to the fluvial source initially, with sediments eventually transported to deeper regions of the mid-shelf (Ogston et al., 2000). Also on the Eel River, dry storms resuspend and transport sediments as wave-supported sediment gravity flows from the shelf to deeper regions (i.e., submarine canyons and the continental slope; Puig et al., 2003). Interestingly, sediments are dispersed on the Waiapu shelf through both wave- and current-supported gravity flows (Ma et al., 2008, 2010). Wave-supported sediment gravity flows occur in water depths  $< 60$  m, whereas current-supported gravity flows occur in deeper waters (Ma et al., 2010). This suggests that water depth is a limiting factor in the generation of wave-supported gravity flows; whereas seabed slope is more important in sustaining current-supported sediment gravity flows (Ma et al., 2010). These examples show the importance of sediment gravity flows in a variety of margin dispersal systems and the complex and variable combination of oceanographic conditions required for their formation.

The loci of sediment deposition and accumulation on continental margins are heavily influenced by fluvial and oceanic interactions and margin morphology (Walsh and Nittrouer, 2009). The amount of sediment discharged by rivers dictates how much material is available for transport upon reaching the marine environment. This amount varies for different fluvial systems and has been complicated by anthropogenic alterations to catchments (e.g., increased soil erosion) and the emplacement of structures (e.g., dams) that starve lower stream reaches of bedload and washload sediment. The latter has caused a global reduction of  $1.4 \text{ BT y}^{-1}$  of terrigenous sediment released to the ocean (Syvitski et al., 2005). However, notwithstanding downstream structures, in many catchments have led to increased landscape sediment yields, the result of anthropogenic activities. In the northeastern New Zealand catchment, by the early 20<sup>th</sup> century, nearly all the forest cover had been removed, landslides proliferated in steep headwaters, and rivers were aggrading rapidly (e.g., Gage and Black, 1979).

Once reaching the coast in systems characterized by a minimum wave and tidal climate, sediments generally are deposited proximal to river mouths (e.g., Mississippi and Po river margins; Walsh and Nittrouer, 2009). However, in energetic systems, there is potential for sediment accumulation in distal shelf regions, and in these cases the morphology may strongly influence the pattern of deposition. Margins with a very high sediment discharge and tidal range (>2 m) generally form thick- elongate deposits (subaqueous delta clinoforms) (e.g., Amazon, and Fly systems). If the continental shelf is narrow, the potential exist for sediments to escape the shelf and accumulate on the continental slope and in the deep ocean (e.g. Eel, and Waipaoa systems; Alexander et al., 1999, 2010).

The distribution and activity of radioisotopes in marine sediments can aid in resolving the impact of complex coastal processes on the seabed, with the half-life of the radioisotope



dictating its application. Due to their short half-lives,  $^7\text{Be}$  ( $t_{1/2} = 53.3$  d) and  $^{234}\text{Th}$  ( $t_{1/2} = 24.1$  d) are powerful tools to evaluate complex processes such as sediment deposition, resuspension, erosion, and mixing occurring on timescales of days to months.  $^7\text{Be}$  is produced naturally via cosmic-ray spallation reactions with nitrogen and oxygen in the atmosphere. This radioisotope is deposited both wet and dry and is quickly adsorbed to soil particles and coastal sediments (Olsen et al., 1986). Catchment sediments enriched in  $^7\text{Be}$  may be eroded, delivered to rivers, and transported and deposited in coastal environments, and thus  $^7\text{Be}$  may act as a tracer of fluvial material (Sommerfield et al., 1999). Time-series sampling allows for the evaluation of seabed changes and interpretation of sediment deposition, erosion, or non-deposition based on the net change in  $^7\text{Be}$  inventory through time (e.g., Canuel et al., 1990; Giffin and Corbett, 2003, Corbett et al., 2004, 2007).  $^{234}\text{Th}$  occurs naturally in the water-column and seabed sediments, produced from the decay of  $^{238}\text{U}$  (Aller and Cochran, 1976; Aller et al. 1980; Waples et al., 2006). As  $^{234}\text{Th}$  has multiple sources, sediment deposition is determined by differentiating between total, supported, and excess  $^{234}\text{Th}$ , where the total is the sum of the supported and excess  $^{234}\text{Th}$ . Supported  $^{234}\text{Th}$  is produced from the continual decay of  $^{238}\text{U}$  in the seabed, whereas excess  $^{234}\text{Th}$  comprises the fraction of total  $^{234}\text{Th}$  that is rapidly scavenged by particles in the water column and deposited on the seabed (Aller and Cochran, 1976). Therefore, excess  $^{234}\text{Th}$  in the surface seabed results from sediment mass accumulation or focusing (e.g., Corbett et al., 2007). However, high surface excess  $^{234}\text{Th}$  may be diffused downward in the seabed through subductive mixing of sediment associated with bioturbation (e.g., Wheatcroft, 2006). The down-core excess  $^{234}\text{Th}$  activity profiles are similar for both sediment deposition and biological mixing, exhibiting a logarithmic decrease with depth in the seabed (Waples et al., 2006). Therefore, these

radioisotopes are most useful in assessing sediment deposition when used in tandem, and with X-radiographs that provide insight into differences in sediment density.

### 2.2.2 *Waipaoa Margin*

The Waipaoa margin is located on the tectonically active northern Hikurangi subduction margin of northeastern New Zealand, where oceanic crust of the Pacific Plate is being subducted obliquely beneath the Raukumara Peninsula (Figure 2-1). The Waipaoa River drains a small and steep catchment (2205 km<sup>2</sup>) but delivers a large amount (15 Mt y<sup>-1</sup>) of sediment to a narrow shelf (~20 km). Much sediment is initially delivered to the Waipaoa River through gully erosion (e.g., DeRose et al., 1998) and mass wasting events (e.g., Jones and Preston, 2012), which are a function of the duration and intensity of precipitation. The Waipaoa catchment is dominantly comprised of highly erodible sandstones, argillites, mudstones, marls, and limestone. Removal of indigenous vegetation following Maori and European colonization led to a six-fold increase in catchment erosion in comparison to the pre-human occupation period (Page et al., 1994, 2000; Wilmhurst, 1997; Wilmhurst et al., 1997; Eden and Page, 1998; Tate et al., 2000), with modern sediment yields in its upper catchment among the highest recorded on Earth (Walling and Webb, 1996).

Previous research has provided insight into sediment transport (Bever et al., 2011), deposition (Rose and Kuehl, 2010), and accumulation on the shelf (Orpin et al., 2006; Miller and Kuehl, 2010) and adjacent slope (Walsh et al., 2007; Alexander et al., 2010). A sediment transport model for Poverty Bay suggests that sediments are sequestered in the nearshore during wet storms, with seaward sediment transport taking place within three weeks as the result of wave activity (Bever et al., 2011).

Sediment deposition and accumulation have been quantified on the shelf using radioisotopes. Three prominent loci of sediment accumulation have been identified: the northern

mid-shelf, the southern mid-shelf, and the outer shelf lobe (Orpin et al., 2006; Miller and Kuehl, 2010). Samples collected from these regions in January 2005 had high  $^7\text{Be}$  inventories suggesting recent sediment deposition (within the last 250 d) and long-term accumulation (over the last ~100 y) are similar in their distribution and extent (Rose and Kuehl, 2010; Miller and Kuehl, 2010). However, a sediment budget calculated over the last 100 y for the Waipaoa margin shows that only 18-30 % of the 15 Mt of sediment discharged annually from the Waipaoa River accumulates on the shelf (Miller and Kuehl, 2010), with an additional 11-15 % accumulating on the upper continental slope and mid-slope plateau (Alexander et al., 2010) and filling local areas of the shelf break (Walsh et al., 2007). This leaves 55-71 % of the sediment discharge unaccounted for, suggesting transport of sediment to more distal locations (Alexander et al., 2010). However, a small fraction of this sediment discharge (<10 %) potentially may be retained in near shore sands, based on observations on the Eel River margin (Crockett and Nittrouer, 2004), an analog to the Waipaoa system in size, setting, and dispersal behavior.

## **2.3 Methods**

### *2.3.1 Meteorological, River, and Oceanographic Conditions*

Hourly river gauge data were obtained from the Kanakania station located 80-km upriver beyond any tidal influence (provided by G. Hall and D. Peacock). Wave data for a site located in the southern region of the mid-shelf was acquired from the National Institute of Water and Atmospheric Research (NIWA) (Figure 2-1, asterisk); data were produced using the New Zealand Wave (NZWAVE) model, a regional application of the global NOAA Wave Watch 3 model (WW3; Tolman et al., 2001). Precipitation and wind measurements were recorded at Gisborne airport and obtained from NIWA via their National Climate Database (<http://cliflo.niwa.co.nz/>).

### 2.3.2 Sample Collection and Analyses

Samples were collected on four cruises (January 2010, May 2010, September 2010, and February 2011) over 13 months. Their timing was scheduled to capture seasonal changes in riverine and oceanic processes. Short sediment cores were taken using an Ocean Instruments MC-800 multi-core, which collects eight individual 10 x 70 cm cores simultaneously. Slabs from one or more of the eight cores were X-rayed using a Varian Paxscan 4030E flat panel imaging system and an Ecotron EPX-F2800 portable X-ray generator, whilst others were sub-sampled for analysis of radionuclides and physical sediment properties.

Sediment samples were analyzed for  $^7\text{Be}$  (477 keV) and  $^{234}\text{Th}$  (63.3 keV) using gamma spectroscopy (Giffin and Corbett, 2003). Samples were dried, homogenized, packed in a standard-geometry container and counted for approximately 24 hours on low-background, high-efficiency, high-purity Germanium detectors (BEGe-, Coaxial-, LEGe-, and Well-type) coupled to a multi-channel analyzer. Calibration of detectors was achieved using natural matrix standards (IAEA-300, 312, 314, 315), to determine the regions of interest (ROI) for specific radioisotopes. Self-adsorption corrections were made to account for compositional differences between samples using the direct transmission method, allowing for accurate calculation of  $^{234}\text{Th}$  sample activity (Cutshall et al., 1983). For the purpose of consistency, cores were counted from the surface to the depth just beyond  $^7\text{Be}$  detection. Sediment X-radiographs were interpreted to highlight potential event strata, aiding in determination of the cutoff depth for the measurement of radioisotope activities. Samples were analyzed for  $^{234}\text{Th}$  within 3 months (~3.5 half-lives) and for  $^7\text{Be}$  within 4 months (~2 half-lives) of collection. Activities were corrected for decay between sample collection and analysis.

The differentiation of total, supported, and excess  $^{234}\text{Th}$  is important when assessing sediment dynamics. Samples were recounted for supported  $^{234}\text{Th}$  after 6 months to ensure that

no measureable excess  $^{234}\text{Th}$  remained. However, due to time constraints and high demand for gamma detectors, only a limited number of samples (110 total) were recounted. For the samples that were recounted, the measured supported  $^{234}\text{Th}$  was used, but for samples that were not recounted the overall average supported  $^{234}\text{Th}$  value of  $1.63 \pm 0.05 \text{ dpm g}^{-1}$  was used.

Excess  $^{234}\text{Th}$  and  $^7\text{Be}$  inventories were calculated using the following equation:

$$I = \sum X_i (1 - \varphi_i) \rho_i (A_i) \quad (1)$$

where  $I$  represents the total inventory of the sediment core ( $\text{dpm cm}^{-2}$ );  $X_i$  is the subsection thickness (cm);  $\varphi_i$  is the porosity of the subsection (unitless);  $\rho_i$  is the sediment density ( $\text{g cm}^{-3}$ ); and  $A_i$  is the activity ( $\text{dpm g}^{-1}$ ) (Canuel et al., 1990). The salt-corrected porosity for a sample was calculated using both wet and dry sediment mass and constants for porewater density ( $1.025 \text{ g cm}^{-3}$ ), particle density ( $2.650 \text{ g cm}^{-3}$ ), and salt fraction (35 ‰). Errors associated with counting, background, and detector efficiency were propagated to determine the total error associated with each sample measured and the calculated radioisotope activities (Sommerfield et al., 1999). The combined error associated with count rate, count time, peak fit, and the area encompassing the ROI is the counting error. A sample blank was run on each detector to determine the error associated with background radioisotope activities. Lastly, errors in efficiency account for any errors associated with detector calibration.

Following the methods of Corbett et al. (2004), the dependence of excess  $^{234}\text{Th}$  inventories on salinity and water depth was removed by normalizing excess  $^{234}\text{Th}$  inventories to the water-column  $^{238}\text{U}$ -supported  $^{234}\text{Th}$  inventories. Ship-based measurements of water depth and average salinity measurements from CTD casts (when available) were used in calculations. For sites where salinity measurements were unavailable, a constant (35 ‰) was assumed. Water

column supported  $^{234}\text{Th}$  ( $^{234}\text{Th}_{\text{WCS}}$ ) was then calculated using an established relationship between salinity and  $^{238}\text{U}$  in the water column (Chen et al., 1986).

New  $^7\text{Be}$  inventories ( $^7\text{Be}_{\text{new}}$ ) were calculated for May, September, and February at sites where a time-series of samples were collected by determining the  $^7\text{Be}$  inventory lost due to decay from the previous cruise and then subtracting the residual inventory from the  $^7\text{Be}$  inventory measured during the current cruise (Canuel et al., 1990; Corbett et al., 2007). Measureable  $^7\text{Be}_{\text{new}}$  indicates recent (since the last cruise) sediment deposition. Conversely, a negative value of  $^7\text{Be}_{\text{new}}$  is suggestive of net erosion.

The  $^7\text{Be}:\text{excess } ^{234}\text{Th}$  ratio was calculated to help assess the relative influence of fluvial versus marine processes on sedimentation (Feng et al., 1999; Allison et al., 2005; Corbett et al., 2007; Dail et al., 2007). As the sediment-bound activity ratio of  $^7\text{Be}$  and  $^{234}\text{Th}$  is not assumed to be 1:1, the range of data over all cruise periods was separated into quartiles using the median values of the entire data set. Samples with ratios that fall in the lower and upper 25 % of the entire data set are likely beyond the range of measurement error and therefore probably reflect the dominant processes influencing margin sedimentation (marine versus fluvial, respectively).

Grain-size was determined via sieving for the sand fraction ( $>63 \mu\text{m}$ ) and the remaining material was measured using a Micrometrics Sedigraph 5100 (Jones et al., 1988; Coakley and Syvitski 1991;). The amount of sample analyzed was dependent on the sand content; coarser sediments required a greater amount of sample to attain the desired turbidity. However, in most instances 5 to 10 g of wet sediment was analyzed. For the fine fraction, a detailed measurement of mass percentages was determined for user-defined size classes (Alexander et al., 2010). Sand, silt, and clay percentages were determined by back calculating the total dry weight of the wet sample using calculated sample porosities.

Loss on ignition (LOI) was analyzed as a proxy for organic matter content.

Approximately 5 g of sediment was placed in a muffle furnace at 550 °C for an hour. The difference in mass before and after combustion was assumed to be from ignition of organic matter (Dean, 1974).

## **2.4 Results**

### *2.4.1 Discharge, Modeled Waves, and Wind Observations*

While numerous sediment discharge and wave events punctuate the study period, a discernible pattern in wind speed variation (e.g., strong seasonality) was not evident (Figure 2-2). Note, major sediment discharge events occurred within the intervening period between all research voyages, but not within 60 days of sampling (Figure 2-2). However, several minor discharge events transpired prior to sample collection in September 2010 and February 2011 (Figure 2-2). Energetic wave conditions, with wave heights exceeding 3.5 meters and associated with high discharge periods, also occurred prior to these samplings events (Figure 2-2). Mean fluvial, oceanographic, and meteorological conditions were similar for all pre-sampling periods with the exception of the time prior to September sampling which had higher average river discharge, sediment discharge, wave height, and precipitation (Table 2-1). However, the year of observations did include several sizeable floods (10/4/09, 1/31/10, 7/6/10, and 10/13/10) and large wave events (from 3/10/2010 to the end of record) (Figure 2-2).

### *2.4.2 Radioisotopes*

Numerous samples were collected in this study, across the shelf system and over time. To help assess spatial and temporal changes in measured sediment properties, sites were grouped into distinct regions (Poverty Bay, Poverty mouth, the sediment depocenter, and the outer shelf) (Figure 2-1). Calculation of the mean and variance of  $^7\text{Be}$  penetration depths suggests spatial and temporal variability in sediment deposition (Figure 2-3). On the mid-shelf where  $^{210}\text{Pb}$ -

based sediment accumulation rates are  $>0.75 \text{ cm y}^{-1}$  (i.e., the center of the depocenters),  $^7\text{Be}$  penetration depths are  $\geq 3 \text{ cm}$  with the exception of one site to the north (Figure 2-3). Mean  $^7\text{Be}$  penetration depths  $< 3 \text{ cm}$  are more common in the regions accumulating  $< 0.25 \text{ cm y}^{-1}$  of sediment (Figure 2-3). In the Poverty Bay and Poverty mouth, mean  $^7\text{Be}$  penetration depths are fairly variable (Figure 2-3). Spatial patterns of variance in  $^7\text{Be}$  penetration depths seem to be more variable than those determined for the means. For example, sites 20 and 23 in the southern mid-shelf depocenter display high variance in  $^7\text{Be}$  penetration depths, whereas Sites 30 and 32 in the northern mid-shelf sediment depocenters are characterized by a lower variance (Figure 2-3).

$^7\text{Be}_{\text{total}}$  inventories also vary through space and time (Figure 2-4). In January 2010,  $^7\text{Be}_{\text{total}}$  inventories are greatest in Poverty Bay ( $> 6 \text{ dpm cm}^{-2}$ ) with moderately high inventories ( $1.5 - 2.5 \text{ dpm cm}^{-2}$ ) found in mid-shelf regions of long-term sediment accumulation (i.e., see areas  $> 0.5 \text{ cm y}^{-1}$  in Figure 2-3; Figure 2-4A). For May 2010,  $^7\text{Be}_{\text{total}}$  inventories mostly range from 1 to  $3 \text{ dpm cm}^{-2}$  across the margin, with the highest inventories located landward of the 50-m isobath (Figure 2-4B). In September 2010,  $^7\text{Be}_{\text{total}}$  inventories are greatest in the northern mid-shelf sediment depocenter ( $2.5 - 5.0 \text{ dpm cm}^{-2}$ ), while other regions display variable  $^7\text{Be}_{\text{total}}$  inventories (Figure 2-4C). In February 2011,  $^7\text{Be}_{\text{total}}$  inventories  $> 6 \text{ dpm cm}^{-2}$  are positioned in the Poverty mouth area: however, there is much variability in  $^7\text{Be}_{\text{total}}$  inventories in this region. Sites located at water depths  $> 70 \text{ m}$  generally have  $^7\text{Be}_{\text{total}}$  inventories  $< 1 \text{ dpm cm}^{-2}$  (Figure 2-4D).

Sediment deposition variability through time can be estimated using  $^7\text{Be}_{\text{new}}$  inventories and the calculated ratios of seabed versus estimated water-column  $^{234}\text{Th}$ . As no samples were collected in January,  $^7\text{Be}_{\text{new}}$  inventories could not be determined for the first cruise. However,  $^{234}\text{Th}$  ratios  $> 1$  suggest enhanced sediment deposition (reflected by an elevated seabed



inventory) was not widespread, generally occurring only in water depths >50 m (Figure 2-5). In May 2010, the majority of mid-shelf sites (30- to 60-m water depth) with the exception of the southern depocenter had measureable  $^7\text{Be}_{\text{new}}$  inventories and  $^{234}\text{Th}$  ratios greater than unity, likely indicating sediment deposition (Figures 2-5 & 2-6). Erosion or non-deposition is inferred for most other shelf sites as the majority had no measureable  $^7\text{Be}_{\text{new}}$  inventories and  $^{234}\text{Th}$  ratios were < 1 (Figures 2-5 & 2-6). In September 2010,  $^7\text{Be}_{\text{new}}$  inventories and  $^{234}\text{Th}$  ratios suggest sediment focusing on the outer shelf. However, the two radiotracers show disagreement in their prediction of sediment deposition on the mid-shelf; measureable  $^7\text{Be}_{\text{new}}$  inventories imply sediment deposition in the southern depocenter, whereas  $^{234}\text{Th}$  ratios argue for sediment focusing in the northern depocenter. For February 2011, measureable  $^7\text{Be}_{\text{new}}$  inventories and  $^{234}\text{Th}$  ratios reflect sediment deposition in close proximity to the Waipaoa River, in Poverty Bay, Poverty mouth, and at a few sites in the mid-shelf located between northern and southern mid-shelf sediment depocenters (Figures 2-5 & 2-6).

The relative influence of marine or fluvial sedimentation can be evaluated with a  $^7\text{Be}:\text{excess } ^{234}\text{Th}$  ratio. Because of differences in the rate of production and decay rate, and inconsistent fluxes, the equilibrium in the ratio between  $^7\text{Be}$  inventories and the excess  $^{234}\text{Th}$  ratio should not be assumed to be 1:1. After assessing the entire data set, cutoffs for fluvial ( $^7\text{Be}:\text{excess } ^{234}\text{Th} > 3$ ) and marine ( $^7\text{Be}:\text{excess } ^{234}\text{Th} < 1$ ) influence were determined. Ratios between 1 and 3 likely fall within the measurement error and are not designated as fluvial or marine. The important point here is that values >3 may reflect more fluvial impact, whereas values <1 indicate more marine influences on sedimentation. For January 2010,  $^7\text{Be}:\text{excess } ^{234}\text{Th}$  ratio values suggest fluvial dominance on sedimentation in Poverty Bay and the southern mid-shelf sediment depocenter. Some sites located to the north and on the outer shelf have a

marine signature, but most others are within the end-member sources (Figure 2-7). Parts of Poverty Bay, the southern mid-shelf sediment depocenter, and outer shelf sediments exhibit a marine signature for the May sampling period (Figure 2-7); however, fluvial dominance on sedimentation is indicated for Poverty mouth at this time (Figure 2-7). No clear trends were observed in September 2010. However, the majority of sites in Poverty Bay suggest a marine influence on sedimentation (Figure 2-7). Finally, the majority of sites sampled in February 2011 are characterized by  ${}^7\text{Be}:\text{excess } {}^{234}\text{Th} < 1$ , suggesting a margin-wide marine influence on sedimentation (Figure 2-7). There are a few exceptions, as a few sites in Poverty mouth have a stronger fluvial signature (Figure 2-7).

#### 2.4.3 Seabed Character

Clay and organic content (LOI percentages) exhibit similar spatial and temporal patterns (Figure 2-8). Northern and southern mid-shelf sediment depocenters had the highest mean clay (>40 %) and LOI (>4 %) percentages (Figure 2-8). Surprisingly, the few sites in Poverty Bay with time-series measurements had high mean clay and LOI percentages, comparable to those of the mid-shelf sediment depocenters. The Poverty mouth sites had lower mean clay (<30 %) and LOI (<4 %) contents (Figure 2-8). The greatest variance in clay and LOI percent was observed in Poverty Bay and Poverty mouth, while the sediment depocenters exhibited little change in these properties throughout the study (Figure 2-8).

A one-way ANOVA was used to assess the differences in both surface clay percent and LOI content through space and time. Significant differences (p-value <0.01) in both clay percent and LOI content are observed in space but not time. More specifically a post-hoc Tukey Test suggests significant differences in clay percent between Poverty mouth and the sediment depocenter (p-value < 0.01), Poverty mouth and the outer shelf (p-value = 0.05). Also, the LOI

content was significantly different between Poverty mouth and the sediment depocenter (p-value <0.01).

## **2.5 Discussion**

### *2.5.1 Spatial and Temporal Variation of Sediment Deposition*

Significant changes in fluvial and oceanographic conditions during pre-sampling periods are very evident over the course of the study (Figure 2-2), as are spatial and temporal variability in radioisotope inventories and seabed character (Figures 2-3 to 2-8). The following are a few possible reasons for the observed spatial and temporal complexity in sediment deposition and seabed character: 1) timing of sediment discharge events relative to sampling; 2) the number of sediment discharge events and wave events; 3) the concurrence (or lack) of both sediment discharge events and wave events was inconsistent; and 4) sedimentation on the shelf at scales <3 km may be more heterogeneous than appreciated by earlier studies. Some recent research discussed below has touched on the possible importance of all of these items, and the results here help support these ideas.

A major fluvial discharge event occurred prior to each sampling period. More specifically, floods in January, May, September, and February represent a hiatus of 109, 114, 67, and 126 days between major discharges and the cruise start date, respectively. Research on the Eel shelf, a modern equivalent to the Waipaoa system has shown that flood sediments may be transported across the shelf and to the upper slope in as little as 2 weeks after peak river discharge (Sommerfield et al., 1999). Therefore, their work documents how sediment discharged during flood events may be rapidly recorded in mid-shelf strata, an important region of long-term sediment accumulation. Overall, interpretation of sediment depositional patterns is complicated by multiple sediment discharge events (large and small) and variability in sediment transport, associated with changing oceanographic conditions. On the Waipaoa margin, sediment deposits

with thick  $^7\text{Be}$  penetration were observed in Poverty Bay and Poverty mouth, but the energetic wave climate and seabed variability (e.g., Figure 2-4) suggests that this material was most likely ephemeral. Previous researchers have hypothesized that Poverty mouth and the region between mid-shelf sediment depocenter acts as a zone of fine-sediment bypassing (Miller and Kuehl, 2010; Rose and Kuehl, 2010); in this region, physical reworking favors the dispersal of sediment to distal shelf regions and has created interbedded laminated sands and muds characterized by low uniform  $^{210}\text{Pb}$  activities. Variability in  $^7\text{Be}$  (Figure 2-4),  $^{234}\text{Th}$  (Figure 2-5), clay content, and LOI percent (Figure 2-8) in the surface seabed support this assertion of sediment bypassing, suggesting the periodic emplacement but not permanent accumulation of organic-rich fine-grained sediments.

Inspection of sediment deposition patterns and the timing of pre-sampling fluvial and oceanographic events for January and September 2010 suggest that the coherence of wave and discharge events may be important. The major sediment discharge event occurring prior to sampling in January 2010 (10/4/09) did not occur with nor was followed by a significant wave event ( $>3.5$  m). In contrast, the September 2010 sampling period was preceded by a major sediment discharge event concurrent (7/6/10) with a large wave event ( $>3.5$  m). The sediment depositional patterns for these two time periods were different (Figures 2-4 to 2-6). In January 2010, deposition occurred in close proximity to the Waipaoa River in Poverty Bay; whereas in September 2010 sediment deposition is inferred significantly further seaward, on the mid- and outer shelf. Based on these observations, it appears that increased wave activity may be responsible for remobilizing and flushing sediment out of Poverty Bay and shelf-wide dispersal. This assertion is supported by sediment transport models for Poverty Bay that show during wet storms sediments are moved out of the bay by waves and currents (Bever et al., 2011). Dispersal

is further encouraged by favorable wind direction. Initially winds blow onshore, building easterly swells, but switch direction during later phases of river flooding as low pressure cyclonic systems tract westward across northeastern New Zealand, reversing the direction of surface currents, and facilitating movement of sediments toward the mouth of Poverty Bay (Bever et al., 2011). The movement of sediments out of Poverty Bay is accomplished by waves at a later time (Bever et al., 2011). During these wet storms current velocities can reach  $0.25 \text{ m s}^{-1}$  and wave heights of 2-3 m in water depths of only 10 m (Bever et al., 2011). Data from the Eel River margin also show that wet storms are responsible for transporting sediment to the mid-shelf (Ogston et al., 2000), and that deposition at more distal locations is less dependent on river discharge than wave events and currents (Walsh and Nittrouer, 1999; Puig et al., 2003). However, this is not the case for all margin systems. For instance, sediment deposits formed on the Tet River inner shelf could not be linked directly to the occurrence of wet storms. Rather, their development was dependent on the initial deposition of sediment in close proximity to the river mouth (during wet storms) and the subsequent reactivation and transport of this sediment during dry storms (Guillen et al., 2006). Also, study of flood deposition on the Mississippi Shelf has shown that sediments are deposited proximal to the river mouth and may remain there, even if there is a large time gap between sampling and the occurrence of the sediment discharge event responsible for their creation (Corbett et al., 2007). This is due to the fact that the Mississippi margin lacks an energetic wave climate with wave heights  $<2 \text{ m}$  for most of the year (Dail et al., 2007). This contrasts quite dramatically with the typical conditions on the Waipaoa (Figure 2-2). That said, the Mississippi margin, can experience massive waves ( $>15 \text{ m}$ ) during hurricane passage, potentially enabling even thicker- spatially extensive shelf event strata. Recent examples include sequences described after hurricanes Ivan and Katrina (Dail et al., 2007; Walsh

et al., 2007; Gőni et al., 2007). But, sample collection on the Waipaoa shelf in January 2010, followed a long period of quiescent wave climate (Figure 2-2), and this is probably the fundamental driver for the large amount of sediment deposition seen in Poverty Bay (Figure 2-4). Therefore, depositional patterns on margins with differing morphologies and mean oceanographic settings may be similar, suggesting that event strata are not necessarily diagnostic of depositional environment. However, all seabed observations represent a sedimentary snapshot in geologic time and thus have their own limitations.

Using the radionuclide data and other observations, four generalized depositional interpretations were developed and can be employed to explain observed patterns of radioisotopes, and may be conceptually related to pre-sampling fluvial and oceanographic conditions on the Waipaoa margin. The patterns are inferred to reflect four fundamental, controlling situations: 1) high sediment discharge coupled with a non-energetic wave climate leads to deposition in Poverty Bay; 2) a large sediment discharge coupled with an energetic wave climate yields sediment deposition on the mid-shelf; 3) successive, concurrent high sediment discharge and wave events induce sediment shelf-wide transport to the mid-shelf and outer shelf (and likely beyond); and 4) a large sediment discharge coupled with an energetic wave climate followed by a second sediment discharge event leads to deposition in Poverty Bay and the mid-shelf (Figure 2-9). The spatial radioisotope pattern observed in January is thought to be captured by interpretation 1; the distribution in May, September and February by maps 2, 3 and 4, respectively (Figure 2-9). Indeed, these interpretations are simplifications of the complexity of the observed natural variability, but insight of fundamental dispersal patterns is provided by generalizing these data.

A notable point to emphasize here is that in addition to generalized pattern changes, the radioisotope data suggests that deposition can be remarkably variable over spatial scales  $\leq 3$  km on the Waipaoa margin. For example, samples collected from sites 13-16 (Figure 2-1) in February 2011 have differing radioisotope inventories (Figure 2-4; Figure 2-5), with X-radiographs that suggest a great deal of variability in the spatial distribution and thickness of sedimentary layers even over a small area (Figure 2-10). Albeit, on a larger scale of  $\sim 15$  km, Goff et al., (2002) showed that beds on the Eel River margin comprised dominantly of very fine sands and silts are predisposed to forming ripples in response to the reworking of surface sediments. Here, the irregular surface of the bed led to further heterogeneity in grain-size, destroying flood layers. Therefore, it is possible that spatial variability in bedforms in water depths  $< 40$  m may be responsible for differences in the thickness and extent of sedimentary layers over small spatial areas.

#### *2.5.2 Change in Seabed Character with Sediment Deposition*

While sediment deposition is variable through both space and time across the entire shelf, variance in the mean character of the seabed is limited to the confines of Poverty Bay inner shelf and mouth. The clay and LOI content at  $> 40$  m water depth have sediment properties that appear to remain relatively stable through time (Figure 2-8). Comparison of variance for  $^7\text{Be}$  inventories (Figure 2-3) and clay and LOI percent data (Figure 2-8) for offshore shelf regions (which show variance in inventories) suggests that sediment deposition does not cause changes in seabed character. Ultimately, the variability measured in seabed character compares well with the facies distribution described on the Waipaoa shelf (Rose and Kuehl, 2010) and observed in  $^{210}\text{Pb}$  profile patterns (Miller and Kuehl, 2010). Specifically, the greatest variability in clay content and LOI percent occurs in the inner-shelf region, which is characterized by interbedded laminated muds. Physical reworking of sediment in this region is suggested based on graded

bedding and high-bulk density of strata (Rose and Kuehl, 2010). Seaward, the shelf is characterized by steady-state and non-steady-state  $^{210}\text{Pb}$  profiles associated with mixed layers and mottles and mottled muds, respectively (Miller and Kuehl, 2010; Rose and Kuehl, 2010). The variability in seabed character in Poverty Bay and Poverty mouth can be explained by the temporary emplacement of fine-grained sediment deposits. Sediment deposition is punctuated in deep (>50 m) regions of the shelf, yet the character of the supplied sediment remains relatively unchanged through time. This explains the lack of correlation between sediment deposition and changes in seabed character at deeper sites (>50 m).

## **2.6 Conclusions**

Over the duration of the study, the locus of sediment deposition coincided with the regions of long-term sediment accumulation and thick sequences. However, temporal variability in radioisotope inventories suggests that the supply of sediment to these major accumulation regions is variable through time. Clay and LOI percentages in the surface seabed remained relatively constant in these locations, suggesting relatively little change in the character of the sediment supplied or after it's reworking.

Sediment deposition was variable in water depths <40 m, including Poverty Bay and Poverty mouth, and dependent on both the timing of sample collection relative to sediment discharge events and the synchronicity (or lack of) between river sediment discharge and wave events. Identification of ephemeral sediment deposits suggests that Poverty Bay and its mouth function as sediment transport pathways, regions of fine-sediment bypassing. Localized bathymetry and a high energy wave regime in the nearshore and inner shelf probably complicate interpretation of the dominant controls on variability in seabed character.



It appears that fluvial and oceanographic conditions dictate the formation of sedimentary strata on the Waipaoa shelf. There was considerable spatial complexity in sediment deposition observed during four sampling periods (January 2010, May 2010, September 2010, and February 2011). A qualitative interpretation of radionuclide observations suggests the importance in the relative timing of sediment discharge and wave events in relation to patterns of sediment deposition. The time-series observations of radioisotope inventories and surface seabed clay and LOI percent and subsequent interpretations of sediment deposition patterns will provide researchers with an opportunity to develop and test the validity of sediment transport models for the Waipaoa shelf. The small-scale spatial variability in the thickness and horizontal extent of sedimentary layers is complex and deserves more research.

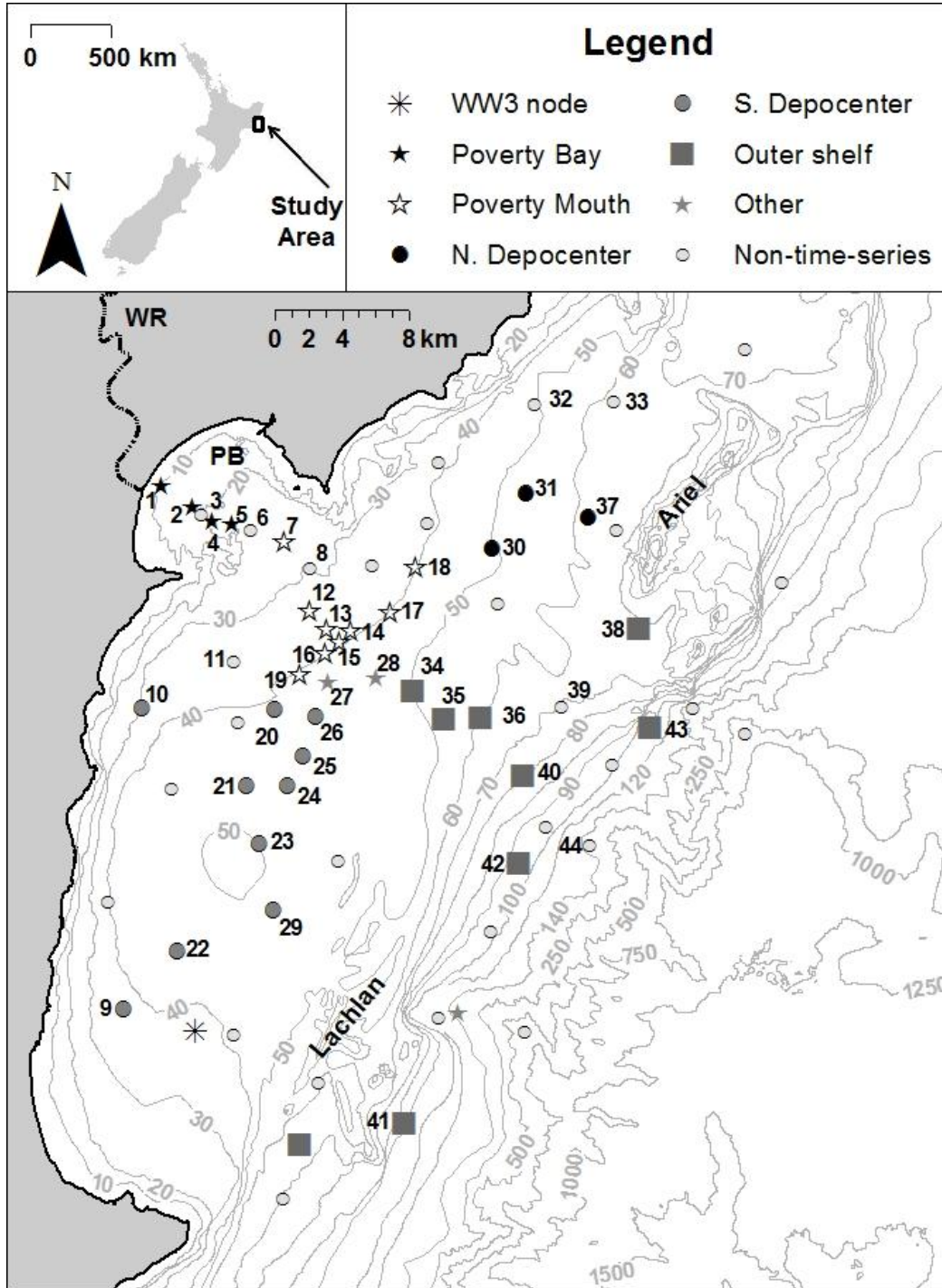


Figure 2-1 Basemap showing the location of samples in relation to the Waipaoa River (WR), Poverty Bay (PB), and Lachlan and Ariel anticlines. Sites where time-series radioisotope inventories were calculated are presented as symbol indicating the shelf region (Poverty Bay, Poverty mouth, sediment depocenters, outer shelf, and other) and are numbered.

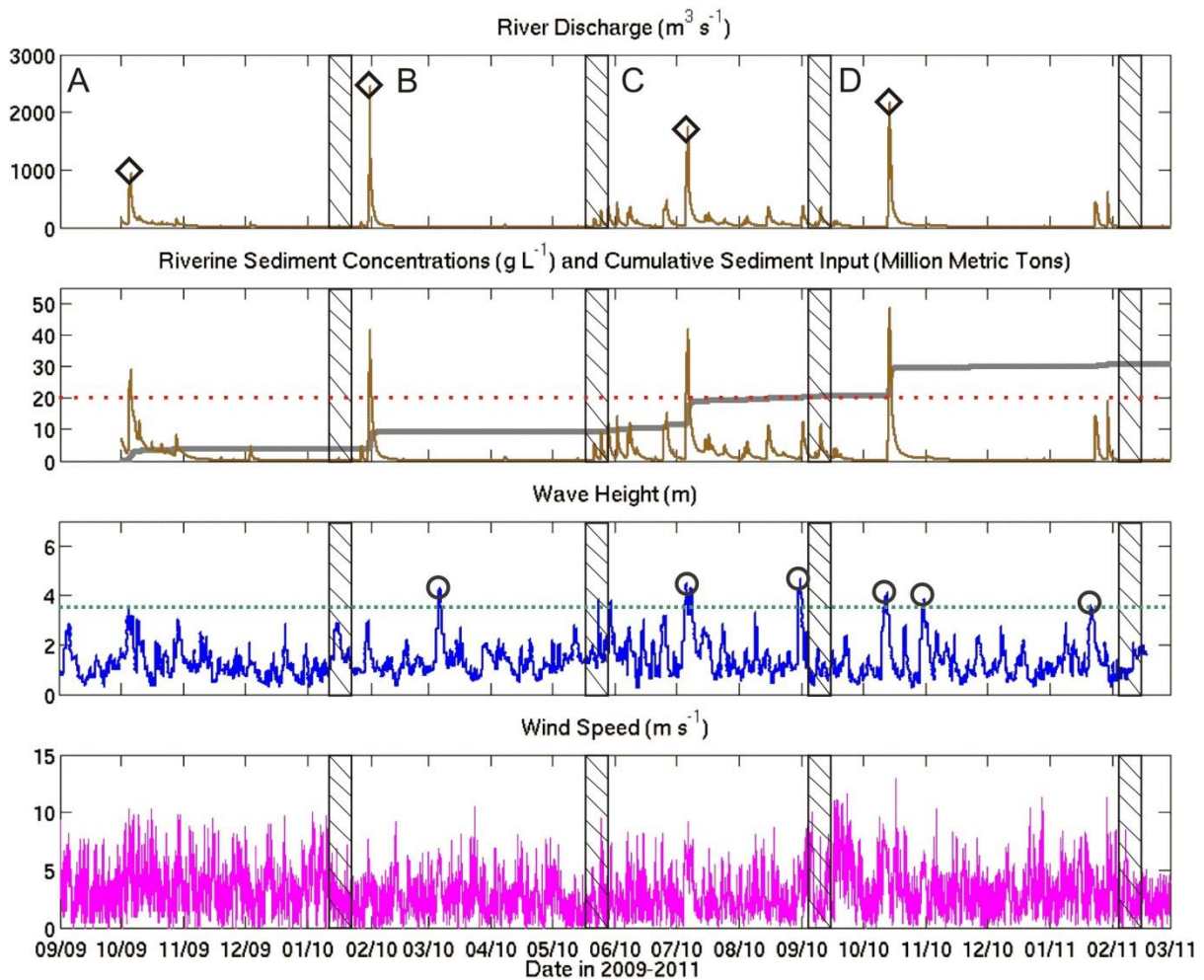


Figure 2-2 Fluvial, oceanographic, and meteorological data for the periods of time prior (A-D) to sampling during cruises (black hatched boxes). An arbitrary cutoff of 3.5 m and 20  $\text{g l}^{-1}$  were chosen to represent wave and high sediment discharge events (dotted lines), respectively. Data indicate temporal variability in river discharge, sediment concentration, wave height, and wind speed including several flood periods (diamonds) and wave events (circles).

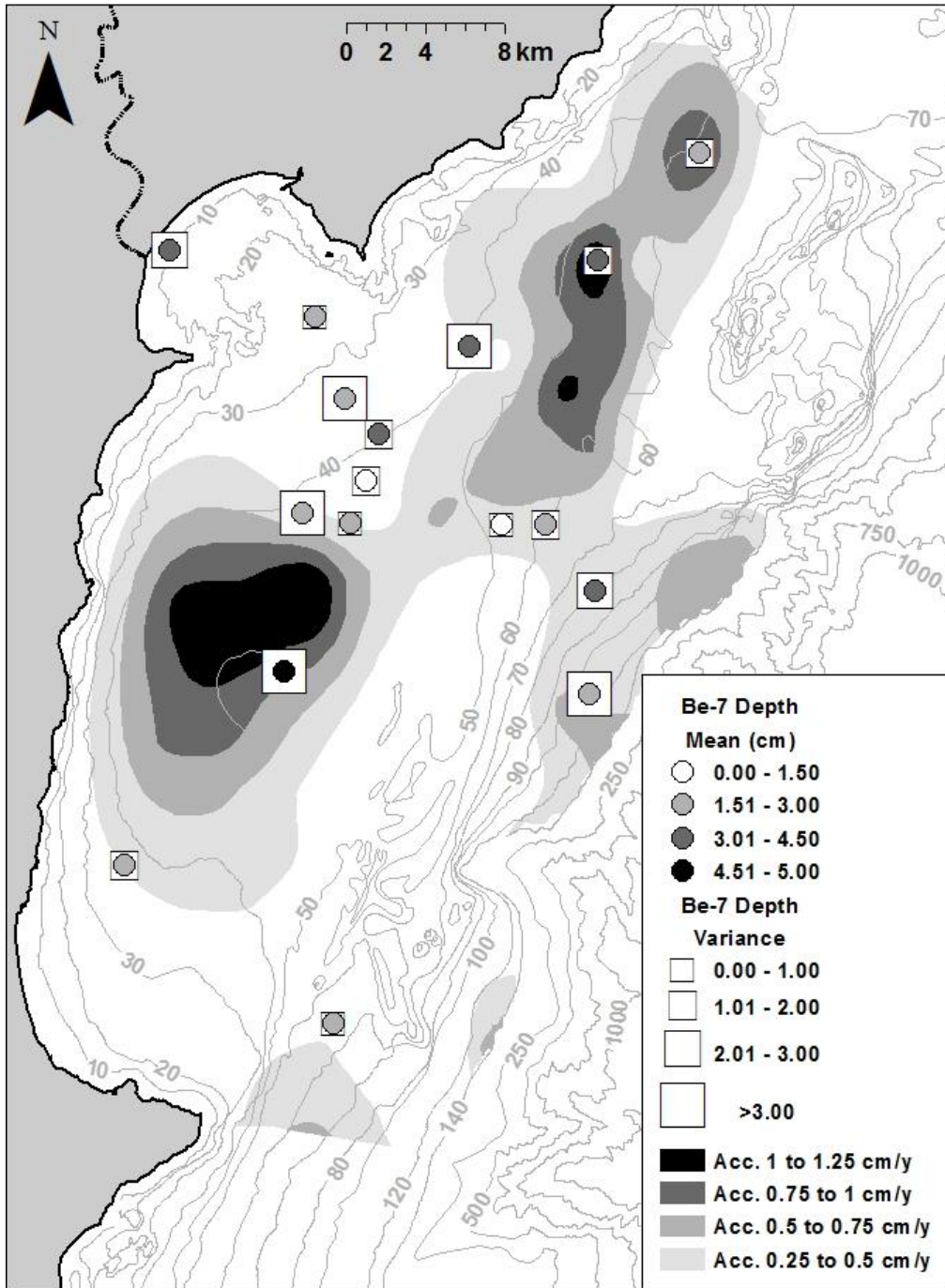


Figure 2-3 A comparison of short-term sediment deposition (evidenced by mean <sup>7</sup>Be penetration depths) and long-term <sup>210</sup>Pb based sediment accumulation patterns (from Miller and Kuehl, 2010 using <sup>210</sup>Pb). Variability through time is shown as the variance of values using data from all sampling periods. Data show that sediment deposition is punctuated through time and does not necessarily correspond to areas of long-term accumulation.

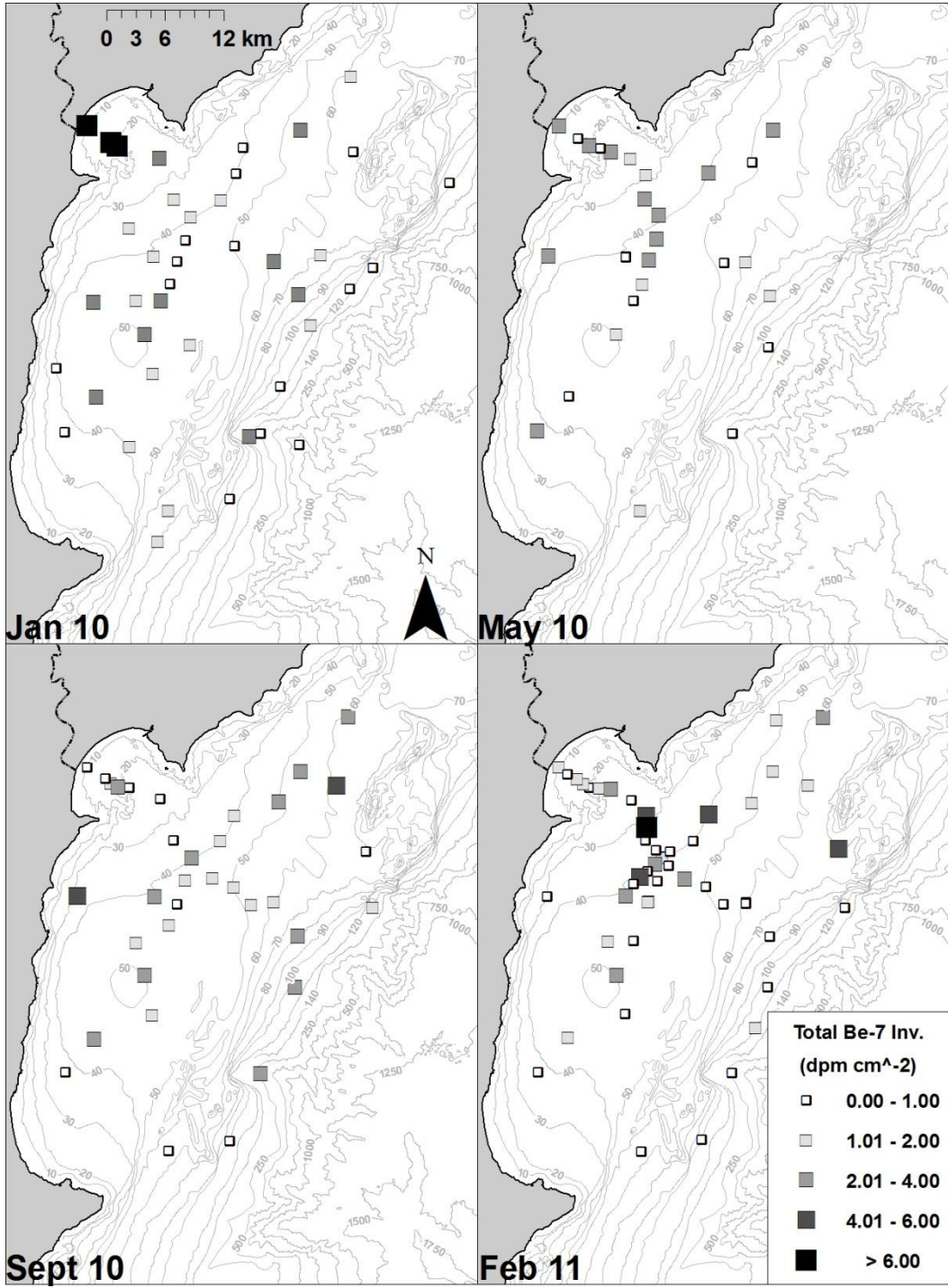


Figure 2-4 Total <sup>7</sup>Be inventories for each sampling period. Variability in total <sup>7</sup>Be inventories through time indicate that sediment deposition is punctuated over the course of the study.

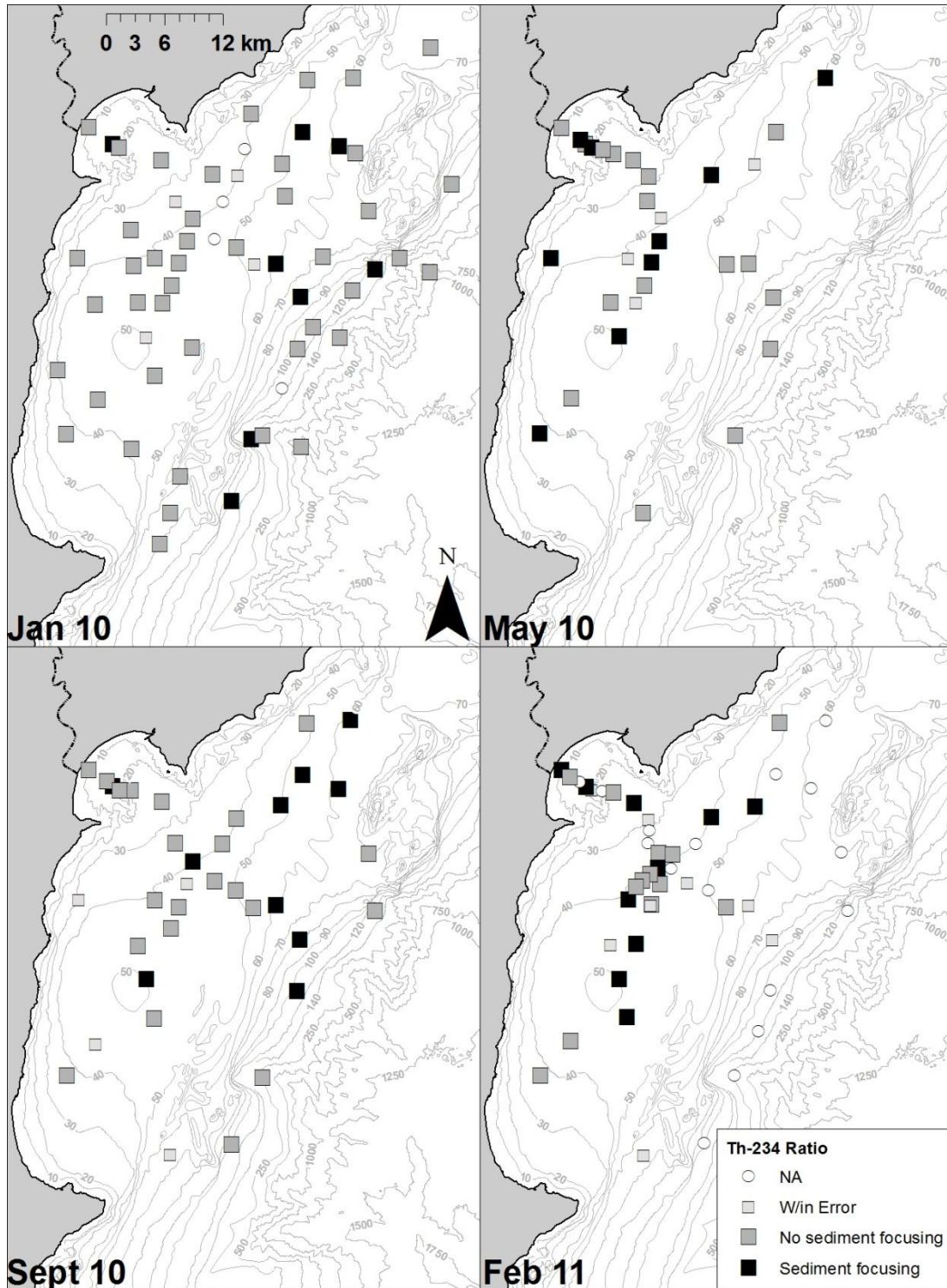


Figure 2-5 Sediment focusing inferred from  $^{234}\text{Th}$  ratios  $>1$  for each sampling period. Differences in sediment focusing suggest variable sediment dispersal over the duration of this study.

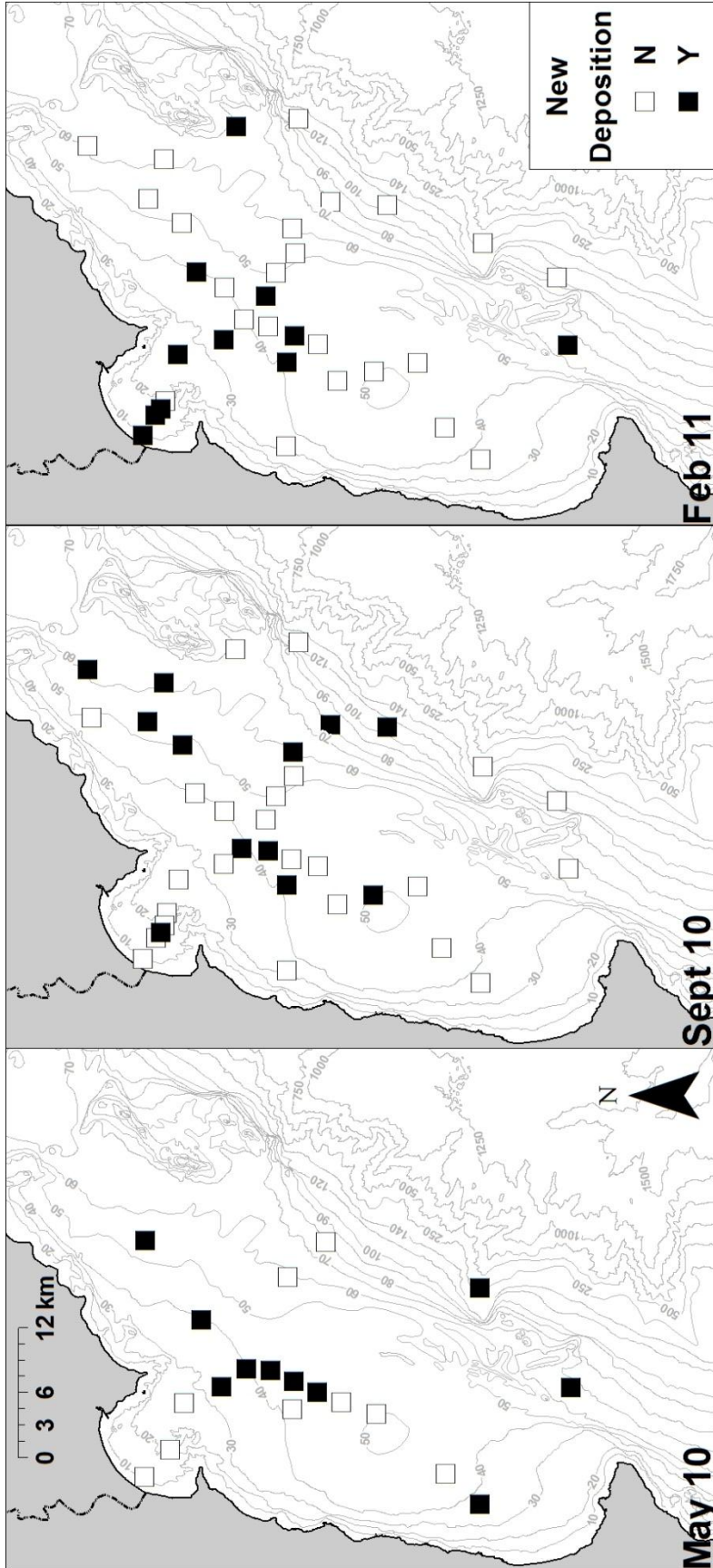


Figure 2-6 Sediment deposition inferred from measureable new  $^7\text{Be}$  inventories at repeat sites for May and September 2010 and February 2011. Data indicate that sediment deposition is sporadic through time.

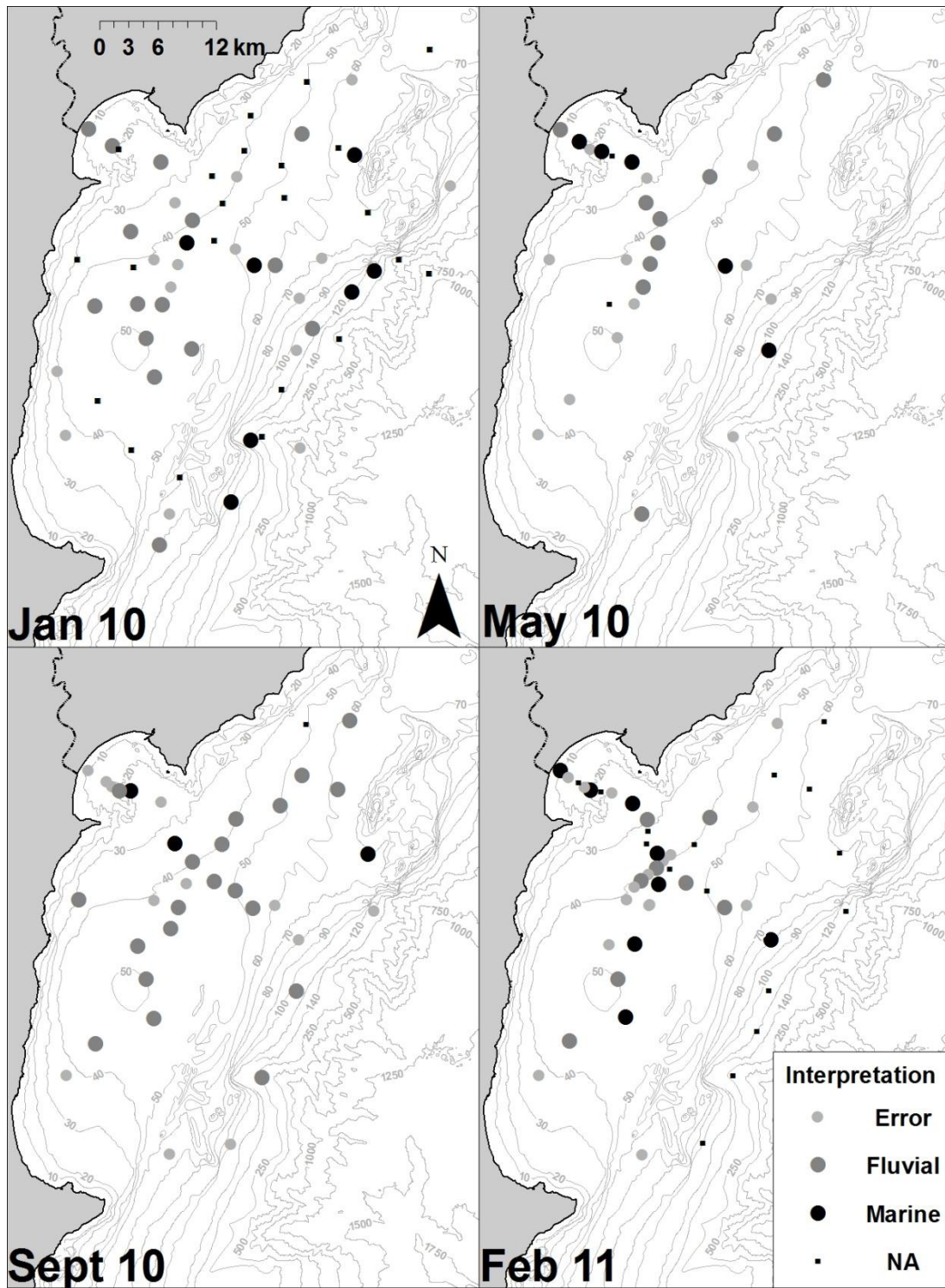


Figure 2-7 The relative influence of fluvial and marine processes on sedimentation inferred from the  $^7\text{Be}:\text{excess } ^{234}\text{Th}$  ratio for four sampling periods. Maps show temporal variability in the dominant influences on deposition.



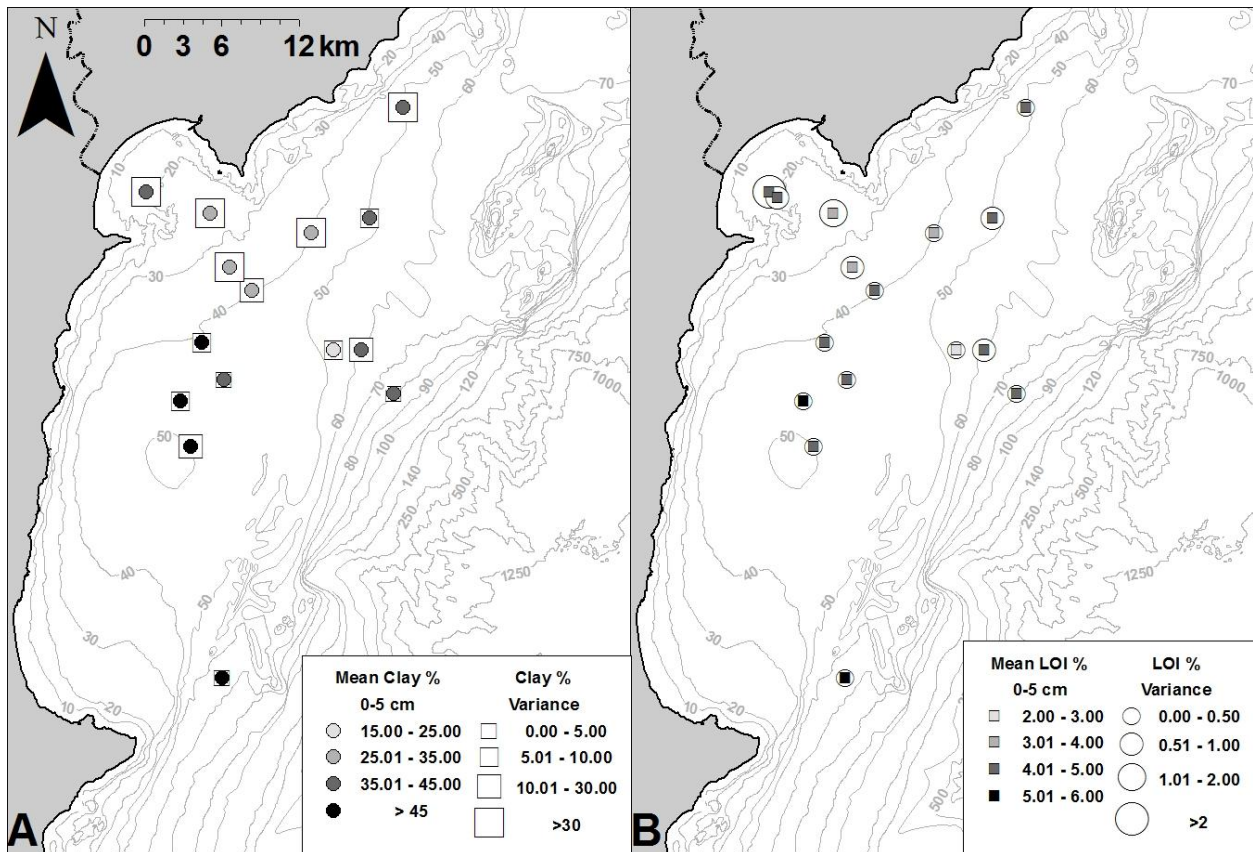


Figure 2-8 The mean and variance of clay percent (A) and LOI percent (B) for the period of study. Note that patterns are comparable for the two datasets.

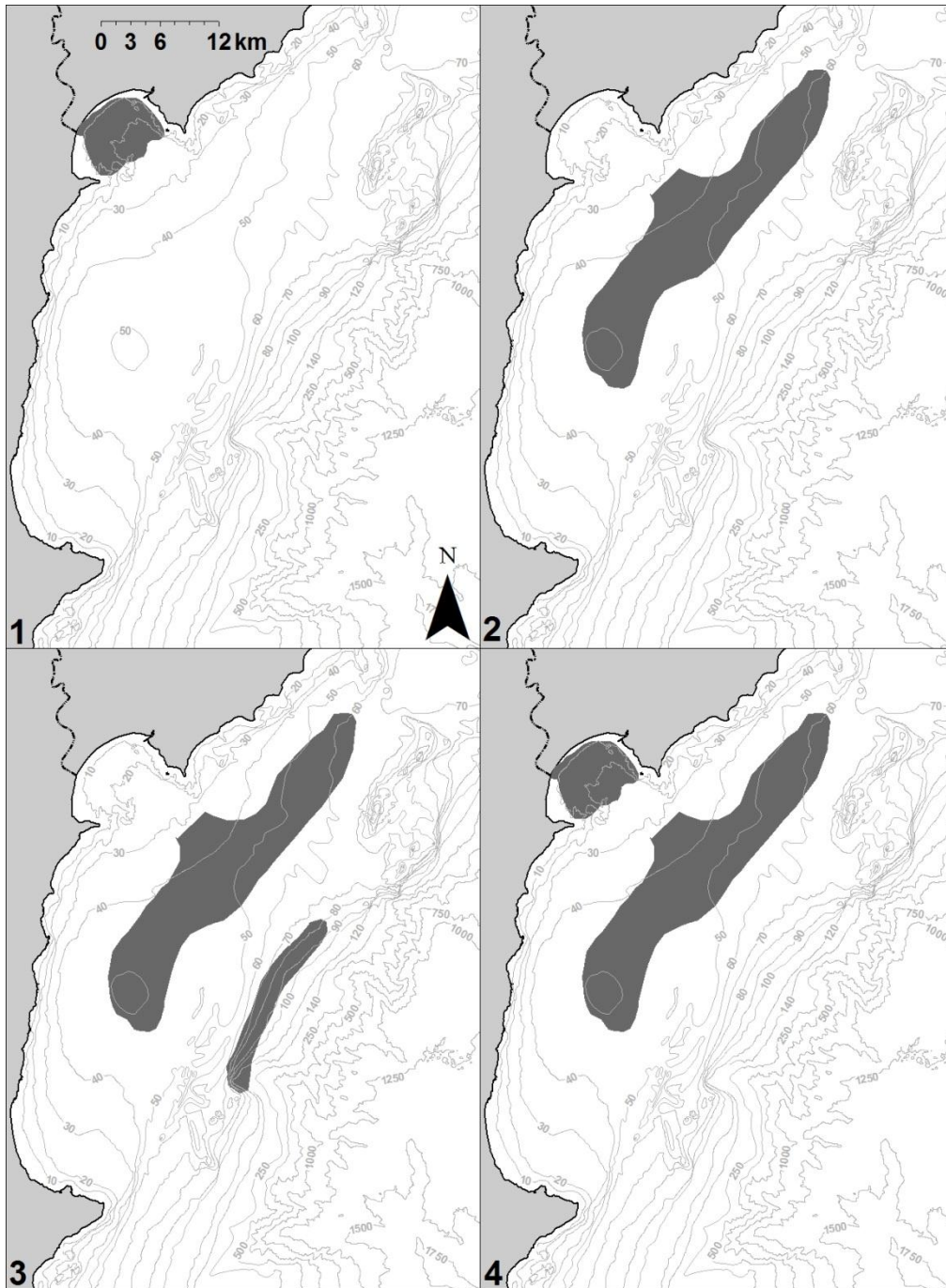


Figure 2-9 Sediment depositional interpretations for the Waipaoa shelf relating pre-sampling fluvial and oceanographic conditions to observed sediment deposition patterns, determined by spatial changes in radioisotope inventories (indicated by shaded black regions). Interpretations (1-4) are referenced in the text and suggest that pre-sampling conditions dictate the patterns of sediment deposition on the short-term.

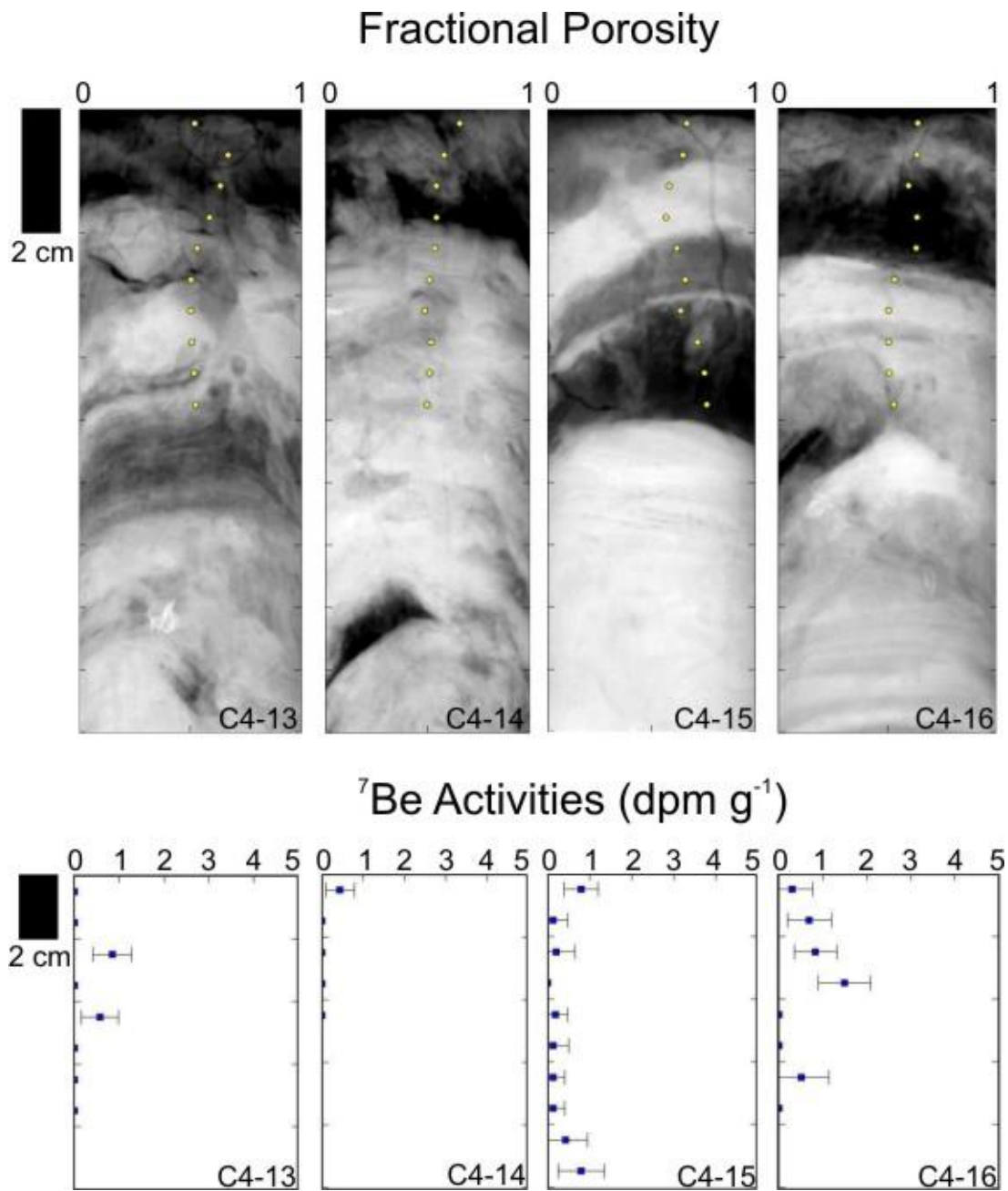


Figure 2-10 Evidence for variability in strata thickness (X-radiographs) and deposition ( $^7\text{Be}$  down-core profiles) over a small spatial scale (sites 13-16; Figure 2-1).

Table 2-1 Summary of average fluvial, oceanographic, and meteorological conditions.

<b>Pre-cruise period</b>	<b>Number of days</b>	<b>Average discharge (<math>10^6 \text{ m}^3 \text{ s}^{-1} \text{ d}^{-1}</math>)</b>	<b>Total sediment discharged (Mt)</b>	<b>Average wave Height (m)</b>	<b>Total precipitation (cm)</b>	<b>Daily average precipitation (mm)</b>
<b>Pre-C1</b>	113*	151	3.36	1.5 ± 0.03	24.4	2.16
<b>Pre-C2</b>	124	101	4.54	1.6 ± 0.02	38.8	3.13
<b>Pre-C3</b>	109	227	5.73	2.0 ± 0.04	48.9	4.49
<b>Pre-C4</b>	158	130	4.98	1.5 ± 0.02	41.5	2.63

\*Number of days does not represent days between sampling events, as the first samples were collected in January.

### 3 Spatial and Temporal Variation in Sediment Erodibility on the Waipaoa River Margin, New Zealand

#### Abstract

Erodibility is a measurement of the ease at which material is eroded from the seabed, and therefore, it is critical to modeling coastal sediment dynamics. Seabed erodibility measurements collected on four research cruises (January 2010 – February 2011) on the Waipaoa margin, New Zealand suggest spatial and temporal complexity in sediment erodibility. Erodibility measurements are low in water depths >40 m and higher but more variable in shallower regions of the Waipaoa shelf. Cores with fluid-mud layers, collected from the inner shelf all showed a moderate level of erodibility and time-series seabed observations suggests that these deposits are ephemeral, the result of being more easy to erode. Radionuclide data indicate that the erodibility may be related to the recency of sediment deposition with  $^7\text{Be}$ - and  $^{234}\text{Th}$ -rich sediment deposits being easier to erode. This observation is supported by previous work in the York River estuary, VA. Also, high sand-content sediments (> 65 %) were more erodible than sediments containing finer material, providing a mechanism for temporal seabed variability at sites landward of the 40-m isobath. Observations highlight how changes in the physical character of the seabed alter the erodibility. Interestingly, time-series core data from the outer shelf showed how a flood layer and its subsequent reworking caused little change in erodibility, and this suggests lithologic homogeneity in seabed sediment may limit erodibility variations in some shelf areas. Future studies with rapid-response sampling schemes or laboratory studies focused on simulating sediment deposition events are needed to better determine erodibility response over time.

#### 3.1 Introduction

The erodibility of the seabed is dependent upon the surface sediment properties and the forces (e.g., bed stress from waves and currents) acting upon them (Sanford, 2006) and these

data are important to accurately model sediment transport in marine environments. The fate of fine-grained sediment in the coastal environment is especially important as these particles have a high affinity for anthropogenic pollutants, chemicals, trace metals (Horowitz, 1995), and organic and inorganic carbon (Bonniwell et al., 1998). Sediment resuspension facilitates the availability and mobility of these materials in marine environments and thus affects the flux of nutrients (e.g., Fanning et al., 1982) and pollutants (Håkanson, 2006) from the seabed to the water column. The burial of carbon in the ocean forms an important part of the carbon cycle and has implications for global climate (Mckee et al., 2004). Suspended sediment in shallow water attenuates sunlight, reducing primary productivity and impacting dissolved oxygen concentrations (Lawrence et al., 2004). For these many reasons, understanding sediment dynamics in the marine environment is important, and erodibility is a key parameter controlling these biogeochemical processes. Considerable research (e.g., Grabowski et al., 2011 and references therein) has focused on discerning the relationship between erodibility and properties of the seabed (e.g., Thomsen and Gust, 2000; Stevens et al, 2007; Law et al., 2008); however, few studies have examined sediment erodibility on continental shelves over time across a shelf-wide scale.

This study aims to resolve seasonal changes in sediment erodibility on the Waipaoa River margin, New Zealand through time-series seabed observations. A large sediment supply coupled with variable fluvial and oceanographic conditions factored into the selection of this system. The objectives of this research are to: 1) determine the manner in which sediment erodibility varies through space and time; 2) examine the relationship between sediment erodibility and depositional processes; and 3) relate the findings of this research to previous studies.

## 3.2 Background

### 3.2.1 Sediment Erodibility

Sediment erodibility is typically defined as an erosion threshold (e.g., Thomsen and Gust, 2000) or critical shear stress (e.g., Jepsen et al., 1997; Dickhudt et al., 2009), both of which represent the applied force on an area of the seabed necessary to generate sediment motion. No standard protocol currently exists for defining the rate of or applied stress at which sediment erosion begins (e.g., Sanford 2006 and references therein). Current knowledge of sediment erosion and transport may be advanced by standardizing sediment erodibility measurements, thereby allowing sediment erodibility data sets over a range of geologic environments and forcings to be compared (Sanford, 2006).

Equations relating erosion rate to shear stress are dependent on the nature of erosion (i.e., depth-limited or time dependent) and many formulations exist (see Sanford and Maa, 2001 and references therein). Depth-limited erosion is referred to as Type 1, whereas Type 2 is time dependent. When examining experimental data, depth-limited, or Type 1, erosion shows a decrease in erosion rate through time while time dependent, Type 2, has a constant erosion rate through time. Experimental design may influence the type of erosion observed. For example, experiments applying a small number of step-wise increases in applied stress over a longer duration of time may resemble Type 1 erosion, whereas experiments with small step-wise increases in applied stress over a short period of time may resemble Type 2 erosion.

The erodibility measurement methodology and erosion formulation derived by Sanford and Maa (2001) is used in this study as it may be applied to both Type 1 and Type 2 erosion:

$$E(m,t) = M(m)[\tau_b(t) - \tau_c(m)] \quad (1)$$

where  $E$  is the rate of erosion ( $\text{kg m}^{-2} \text{s}^{-1}$ ),  $M$  is the erosion rate parameter ( $\text{kg m}^{-2} \text{s}^{-1} \text{Pa}^{-1}$ ),  $\tau_b$  is the applied bed stress (Pa), and  $\tau_c$  is the critical stress for erosion (Pa),  $m$  refers to the

experiment eroded mass ( $\text{kg m}^{-2}$ ), and  $t$  is time (s). Assuming an increasing resistance to erosion ( $\tau_c$ ) with depth in the seabed (i.e., as more sediment is eroded), the exponential decay of  $E$  with time is fit to measurements of  $m$  for the duration of each experimental time step (Dickhudt et al., 2010). The critical stress as a function of mass eroded (i.e.,  $\tau_c(m)$ ) is then evaluated using Equation 1. This erodibility formulation is basic, but the experimentally derived erodibility variables provide valuable insight into the character of sediment erosion. Comparing  $\tau_c$  and  $m$  may be used as a means of assessing spatial (horizontal and vertical) and temporal differences in sediment erodibility. A comparison of  $M$  to  $m$  shows how the erosion rate changes with depth in the seabed. These relationships shed light on the bed response to an applied stress and the amount of material available for transport both of which are important aspects of modeling sediment transport.

### *3.2.2 Controls on Erodibility*

Lab and field studies have shown that erodibility is influenced by several sediment properties and processes, including grain-size distribution (Roberts et al., 1998; Thomsen and Gust, 2000), clay content (Panagiotopoulos et al., 1997; Houwing, 1999), wet-bulk density (Amos et al., 2004; Bale et al., 2007), organic content (Righetti and Lucarelli, 2007), sediment disturbance (Sgro et al., 2005), feeding and egestion by organisms (Andersen et al., 2005), bioturbation (Fernandes et al., 2006; Widdows et al., 2009), and biofilms and extracellular polymeric substances (EPS) (Sutherland et al., 1998; Friend et al., 2003; Lundkvist et al., 2007). Grabowski et al. (2011) summarizes the complex relationship between erodibility and sediment properties in a review paper on cohesive sediment erodibility.

At present, no universal empirical formula exists to predict erodibility through single measurements or observation of the aforementioned sediment properties or post-depositional processes. For this reason, controls on sediment erodibility are still assessed in both laboratory



settings and the natural environment. Laboratory studies often aim to isolate controls on erodibility through creation of artificial sediment beds. The majority of research has focused on the influence of physical sediment properties on erodibility, especially particle size and bulk-density. For example, the study of homogenous grain-size beds has shown that as sediment bulk density increases, the erosion rates decrease (Jepsen et al., 1997; Roberts et al., 1998). However, fine-grained sediment with a low bulk density may be less erodible due to inter-particle cohesion. Experiments varying the grain-size of artificial beds (i.e., mixed or heterogeneous beds) provide insight into the mud content necessary to induce sediment cohesion. Results show that beds comprised of as little as 3-15 % mud may act more cohesive and better resist erosion (Mitchener and Torfs, 1996). Panagiotopoulos et al. (1997) distinguished between silt and clay, and their study revealed that artificial beds with clay mineral content <11-14 % by dry weight are difficult to erode. Therefore, in lab studies, bed grain-size distribution, especially bed clay content, has been well established as an important determinant of sediment erodibility. However, in the natural environment biogeochemical alteration of surface sediment and the addition of event layers also affects surface seabed character, and these may have a compounding control on sediment erodibility variation through space and time (Stevens et al., 2007 and references therein).

Unfortunately, field studies have had limited success in disentangling individual parameters that control sediment erodibility, a testament to the complexity of physical, biological, and chemical interactions in natural sediments. For example, Stevens et al. (2007) determined sediment erodibility to be spatially and temporally complex in the Western Adriatic Sea. During winter, porosity appeared an important determinant of sediment erodibility. However, less porous sediments were more erodible, a relationship opposite to what was

expected based on laboratory studies (e.g., Jepsen et al., 1997; Lick and McNeil, 2001). As no correlation between erodibility and sediment properties was observed in the summer, it is likely that the relationship between porosity and erodibility is possibly related to other bed properties or the complex interaction of many properties (Stevens et al., 2007).

Seasonal variation in sediment erodibility was also observed in the York River estuary, VA but no strong correlations between bed erodibility and properties of the seabed were identified (Dickhudt et al., 2009), including solids volume fraction, surface concentrations of organic matter, colloidal carbohydrates, and exopolymeric substances. This study consisted of monthly to bi-monthly measurements of sediment erodibility over an 18-month period. Sediment erodibility increased in response to recent deposition events associated with flooding of the York River (Dickhudt et al., 2009). However, these event layers were ephemeral in nature and for the majority of the study erodibility was low, the result of post-depositional processes acting on the seabed (Dickhudt et al., 2009).

Benthic organisms disturb the surficial seabed through locomotion, feeding, and bioturbation. These activities influence bed roughness, the momentum of fluid forces, exposure of the bed, and the biologically-enhanced adhesion of particles (Jumars and Nowell, 1984). In the seabed, sediment reworking is greatest in the surface mixed layer where recently deposited sediments are impacted in potentially less than a few weeks after their emplacement (Wheatcroft and Drake, 2003). Burrows are void spaces in sediment that decrease the original bulk density of sediments (e.g., Gerdol and Hughes, 1994; Mazik and Elliot, 2000), and as a result of increased porosity may increase the rate of erosion. Conversely, exopolymeric substances secreted by organisms may make the seabed more cohesive and decrease the rate of erosion (Sutherland et al., 1998; Friend et al., 2003; Lundkvist et al., 2007). However, it is hard to isolate one

controlling variable on sediment erodibility, as certain properties are related and may co-vary (e.g., grain-size and organic content).

Research in the western Gulf of Lions focused on determining if seabed characteristics facilitate what material is eroded (Law et al., 2008). Before and after erodibility experiments, the grain-size of the bed was measured. Beds with <7.5 % clay were easily winnowed of their fine fraction at low applied stresses, whereas beds with >7.5 % clay acted cohesively, eroding all grain-sizes up to medium silts at the same rate. This finding may have important implications with regard to spatial patterns of erodibility on continental shelves as sediments are sandier in the nearshore and get progressively finer-grained with increasing water depths, the result of a decrease in the magnitude of sediment redistributive forces (Law et al., 2008). Therefore, spatial and temporal measurement of seabed properties and erodibility are necessary to improve current continental shelf sediment transport models.

### *3.2.3 Waipaoa Sedimentary System*

The Waipaoa Sedimentary System is situated on the tectonically active boundary, where the Pacific plate is being subducted obliquely beneath the Raukumara Peninsula of northeastern New Zealand resulting in a maximum uplift of  $3 \text{ mm y}^{-1}$  in the Waipaoa upper catchment (Reyners and McGinty, 1999). The  $2205 \text{ km}^2$  Waipaoa catchment is dominantly comprised of highly erodible sandstones, argillites, mudstones, marls, and limestone. Removal of indigenous vegetation following Maori and European colonization led to a six-fold increase in catchment erosion in comparison to the pre-human occupation period (Page et al., 1994, 2004; Wilmhurst, 1997; Wilmhurst et al., 1997; Eden and Page, 1998; Tate et al., 2000) with modern sediment yields in its upper catchment among the highest recorded on Earth (Walling and Webb, 1996). Extensive gully erosion, earthflows, and shallow landslides in the upper reaches result in a high

annual sediment load of  $15 \text{ Mt y}^{-1}$ , but up to  $40 \text{ Mt}$  might be delivered during 1-in-100 year flood (e.g., Hicks et al., 2004).

The continental shelf extends  $\sim 20 \text{ km}$  seaward of Poverty Bay and the mouth of the Waipaoa River (Figure 3-1). Tectonic activity has created a subsiding ( $2 \text{ mm y}^{-1}$ ) mid-shelf synclinal-basin and adjacent growing Lachlan and Ariel anticlines indicative of ongoing tectonic deformation of the margin (Foster and Carter, 1997; Gerber et al., 2005). Previous research has provided insight into sediment accumulation and deposition on the shelf (Orpin et al., 2006; Rose and Kuehl, 2010; Miller and Kuehl, 2010) and adjacent slope (Walsh et al., 2007; Alexander et al., 2010). Holocene sediment accumulation is most prominent in three shelf regions: the northern mid-shelf, the southern mid-shelf, and the outer shelf lobe (Orpin et al., 2006; Miller and Kuehl, 2010), with sediments ranging from sandy-silts to clayey-silts (Wood, 2006). A comparison of short-lived (i.e.,  $^7\text{Be}$ ) (Rose and Kuehl, 2010) to long-lived radionuclide inventory patterns (i.e.,  $^{210}\text{Pb}$ ) (Miller and Kuehl, 2010) suggests that regions of millennial-scale sediment deposition and decadal accumulation are similar. Calculation of a modern (100 y) sediment budget for the Waipaoa River margin shows that only 18-30 % of the  $15 \text{ Mt}$  of sediment discharged from the Waipaoa River accumulates on the shelf annually (Miller and Kuehl, 2010), with 11-15 % accumulating on the upper continental slope and mid-slope plateau (Alexander et al., 2010) and filling local areas of the shelf break (Walsh et al., 2007). The remaining 55-71 % of the modern sediment discharge is unaccounted for, suggesting efficient transport and widespread sediment deposition (Alexander et al., 2010). This is not surprising considering the narrow shelf area, minimal mid-shelf accommodation space, high sediment washload supplied to the margin, and the energetic coastal ocean.

### **3.3 Materials and Methods**

### *3.3.1 Sampling Collection and Analysis*

Samples were collected on four cruises over a 13-month period (January 2010, May 2010, September 2010, and February 2011) to capture events and seasonal changes in riverine and oceanic conditions. Short sediment cores (generally <50 cm) were collected using an Ocean Instruments MC-800 multi-core which obtains up to eight individual cores simultaneously. After collection, cores were visually inspected to make sure they were not significantly disturbed. Slabs from one or more of the eight cores were analyzed by X-radiography using a Varian Paxscan 4030E flat panel imaging system and an Ecotron EPX-F2800 portable X-ray generator. Other cores were sub-sampled for analysis of radionuclides and physical sediment properties. At selected sites two cores with level surfaces and no large burrows were saved for erodibility analysis.

This study assesses erodibility variation through space and time on the Waipaoa River margin. Such interpretation may be complicated by sample collection, preparation, and analysis, including error associated with reoccupation of time-series sampling sites, and variability over small spatial scales. Sediment erodibility measurements were made shipboard with a Gust Microcosm device (Gust and Muller, 1997; Dickhudt et al., 2011) within a few hours after collection to minimize effects of sediment consolidation. The experimental setup (Figure 3-2) and analysis procedure was identical to Dickhudt et al. (2009), where cores were subjected to discrete increases in applied shear stress (0.01, 0.05, 0.1, 0.2, 0.3, 0.45, 0.6 Pa). The initial step of 0.01 Pa ran for 30 minutes served to flush out suspended material; all subsequent steps were run for a 20-minute duration. The eroded mass for each step was determined by filtering the sediment-laden effluent through a 14.2-cm-diameter pre-weighed Whitman glass-microfiber GF/F 0.7  $\mu\text{m}$  filter. Filters were dried and weighed to determine the mass of eroded sediment during each time step. After inspecting the erodibility data, it was determined that the erosion

chamber was not completely flushed until after the 0.05-Pa erosion time step. Therefore, eroded mass for the 0.01- and 0.05-Pa time steps were combined to determine a background suspended-sediment concentration (SSC), and these masses were excluded from any total eroded mass calculations.

Some disturbance during sample collection and analysis was not uncommon. Notes taken for each experiment were used to identify disturbed samples allowing the associated data to be removed. Measurement error was estimated and factored into the determination of step-wise increases in eroded mass during erodibility experiments. This error was determined by calculating the standard error in eroded mass for the 0.1-Pa time step for samples collected from the Sediment Depocenter ( $n = 19$ ). Sites from this region were chosen as they display similar values and fairly consistent sediment properties for the duration of the study. Based on this analysis, the error associated with filtering and measurement of sediment mass for individual experimental steps was determined to be 0.02 g ( $0.002 \text{ kg m}^{-2}$ ). Propagating this error over the five experiment steps (0.1, 0.2, 0.3, 0.45, and 0.6) yields an error of 0.04 g ( $0.005 \text{ kg m}^{-2}$ ) for total eroded mass calculations. After quality-control assessment, results from 93 of the 161 cores analyzed are presented herein. The majority of data for cores not used were from the first research cruise, during which technical difficulties were encountered in operating the Gust Microcosm.

During this study, replicate, repeat, and time-series cores were collected to assess variability at a single core site, associated with reoccupation of a site within a short time window, and at a site between cruises. Here we use explicit terminology to identify these cases. Replicate samples were those collected from the same site (i.e. same multi-core cast) and run simultaneously on the Gust Microcosm. Repeat samples were those that were collected on the

same research cruise but at different times from the same locality (i.e., different multi-core cast). Time-series samples were those collected at the same site but on different cruises.

For the analysis of erodibility parameters, a relationship between normalized turbidity units (NTU) and total suspended solids (TSS) was made (Dickhudt, 2008). The erosion formulation of Sanford and Maa (2001) was employed to determine specific erodibility parameters.

Sediment samples were analyzed for  $^7\text{Be}$  (477 keV) and  $^{234}\text{Th}$  (63.3 keV) using gamma spectroscopy (Giffin and Corbett, 2003). Samples were dried, homogenized, packed in a standard-geometry container and counted for approximately 24 hours on low-background, high-efficiency, high-purity Germanium detectors (BEGe-, Coaxial-, LEGe-, and Well-type) coupled to a multi-channel analyzer. Calibration of detectors was achieved using natural matrix standards (IAEA-300, 312, 314, 315), to determine the regions of interest (ROI) for specific radioisotopes. Self-adsorption corrections were made to account for compositional differences between samples using the direct transmission method, allowing for accurate calculation of  $^{234}\text{Th}$  sample activity (Cutshall et al., 1983). For the purpose of consistency, cores were counted from the surface to the depth just beyond  $^7\text{Be}$  detection. Sediment X-radiographs were interpreted to highlight potential event strata, aiding in determination of the cutoff depth for the measurement of radioisotope activities. Samples were analyzed for  $^{234}\text{Th}$  within 3 months (~3.5 half-lives) and for  $^7\text{Be}$  within 4 months (~2 half-lives) of collection. Activities were corrected for decay between sample collection and analysis.

The differentiation of total, supported, and excess  $^{234}\text{Th}$  is important when assessing sediment dynamics. Samples were recounted for supported  $^{234}\text{Th}$  after 6 months to ensure that no measureable excess  $^{234}\text{Th}$  remained. However, due to time constraints and high demand for

gamma detectors, only a limited number of samples (110 total) were recounted. For the samples that were recounted, the measured supported  $^{234}\text{Th}$  was used, but for samples that were not recounted the overall average supported  $^{234}\text{Th}$  value of  $1.63 \pm 0.05 \text{ dpm g}^{-1}$  was used.

Excess  $^{234}\text{Th}$  and  $^7\text{Be}$  inventories were calculated using the following equation:

$$I = \sum X_i (1 - \varphi_i) \rho_i (A_i) \quad (2)$$

where  $I$  represents the total inventory of the sediment core ( $\text{dpm cm}^{-2}$ );  $X_i$  is the subsection thickness (cm);  $\varphi_i$  is the porosity of the subsection (unitless);  $\rho_i$  is the sediment density ( $\text{g cm}^{-3}$ ); and  $A_i$  is the activity ( $\text{dpm g}^{-1}$ ) (Canuel et al., 1990). The salt-corrected porosity for a sample was calculated using both wet and dry sediment mass and constants for porewater density ( $1.025 \text{ g cm}^{-3}$ ), particle density ( $2.650 \text{ g cm}^{-3}$ ), and salt fraction (35 ‰). Errors associated with counting, background, and detector efficiency were propagated to determine the total error associated with each sample measured and the calculated radioisotope activities (Sommerfield et al., 1999). The combined error associated with count rate, count time, peak fit, and the area encompassing the ROI is the counting error. A sample blank was run on each detector to determine the error associated with background radioisotope activities. Lastly, errors in efficiency account for any errors associated with detector calibration.

Following the methods of Corbett et al. (2004), the dependence of excess  $^{234}\text{Th}$  inventories on salinity and water depth was removed by normalizing excess  $^{234}\text{Th}$  inventories to the water-column  $^{238}\text{U}$ -supported  $^{234}\text{Th}$  inventories. Ship-based measurements of water depth and average salinity measurements from CTD casts (when available) were used in calculations. For sites where salinity measurements were unavailable, a constant (35 ‰) was assumed. Water column supported  $^{234}\text{Th}$  ( $^{234}\text{Th}_{\text{WCS}}$ ) was then calculated using an established relationship between salinity and  $^{238}\text{U}$  in the water column (Chen et al., 1986).



New  $^7\text{Be}$  inventories ( $^7\text{Be}_{\text{new}}$ ) were calculated for May, September, and February at repeated core sites by determining the  $^7\text{Be}$  inventory lost due to decay from the previous cruise and then subtracting the residual inventory from the  $^7\text{Be}$  inventory measured during the current cruise (Canuel et al., 1990; Corbett et al., 2007). Measureable  $^7\text{Be}_{\text{new}}$  indicates recent (since the last cruise) sediment deposition. Conversely, a negative value of  $^7\text{Be}_{\text{new}}$  is suggestive of net erosion.

The  $^7\text{Be}:\text{excess } ^{234}\text{Th}$  ratio was calculated to help assess the relative influence of fluvial versus marine processes on sedimentation (Feng et al., 1999; Allison et al., 2005; Corbett et al., 2007; Dail et al., 2007). As the sediment-bound activity ratio of  $^7\text{Be}$  and  $^{234}\text{Th}$  is not assumed to be 1:1, the range of data over all cruise periods was separated into quartiles using the median values of the entire data set. Samples with ratios that fall in the lower and upper 25 % of the entire data set are likely beyond the range of measurement error and therefore probably reflect the dominant processes influencing margin sedimentation (marine versus fluvial, respectively).

Grain-size was determined via sieving for the sand fraction ( $>63 \mu\text{m}$ ) and the remaining material was measured using a Micrometrics Sedigraph 5100 (Jones et al., 1988; Coakley and Syvitski 1991). The amount of sample analyzed was dependent on the sand content; coarser sediments required a greater amount of sample to attain the desired turbidity. However, in most instances 5 to 10 g of wet sediment was analyzed. For the fine fraction, a detailed measurement of mass percentages was determined for user-defined size classes (Alexander et al., 2010). Sand, silt, and clay percentages were determined by back calculating the total dry weight of the wet sample using calculated sample porosities.

### *3.3.2 Statistical Analysis*

In an effort to have an adequate number of observations for statistical analysis and to assess gross statistical variability of seabed measurements, data were grouped by shelf location

and are referred here with names based on their sampling area (i.e., Poverty Bay, Poverty Mouth, the Sediment Depocenter, and Outer Shelf; Figure 3-1). The rationale for this approach is that the seabed (and thus erodibility) variability in different areas should reflect the depositional environment. Replicate measurements made were considered separate observations and were not averaged for a given site. A one-way ANOVA was used to assess statistical differences in sediment erodibility through space. Pairwise comparisons were assessed using a post-hoc Tukey's test to determine where significant differences occur. Because the number of measurements in each area changed between cruises, an ANOVA could not be used. As a result, multiple t-tests were conducted to determine significant differences between individual shelf regions through time.

### **3.4 Results**

#### *3.4.1 Data Assessment and Error Determination*

To help evaluate methodological error and erodibility variability (intra-core versus between core/area), the coefficient of variation (CV) was examined for each replicate pair. For all replicated analyses, the total eroded mass had an average CV of 13% (n=27 pairs). Not surprisingly, the CV varied between shelf regions (Figure 3-3). Poverty Bay (n=4), Poverty Mouth (n=9), and the Sediment Depocenter (n=6) experiments had similar average CVs, 14, 17, and 13%, respectively, although there was considerable variation in the CVs. In contrast, the average CV for the Outer Shelf (n=8) was lower, only 8%, and this likely reflects the error in the method as the seabed is more homogenized in this region. Repeat samples were collected in January (1/18/2010 and 1/19/2010) from Site 20 and in February (2/10/2011 and 2/14/2011) from Site 36; these had CVs of 11 and 5%, respectively (Figure 3-3). Therefore, in order to state that values are different, the magnitudes must differ by greater than ~15% (depending on area).

Also, results show that the reoccupation of sites (repeat sampling) can produce very comparable results.

#### *3.4.2 Spatial and Temporal Variability in Seabed Attributes*

Plots of total eroded mass (i.e., the sum of mass eroded for all time steps) illustrate variability over space and time on the Waipaoa shelf (Figure 3-4). For example, along the 40-m isobaths, measured differences are found within and between cruises. Over time, significant differences (p-value  $\leq 0.05$ ) in total eroded mass were calculated between January and September for the Sediment Depocenter, and May and September for Poverty Mouth. Spatially, for the complete study, post-hoc Tukey's test showed that total eroded mass was significantly different between Poverty Mouth and the Sediment Depocenter (p-value  $< 0.02$ ) and Poverty Mouth and the Outer Shelf (p-value  $< 0.01$ ). Not surprising, the erodibility of the Waipaoa shelf seabed exhibits quantifiable differences in response to sedimentation dynamics, but the similarity of the majority of measurements was as remarkable (Figure 3-5).

In a graph of the complete dataset, sites of low, medium, and high erodibility are discernible, and these were qualitatively defined based on clustering of total eroded mass (Figure 3-5). For the Waipaoa shelf, low erodibility was defined as total eroded masses less than  $0.4 \text{ kg m}^{-2}$ , medium erodibility as total eroded masses between  $0.4$  and  $0.9 \text{ kg m}^{-2}$ , and high erodibility as total eroded masses greater than  $0.9 \text{ kg m}^{-2}$  (Figure 3-5). Most samples were classified as having low (63%) or medium (30 %) erodibility.

The sedimentological and radionuclide data collected as part of this study may be related to and help inform the variation in erodibility. They are presented here for this purpose, but a more detailed understanding of sedimentation during this period is described in the preceding chapter. X-radiographs for sites of "low erodibility" indicate that the seabed surface at the majority of these sites is overprinted by bioturbation (e.g., C4-30; Figure 3-6). Examination of

the entire low erodibility data set showed that surface grain-size and down-core  $^7\text{Be}$  activities were variable; sand content ranged from 1.3 to 67.8 % and clay content varied from 19.0 to 50.7 %. Many cores exhibit low  $^7\text{Be}$  activities down-core, and excess  $^{234}\text{Th}$  profiles (not presented) generally decrease logarithmically with depth, consistent with sediment mixing by organisms (e.g., Bentley and Nittrouer, 2003; Wheatcroft, 2006).

Sites characterized as having a “medium erodibility” were derived from two distinctive types of cores, “non-fluid mud” and “fluid mud”. X-radiographs of non-fluid-mud sites (e.g., C4-18 and C2-14; Figure 3-6) display laminated sediments with variable bioturbation intensity (relatively well stratified to totally mottled) and surface grain-size distributions. The ranges for sand (1.6 – 69.2 %) and clay (9.6 - 43.5 %) percent at these sites were relatively large. “Fluid mud” sites (e.g., C2-4; Figure 3-6) exhibited finely laminated mud in X-radiographs, with low surface (0-1 cm depth) wet-bulk densities, ranging from 1.15 to 1.31 g cm<sup>-3</sup>. These sites had low surface sand (<1 %) and high surface clay contents (49 – 67 %). The recent emplacement of these layers is indicated by high  $^7\text{Be}$  inventories.

X-radiographs taken from cores categorized as “highly erodible” were dominated by stratified sands (e.g., C2-8, Figure 3-6). Grain-size data for the surface seabed (0-1 cm) showed that these sites had high sand and low clay content, >70 % and ~10 %, respectively. Low calculated  $^7\text{Be}$  inventories, generally below detection level of analytical equipment, were likely the result of the absence of fine-grained sediment which is more effective at scavenging radioisotopes (Olsen et al., 1986).

## **3.5 Discussion**

### *3.5.1 Controls on Sediment Erodibility*

Notable spatial and temporal variation in sediment erodibility was observed on the Waipaoa shelf. More specifically, sediment erodibility in Poverty Mouth was significantly

higher than deeper shelf regions (based on a one-way ANOVA). Over time, both Poverty Mouth and the Sediment Depocenter showed significant variation (based on Tukey's test) in erodibility. The controls responsible for these differences and changes in erodibility are better understood by looking at the measurements of seabed properties and pre-sampling fluvial and oceanographic conditions (see Chapter 2).

Interestingly, the surface (0-1 cm) clay content for Poverty Mouth was significantly lower than both the Sediment Depocenter (p-value <0.01) and the Outer Shelf (p-value = 0.05) (see Chapter 2), and the opposite was true for total eroded mass. This suggests that changes in the grain-size distribution of the seabed surface influenced the erodibility in this area over the period of observation. Differences in surface grain-size between shelf regions may be introduced in two ways: 1) as the result of new deposition which is dependent on sediment supply and the magnitude of transport mechanisms, or 2) the interplay of physical versus biological processes on sedimentation in these regions. Fine-grained ephemeral sediment deposits were identified in Poverty Mouth and closely resembled those of the Sediment Depocenter and Outer Shelf in terms of clay content (see Chapter 2). However, for the majority of this study, Poverty Mouth sites were coarser-grained at the surface with stratified layers down-core. Such sedimentary characteristics suggest that physical reworking of sediments rather than rapid, episodic deposition is more likely in this region. The significant differences in both clay content and erodibility between regions are likely the result of site depositional history, which is driven by physical and biological processes.

Previous work categorized Waipaoa shelf sedimentary facies through identification of primary sedimentary structures and the amount of biological reworking inferred from X-radiography (Miller and Kuehl, 2010; Rose and Kuehl, 2010). Three facies are described with

gradational boundaries, extending in a radial pattern seaward, with the influence of physical processes on the sedimentary strata decreasing with increasing water depth. The Poverty Mouth region is dominated by “interbedded laminated muds and sands”, whereas the Sediment Depocenter and the Outer Shelf areas are characterized by “mixed layers and mottles” and “mottled muds”, respectively. Rose and Kuehl (2010) hypothesize that the creation of these different facies is a function of wave energy and biological sediment reworking, both of which ultimately influence sedimentation and surface seabed character. Interestingly, the highest total eroded masses recorded during this study were in Poverty Bay and Poverty Mouth at sites having relatively low clay percentages. Grain-size data from Wood (2006) in Carter et al. (2010) clearly illustrates how the Sediment Depocenter and the Outer Shelf are more mud-rich than Poverty Mouth. Both laboratory (e.g., Panagiotopoulos et al., 1997) and field studies (e.g., Law et al., 2008) have shown that low percentages of clay can cause a bed to act in a non-cohesive manner leading to more pronounced erosion and winnowing of the fine-fraction of a sandy bed. A similar impact is suggested here, although no statistically significant correlation was found between surface clay percent and total eroded mass (data not shown).

Temporal variation in sediment erodibility is not uncommon and has been observed in the York River estuary, VA (Dickhudt et al., 2009), the western margin of the Adriatic Sea (Stevens et al., 2007), and the Tamar Estuary, SW England (Bale et al., 2006). Figure 3-4 illustrates how erodibility was variable in the Poverty Mouth and the Sediment Depocenter, areas where the deposition of sediment appears to be punctuated and related to fluvial and oceanographic conditions. More specifically, significant differences (p-values <0.05) in erodibility were observed in Poverty Mouth between May and September and the Sediment Depocenter between January and September. The total sediment discharged by the Waipaoa River prior to January

(C1), May (C2), and February (C4) was similar. However, major wave events (>3.5 m) punctuated the period prior to May and February (see Chapter 2). The period of time prior to the September cruise was unique and saw a higher than average river discharge, sediment discharge, wave height, and precipitation in comparison to other pre-cruise periods (see Chapter 2). Therefore the high erodibility observed in September in Poverty Mouth and the Sediment Depocenter may result from the large amount of Waipaoa sediment discharge before sample collection. Differences in clay content and  $^7\text{Be}$  inventories (indicative of sediment deposition) support this assertion (see Chapter 2).

### 3.5.2 *Influence of Depositional History on Sediment Erodibility*

Sediment deposition, erosion, and other post-depositional processes (e.g., bioturbation and compaction) influence the character of the seabed, potentially altering sediment bulk density, grain-size distribution, organic content, and seabed erodibility. As a result, investigation of sedimentation changes (as noted above) may help understand seabed strength. By evaluating the net change in  $^7\text{Be}$  inventory at a site with time, deposition (+) or erosion (-) may be inferred (e.g., Giffin and Corbett, 2003). With this in mind, radionuclide data were categorized in this manner, and for each category total eroded masses were plotted against wet bulk density (a potentially related parameter) to evaluate the relationship with sediment erodibility (Figure 3-7). In theory, the removal of surficial sediment by erosion will expose underlying sediment that is more consolidated and less erodible, whereas addition of material may result in a temporarily more erodible seabed (Jepsen et al., 1997; Roberts et al., 1998). However, no clear relationships between total eroded mass and sediment deposition were observed (Figure 3-7), with the exception of the fact that sites with  $^7\text{Be}$ -rich fluid muds on the seabed (characterized by extremely high water content and low bulk density) had total eroded masses  $>0.5 \text{ kg m}^{-2}$  (Figure 3-7) and were more easily eroded than sites classified as having “low erodibilities”. Similarly,

fluid muds of Hamilton Harbour, Ontario were characterized by low wet bulk densities and more easy to erode in comparison to sediments with higher wet bulk densities (Amos et al., 2004).

From the time-series core observations, a great amount of variability was captured, but for brevity, three examples are presented here (Figures 3-8 to 3-10). At Site 30, X-radiographs and down-core radioisotope profiles indicate sediment deposition in January (C1, ~3 cm), May (C2, ~1 cm), and September (C3, ~3 cm) (Figure 3-8). Over the sampling periods, the character of the seabed remain relatively unchanged, with only a small range in clay and sand content measured, 14.0 % and 4.7 %, respectively. Surface excess  $^{234}\text{Th}$  activities co-varied with total eroded mass suggesting that sediment erodibility may be dependent on the recency of sediment deposition. Wave and Waipaoa River discharge recorded for the 13-month observation period support this assertion (see Chapter 2). Sediments were most erodible in May (C2) followed by September (C3) and January (C1) (Figure 3-8). Sediment erodibility was fairly similar for the May and September periods. These two periods were characterized by both more recent and multiple sediment discharge and wave events in comparison to the January pre-sampling period, providing new and reactivating old material for transport. These findings are similar to previous work in the York River estuary, VA that showed recently deposited sediments were more erodible following seasonal high discharge (Dickhudt et al., 2009).

At Site 8, X-radiographs and down-core radioisotope profiles indicate little to no sediment deposition in May 2010 (C2) but about 6 cm of new deposition by February 2011 (C4) (Figure 3-9). Surface sand and clay content was drastically different for the two sampling periods, and sediment porosity was much higher in February (Figure 3-9). Interestingly, sediments at Site 8 were dramatically more erodible in May 2010 (when sand dominated) in comparison to February 2011, with total eroded mass values of  $3.20 \text{ kg m}^{-2}$  and  $0.240 \text{ kg m}^{-2}$ ,



respectively. This example clearly demonstrates how new deposition can significantly change the physical character of the seabed and in doing so alter the erodibility of a site over time.

Additionally, the enhanced erodibility of a non-cohesive bed is evident.

On the outer shelf, Site 35 has similar total eroded masses for September 2010 (C3) and February 2011 (C4),  $0.26 \text{ kg m}^{-2}$  and  $0.19 \text{ kg m}^{-2}$ , respectively. X-radiographs and down-core radioisotope profiles indicate ~2 cm of new sediment deposition in September, but bioturbation of this layer prior to February sampling (Figure 3-10). Interestingly, there is little change in clay and sand content or porosity, and differences in surface grain-size distribution between September and February are minimal (Figure 3-10). These results suggest that in this case on the outer shelf, sediment deposition and mixing lead to little change in sediment erodibility. Previous erodibility studies suggest the movement of organisms within (e.g., Sgro et al., 2005) and on top (e.g., Moore, 2006) of cohesive beds increases sediment erodibility. However, based on Site 35, little change from bioturbation results, and the fundamental bed characteristics control the erodibility.

These three examples help illustrate that measured erodibility changes may be real and related to complex sedimentary processes. Unfortunately, processes may have subtle or insignificant effects (e.g., in the case of bioturbation on the outer shelf) or prominent and unmistakable impacts, such as from new deposition (e.g., at Site 8; Figure 1). Statistical analyses of multiple measurements are important to defining the variability.

### *3.5.3 Erodibility Measurements in the Context of Previous Work*

The Waipaoa shelf, York River, Baltimore Harbor, and the upper Chesapeake Bay exhibit similar trends in  $\tau_c$  vs.  $m$  profiles (Figure 3-11). However, most of the Waipaoa data are lower than previous measurements. The few erodibility measurements taken in Baltimore Harbor (Sanford and Maa, 2001) and the Upper Chesapeake Bay (Sandford, 2006) are in

agreement with “low” erodibility measurements for the York River (Dickhudt et al., 2009). It is important to note that these other studies did not measure erodibility over large spatial scales, with measurements made at only a few sites. Data for this study are plotted by each shelf region to facilitate spatial comparison (Figure 3-11 C and D) and thus these profiles of  $\tau_c$  vs.  $m$  give insight into both erodibility variation within and between regions (Table 3-1). Measurements from the Sediment Depocenter and the Outer Shelf all fall in the same region of the graph, whereas Poverty Bay and Poverty Mouth showed the potential to be higher but with greater variability. Interestingly, a marked change in the trend of most  $\tau_c$  vs.  $m$  profiles is observed at applied shear stresses greater than 0.45 Pa (Figure 3-11), and this is especially true for measurements from Poverty Bay and Poverty Mouth. Unlike the data presented by Dickhudt et al. (2009), most data are concentrated in a defined (fairly low) range, indicating surprisingly similar behavior across the morphologically complex and dynamic Waipaoa.

The steps of applied stress for erodibility experiments in this study were not identical to those used by Stevens et al. (2007). This coupled with the fact that erodibility was presented as the total eroded mass up to 0.32 Pa rather than 0.60 Pa of shear stress complicated the comparison of Waipaoa and western Adriatic Sea shelf datasets. In the winter, total eroded mass at 0.32 Pa ranged from 0.04 to 0.24 kg m<sup>-2</sup>, whereas in the summer values were between 0.03 to 0.15 kg m<sup>-2</sup> for the western Adriatic Sea. These values are similar to the total eroded mass at 0.3 Pa for the Waipaoa shelf dataset. In the austral summer (C1 & C4), values were between 0.07 and 0.28 kg m<sup>-2</sup>; in autumn (C2) between 0.13 and 0.58 kg m<sup>-2</sup>; in the spring between 0.12 and 0.27 kg m<sup>-2</sup>. Therefore, the western Adriatic Sea and Waipaoa shelves exhibit a similar range of sediment erodibility with the exception of the measurements in autumn.

The erosion rate constant plotted against eroded mass shows similar trends to previous work (e.g., Sanford and Maa, 2001; Figure 3-12; Table 3-2). More specifically,  $M$  increases more rapidly at low eroded mass values ( $m < 0.01 \text{ kg m}^{-2}$ ; Figure 3-12 B). This confirms that sediments at the surface are more erodible than those at depth, supporting previous research showing that the critical shear stress of sediment increases with increasing depth. Profiles of  $M$  vs.  $m$  for the Waipaoa margin are generally an order of magnitude higher than those in the York River. However, Waipaoa measurements are more similar to those of Sanford and Maa (2001) in Baltimore Harbor. Also, similar to Sanford and Maa (2001), power-law fits for the Waipaoa shelf data set overestimate  $M$  at high values of  $m$  (at  $> 1.0 \text{ kg m}^{-2}$ ) (Figure 3-12 A). Sanford and Maa (2001) have suggested that this departure may be associated with changes in sediment density, the volume fraction of sediment and/or a constant ( $\beta$ ) considered locally independent of time and depth.

After all sites were categorized as low, medium, or high, the collection of data was plotted to assess spatial patterns of erodibility variation (Figure 3-13), yielding discernible patterns. The greatest variation in sediment erodibility occurred in Poverty Bay and Poverty Mouth, with some variability in the Sediment Depocenter. Overall, there is a general trend of decreasing erodibility with increasing water depth, and the pattern of erodibility closely resembles the radial distribution of sedimentary facies (Figure 3-13). Sites with potentially high but variable erodibilities are on the inner shelf ( $< 40 \text{ m}$  water depth) which is an area dominated by interbedded muds and sands and anticipated to be strongly and often influenced by physical processes (Miller and Kuehl, 2010; Rose and Kuehl, 2010; Bever et al., 2011) (Figure 3-13). Sediments on the mid- to outer shelf are less erodible and vary little in this regard (Figure 3-13).

Furthermore, observations suggest that even with new deposition, little difference is seen from bioturbation (Figure 3-10).

#### *3.5.4 Considerations and Implications for Modeling*

The Gust microcosm is capable of generating shear stresses up to 0.6 Pa, but model simulations of wave events on the Waipaoa shelf during the period of study period suggests that bed shear stresses may exceed 3.8 Pa (J. Moriarty, personal communication). The bed shear stresses associated with wave events decrease with increasing water depth and this is important as erodibility measurements span depths from shallow (~10 m) to deep (~ 140 m) water across the margin (Figure 3-1). Modeled bed shear stresses were used to assess the differences in the magnitude during periods of both minimal and increased wave activity. Both wet and dry storms occurred during the observation period (see Chapter 2) and generated large waves with the potential to distribute sediment across the shelf. Major wave events occurred on March 7<sup>th</sup> and July 6<sup>th</sup>, 2010. The maximum modeled bed shear stresses provide an estimate during the events. The maximum modeled bed shear stresses leading up to these events (i.e., two weeks prior) were used as an estimate during a quiescent period (i.e., non-event). Modeling results showed that during non-event conditions bed shear stresses of 0.2 to 0.3 Pa are typical in Poverty Bay with values closer to 0.1 Pa for Poverty Mouth. In contrast, the Sediment Depocenter and Outer Shelf had bed shear stresses typically at or below 0.01 Pa, the flushing steps for experiments, during a non-event period, suggesting no erosion in these areas. During wave events, bed shear stresses are much higher in the Sediment Depocenter and the Outer Shelf, reaching 0.6 Pa and 0.3 Pa, respectively. However, modeled bed shear stresses in Poverty Bay and Poverty Mouth far exceed the measurement capabilities of the Gust Microcosm, and while erosion does occur in these regions the amount cannot be quantified.

The cumulative eroded mass most closely associated with modeled non-event and event bed shear stresses was used to estimate sediment erosion associated with both a quiescent and energetic sea. During typical periods of low wave energy, erosion occurs in Poverty Bay and Poverty Mouth; however during large waves sediment erosion occurs across the entire shelf, even in areas of long-term sediment accumulation (Figure 3-14 B). These observations suggest that even though there is net sediment accumulation on the mid-shelf, erosion may occur during storm events providing material for transport to the outer shelf and beyond. This finding has important implications with respect to the sediment budget for the Waipaoa shelf.

Previous research in the western Adriatic Sea was unable to relate sediment erodibility to sediment accumulation (Stevens et al., 2007). However, this study shows that during non-event conditions, which encompass the majority of the observation period, sediment is eroded from the inner shelf but not the mid- and outer shelf, with accumulation occurring in the latter (Figure 3-14 A). In contrast, during energetic waves, which occur only for a small fraction of the record, erosion occurs over the entire shelf (Figure 3-14 B). A sediment budget calculation for the Waipaoa margin suggests that as much as 30% of the total sediment discharged by the Waipaoa is retained on the shelf (Miller and Kuehl, 2010), whereas greater than 55% is unaccounted for (Alexander et al., 2010). These calculations are consistent with our interpretations of net sediment accumulation in the mid-shelf and transport of sediment through this area to more distal shelf sites.

### **3.6 Conclusions**

Spatial and temporal variation in sediment erodibility was apparent on the Waipaoa margin during this 13-month study; however, the mechanisms behind this variability are complex and difficult to isolate and complicated by small- and large-scale lithologic effects and

post-depositional alteration of the seabed. The erodibility data and insights presented in this study are valuable in advancing the understanding of sediment erodibility on continental margins, and this is important to developing accurate sediment transport models.

The most pronounced temporal changes in erodibility observed during this study occurred in Poverty Bay and Poverty Mouth. These two regions also showed some of the greatest changes in sediment properties and sediment deposition. In contrast, little variability was seen in the mid- and outer shelf regions, which are generally characterized by high mud content and moderate to intense biological sediment reworking. Generally speaking, previously identified sediment accumulation regions displayed low sediment erodibility for the majority of sampling periods.

Sites with fluid-mud deposition on the seabed had medium erodibility values, measurably above the widespread low background erodibility character for the Waipaoa shelf. Interestingly, sand-rich/clay-poor sediments showed the greatest erodibility, reflecting winnowing of fine material from the non-cohesive bed. A comparison of Waipaoa margin, York River estuary, and the Chesapeake Bay data sets show magnitudes of erodibility are in the same general range, but with most Waipaoa samples at the low end of the comparison. However, these other localities had relatively few sampling sites. The large number of sampling sites in this study is most likely responsible for the greater degree of variability in critical shear stress versus eroded mass profiles on the Waipaoa shelf.

To better evaluate the effect of consolidation on event beds, future studies should conduct rapid-response sampling after the genesis of an event layer(s) and follow up with subsequent, frequent sampling. This may help provide for a stronger link between consolidation and other margin processes (e.g., bioturbation) and observed erodibility. Laboratory studies that simulate

sediment deposition and vary time allowed for consolidation may provide another more cost efficient means of examining the relationship between sediment emplacement and erodibility.

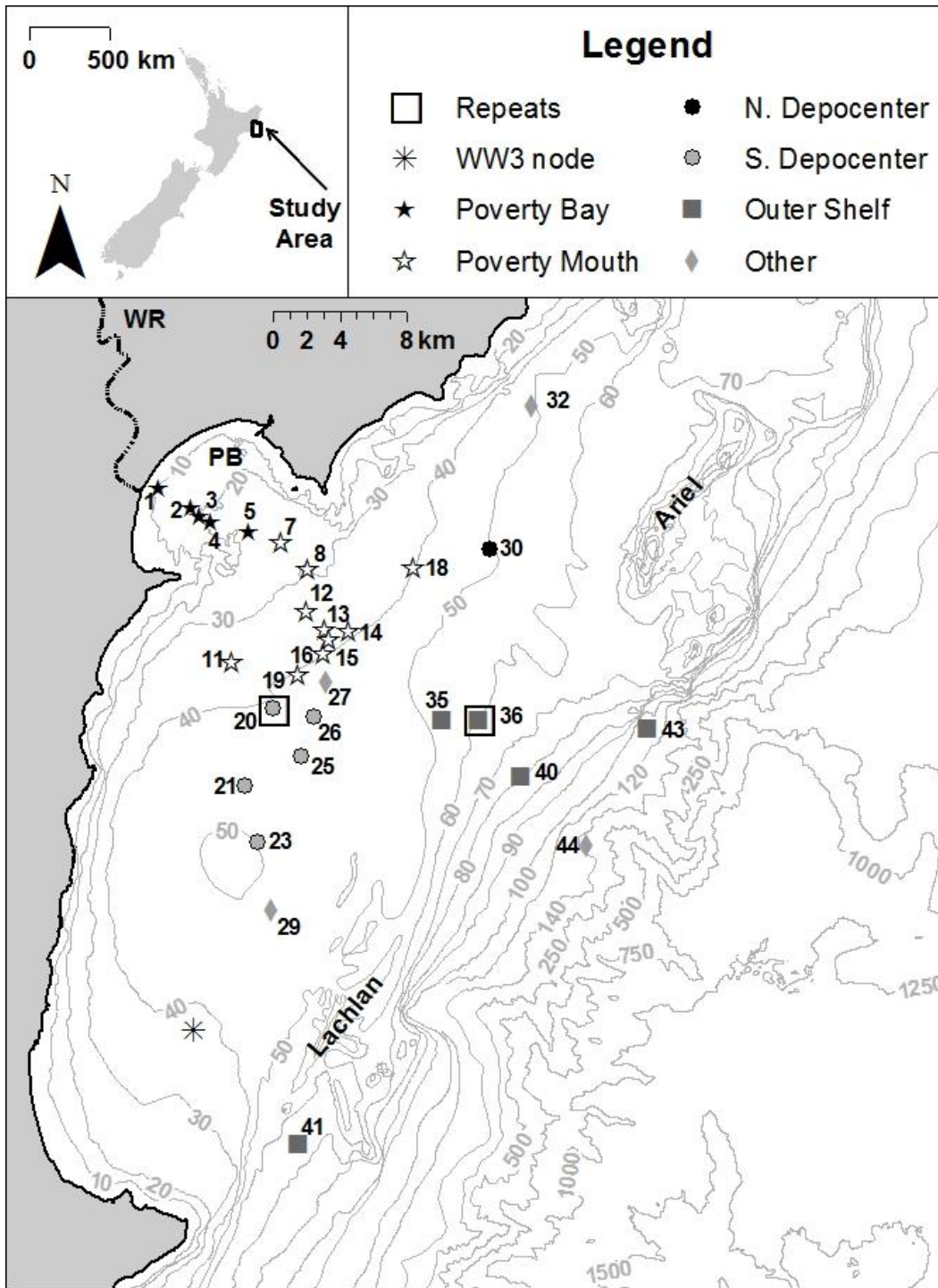


Figure 3-1 The Waipaoa shelf in relation to New Zealand. Sites where erodibility measurements were taken are partitioned based on shelf region. Ariel and Lachlan Anticlines, the Waipaoa River (WR), and Poverty Bay (PB) are referenced.



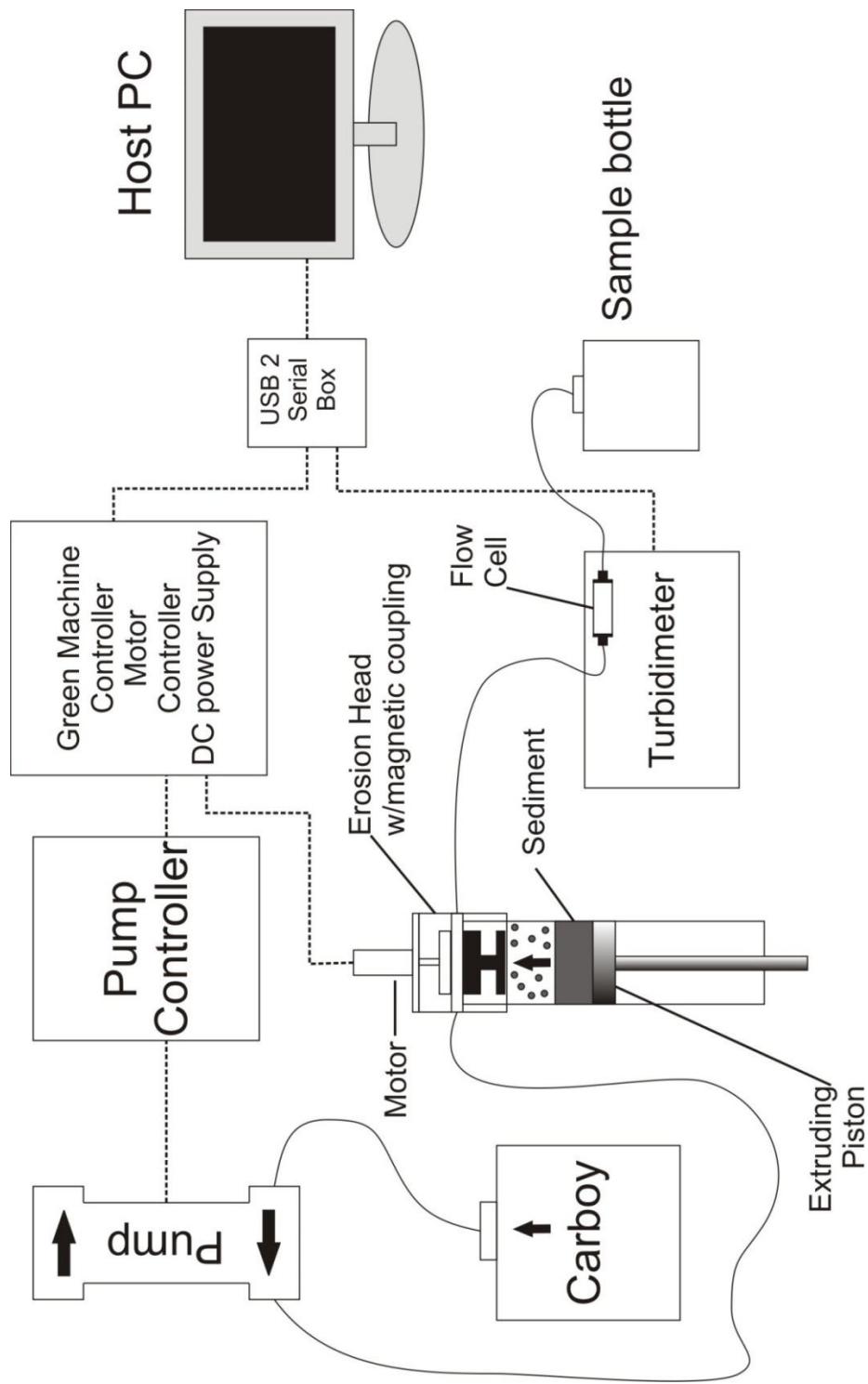


Figure 3-2 Schematic of Gust Microcosm setup (single core) showing major components involved in running an experiment. Rotation of the erosion head and the rate of water throughput dictate the applied stress on the sediment surface and as sediment passes through a flow cell turbidity is measured (modified from Green Eyes, LLC, 2010).

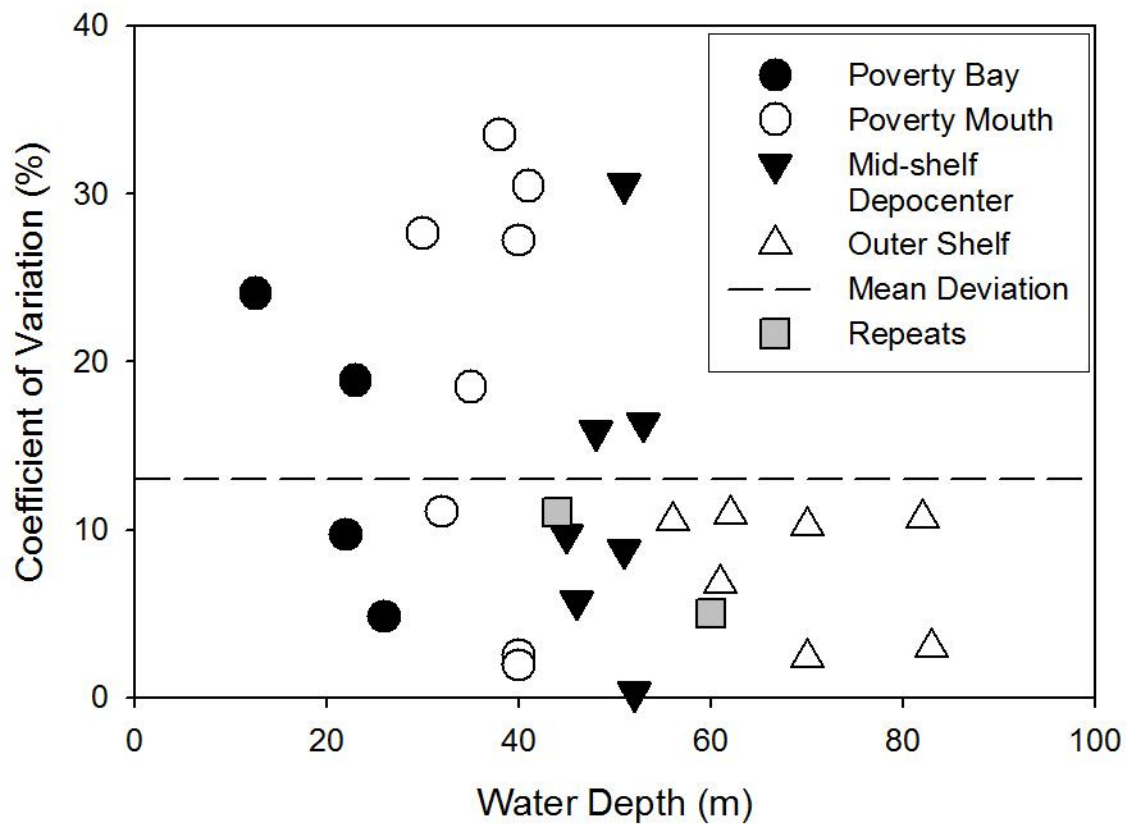


Figure 3-3 Coefficient of variation (CV) for replicate and repeat measurements of total eroded mass. The CV of replicate samples for the entire shelf is relatively low (13%), indicated by the dashed line. The largest CVs are associated with replicate samples collected in <60 m water depth. Repeat measurements taken from the Sediment Depocenter and Outer Shelf (closed gray square) had lower CVs than the overall average CV for replicate samples.

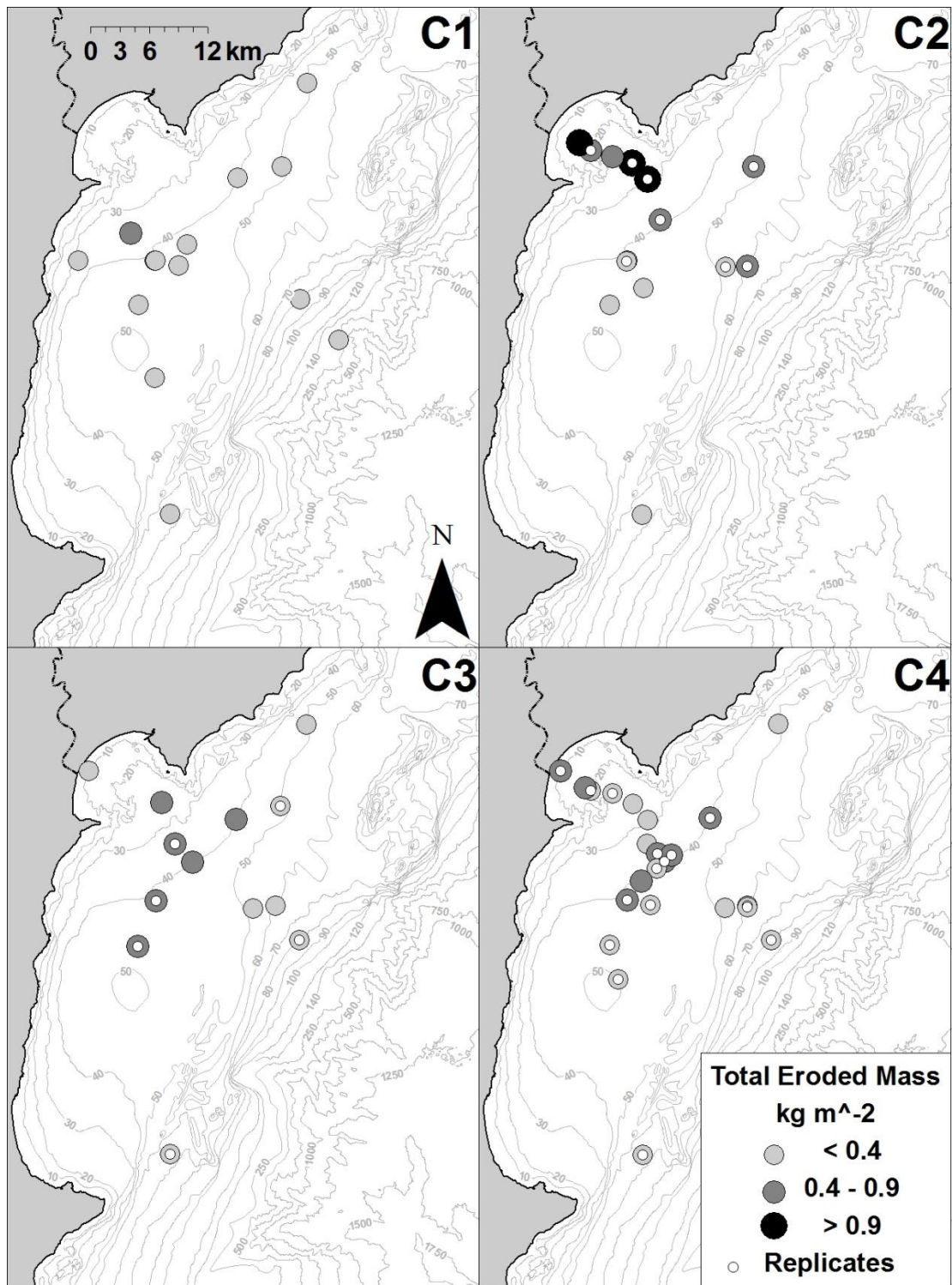


Figure 3-4 Sediment erodibility measurements taken in January 2010 (C1), May 2010 (C2), September 2010 (C3), and February 2011 (C4). The greatest temporal variability occurs seaward of 40 m water depth, in regions of ephemeral sediment deposition.

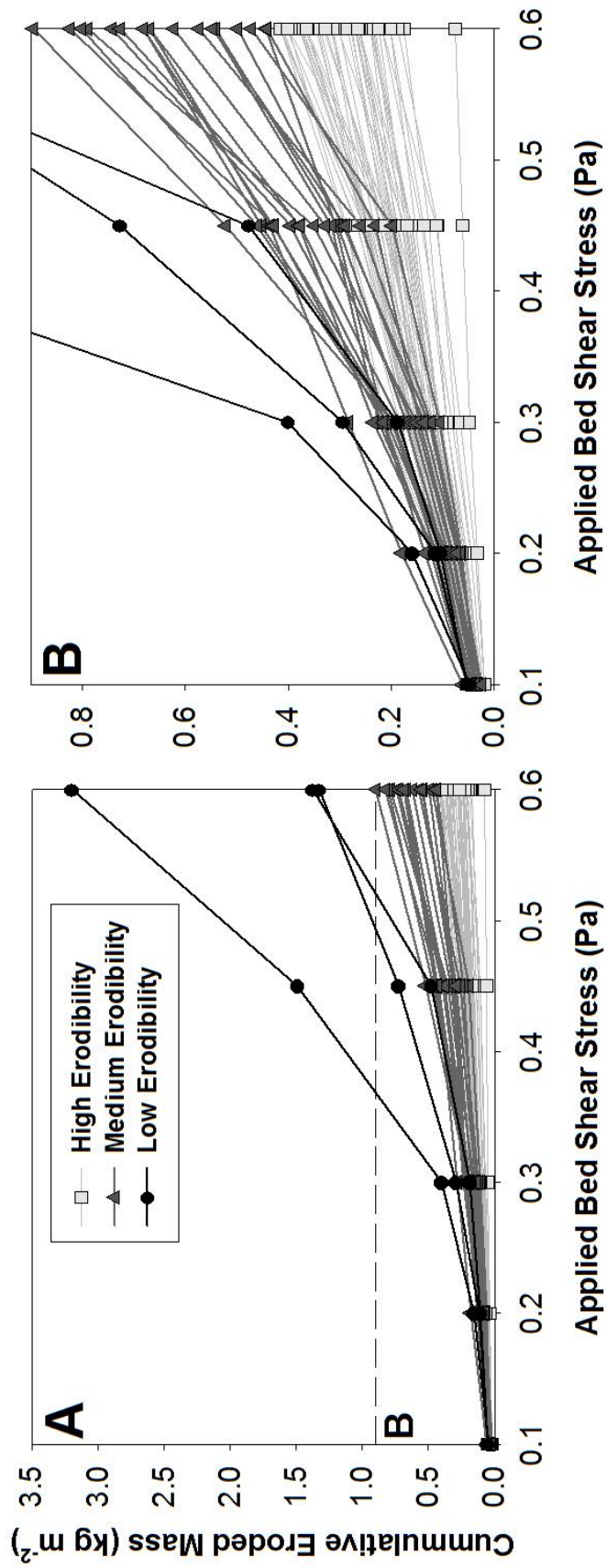


Figure 3-5 Cumulative erodibility plots for all measurements taken during the 13-month period of observation. Cutoffs were determined by clustering of total eroded mass data points (i.e., at 0.6 Pa). Plot B is an expanded view of A. Variability in profiles is seen at applied stress >0.3 Pa.

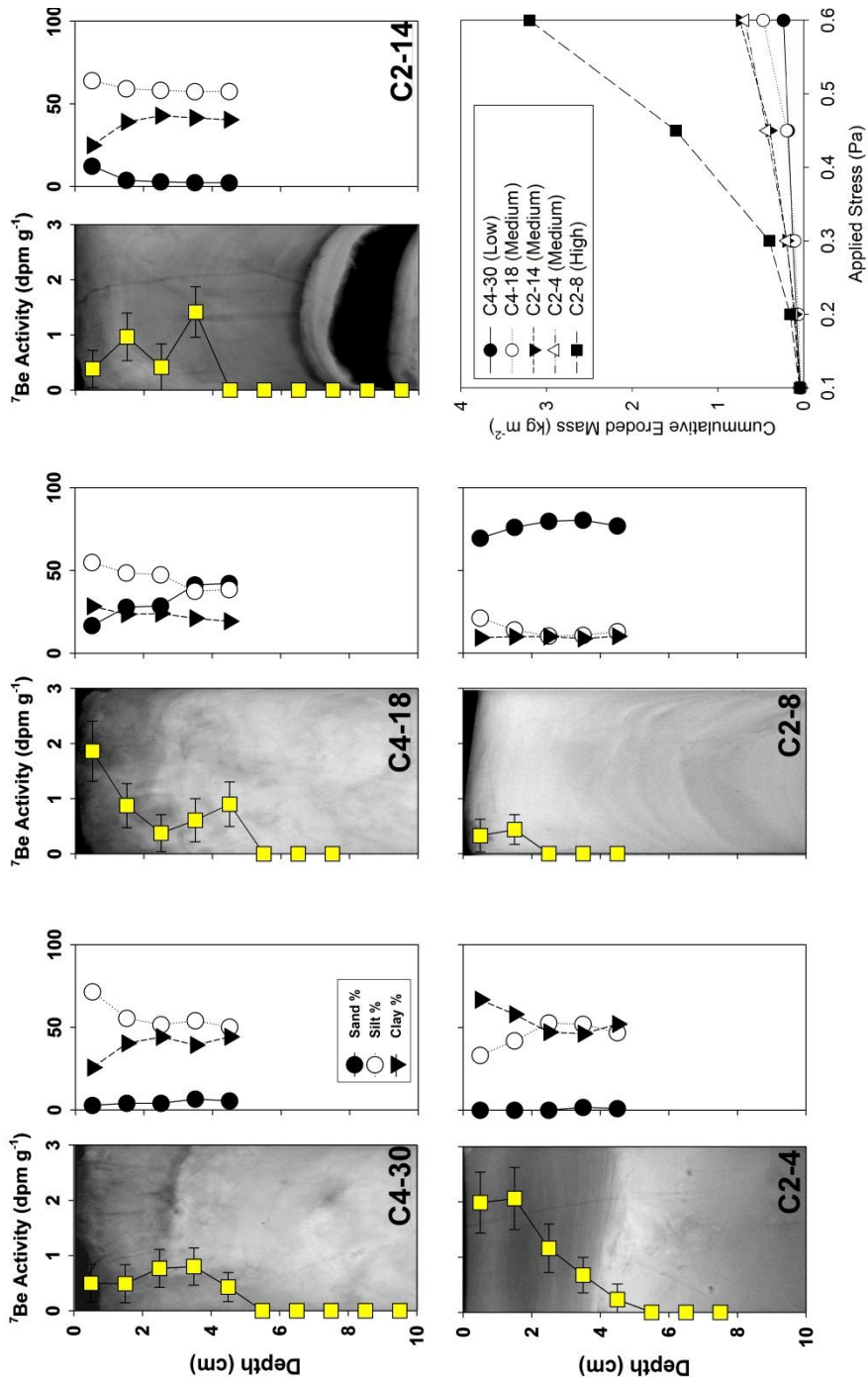


Figure 3-6 Representative examples of bed structure,  $^7\text{Be}$  and grain-size down-core profiles, and cumulative erodibility plots for low, medium, and high erodibility sediments. X-radiographs and surface grain-size measurements suggest that erodibility may be related to depositional history. However, down-core  $^7\text{Be}$  profiles are not that different in the examples presented.

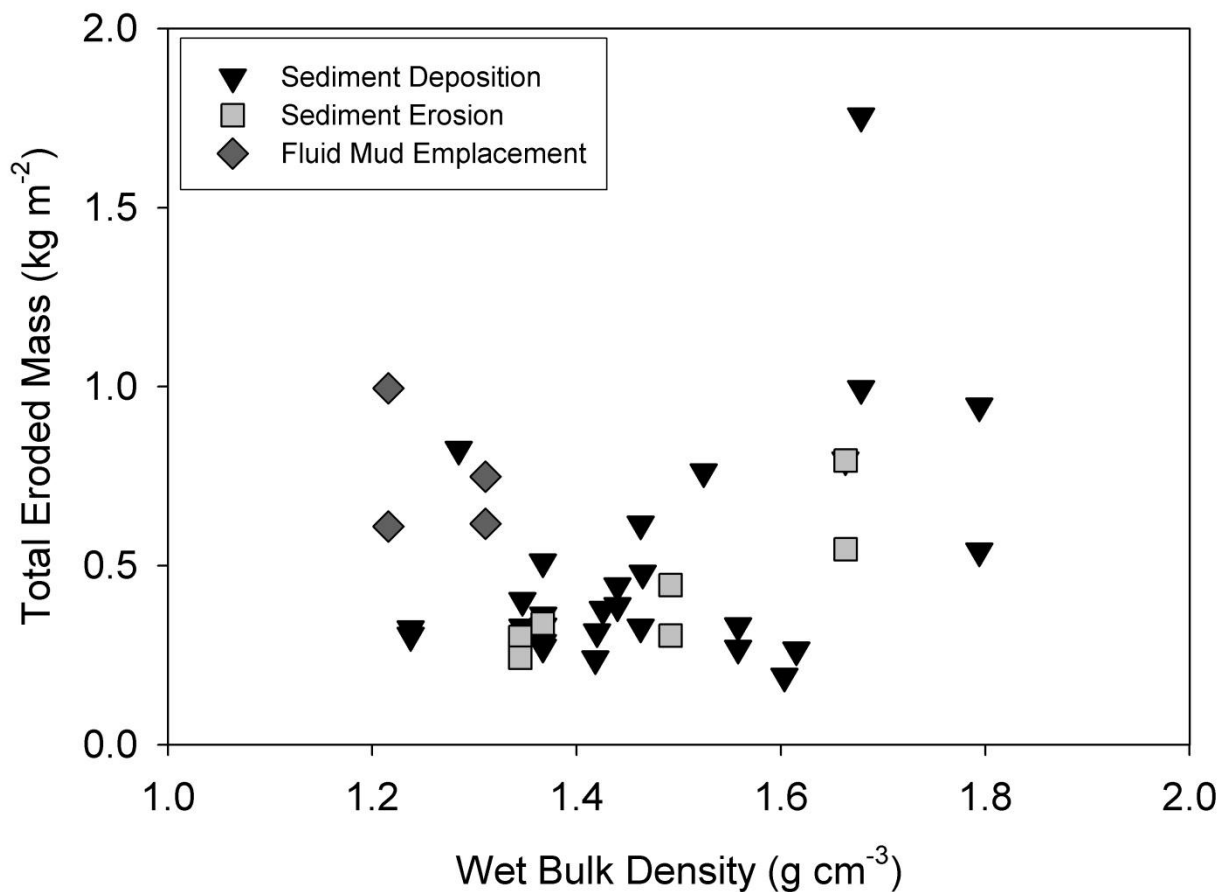


Figure 3-7 A comparison of site depositional history to sediment erodibility and measured wet bulk density. New <sup>7</sup>Be inventories were used to interpret sediment deposition and erosion (see Chapter 2). Site replicates are presented as separate observations; as a result the same site wet bulk density is plotted for each.

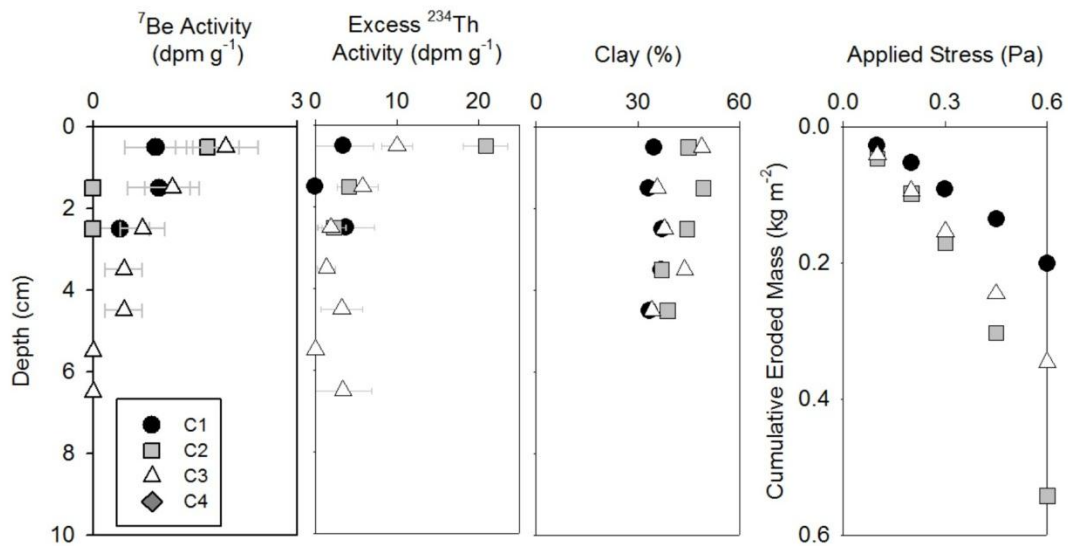
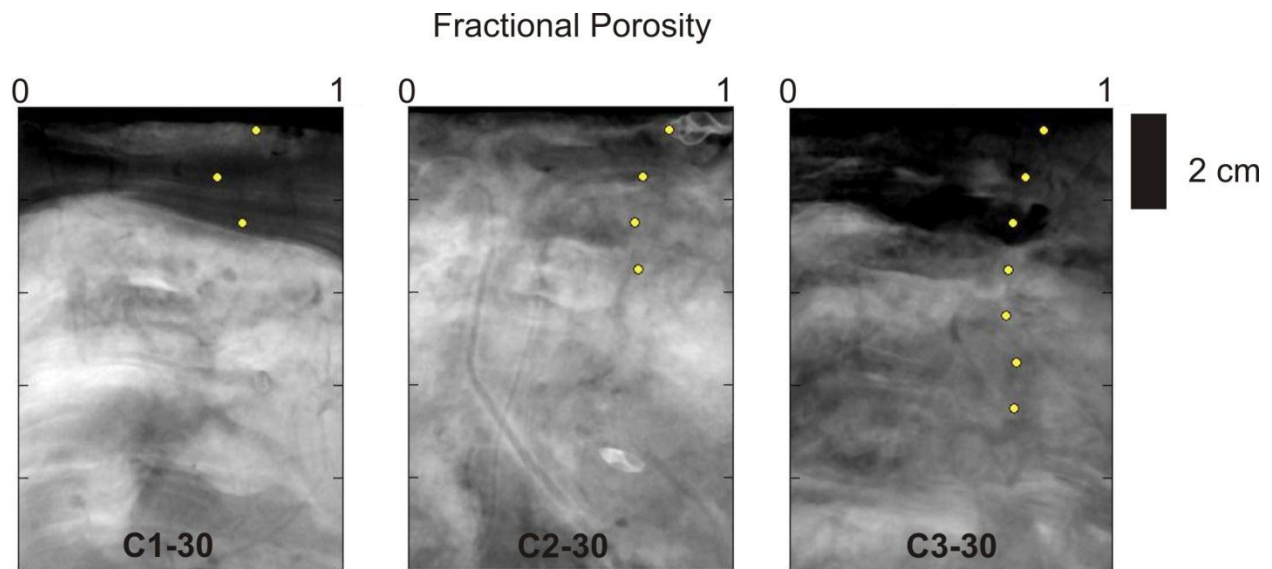


Figure 3-8 Recent depositional events are indicated by high surface  $^7\text{Be}$  and excess  $^{234}\text{Th}$  activities. Changes in erodibility through time suggest that more recently deposited sediments are more erodible. Porosity,  $^7\text{Be}$  down-core activities and grain-size are also presented.

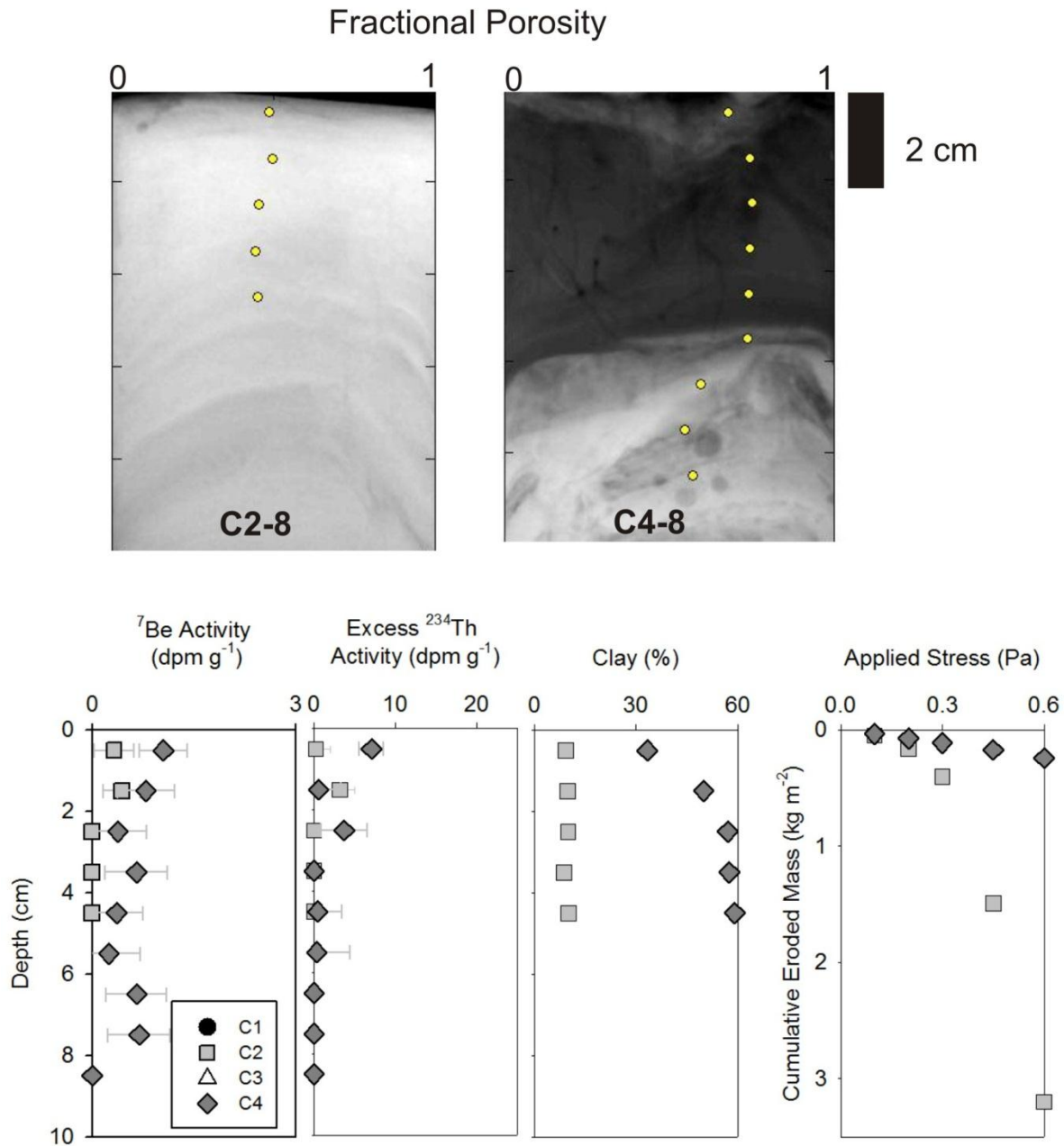


Figure 3-9 Significant changes in surface grain-size were observed from May to February at Site 8, within Poverty Mouth, with 6 cm of deposition measured in February. Porosity,  ${}^7\text{Be}$ , and excess  ${}^{234}\text{Th}$  down-core activities are also presented.



### Fractional Porosity

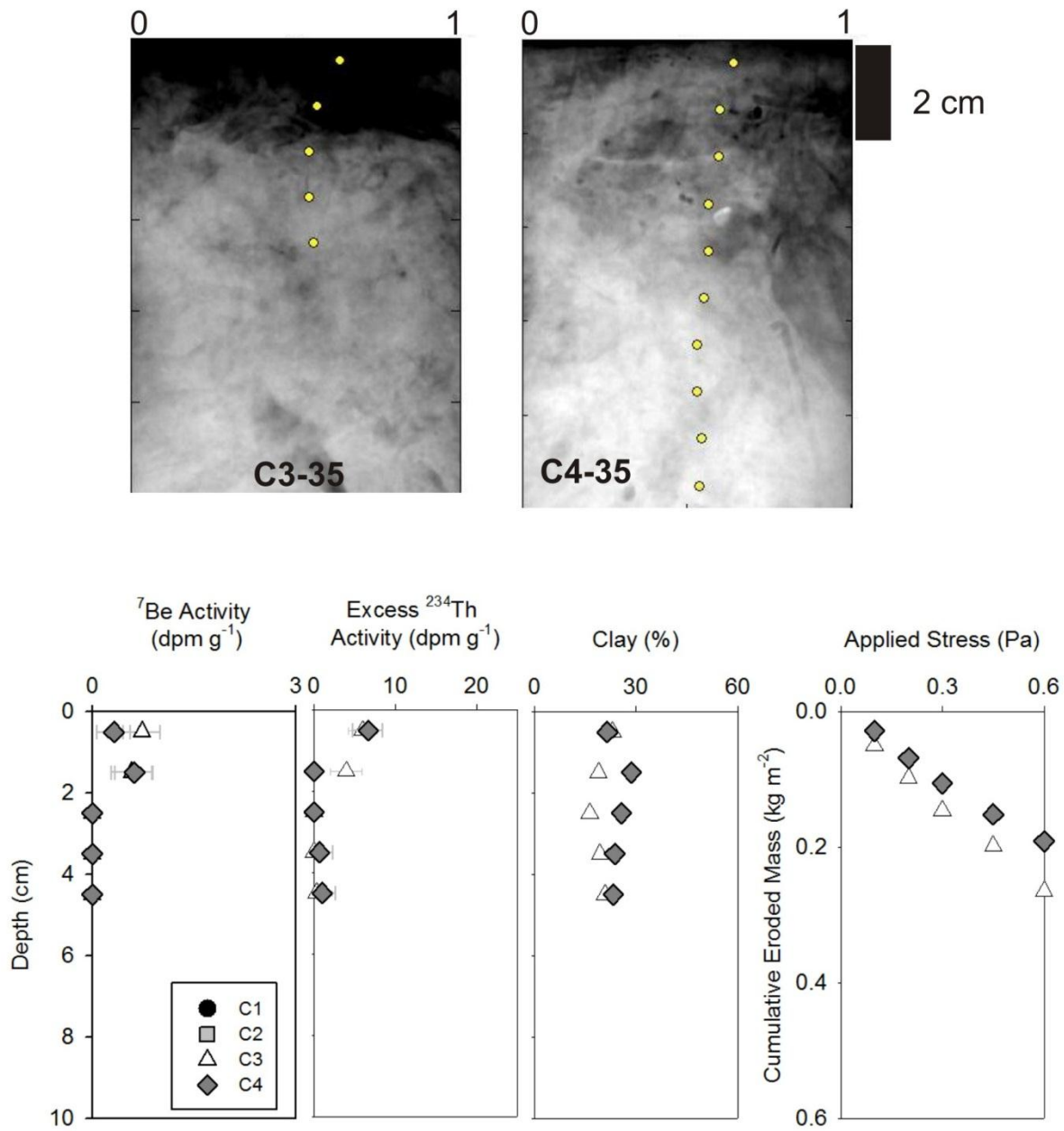


Figure 3-10 Bioturbation of a 2 cm flood layer occurs between September and February at Site 35, on the outer Waipaoa shelf. However, little change is observed in seabed erodibility. Porosity, <sup>7</sup>Be, and excess <sup>234</sup>Th down-core activities and grain-size are also presented.

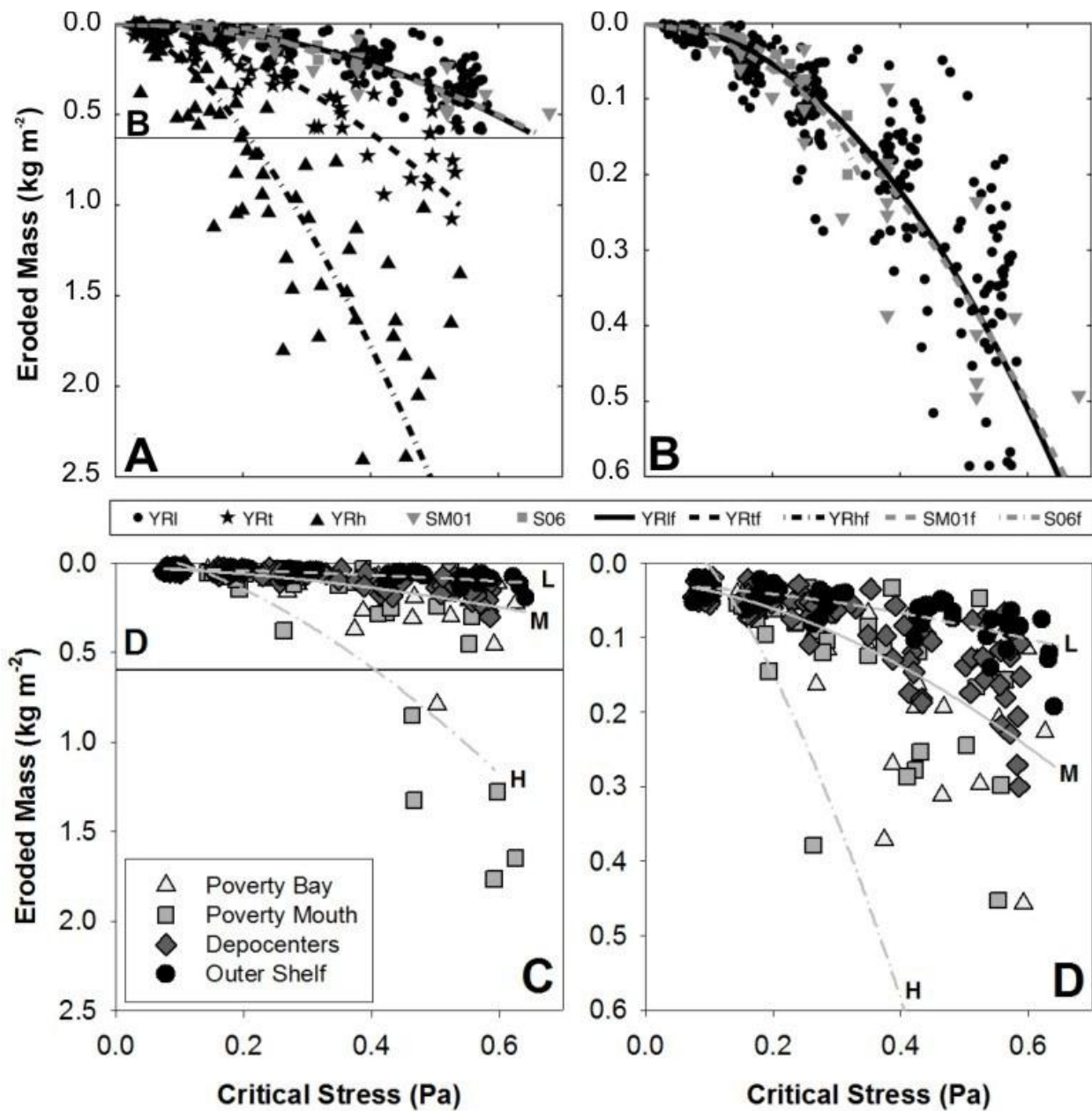


Figure 3-11 Critical shear stress ( $\tau_c$ ) vs. eroded mass ( $m$ ) profiles for previous research (A & B) in the York River, Baltimore Harbor and upper Chesapeake Bay and for the Waipaoa shelf (C & D). Plots B and D are expanded views of A and C, respectively. The two data sets display similar trends. YRI = York River low erodibility; YRt = York River transitional erodibility; YRh = York River high erodibility; SM01 = Sanford and Maa (2001); S06 = Sanford (2006); YRI<sub>f</sub> = fit to YRI; YRt<sub>f</sub> = fit to YRt; YRh<sub>f</sub> = fit to YRh; SM01<sub>f</sub> = fit to SM01; and S06<sub>f</sub> = fit to S06 (from Dickhudt et al., 2009); L = Waipaoa shelf low erodibility; M = Waipaoa shelf Medium erodibility; and H = Waipaoa shelf high erodibility.

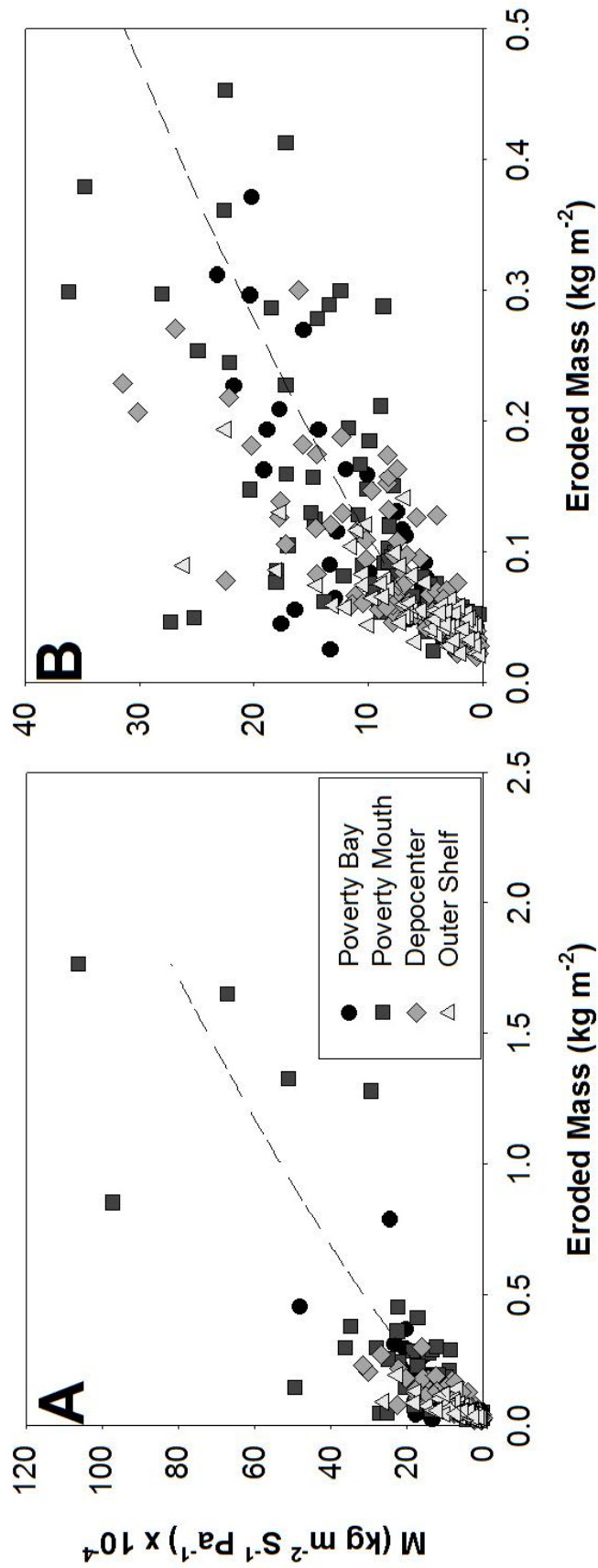


Figure 3-12 Plots of erosion rate constant ( $M$ ) vs. eroded mass (m) for the Waipaoa shelf. Plot B is an expanded view of plot A. The data are described with a power law fit to all sites (equation presented in Table 3-2). Power law fits to data from Poverty Bay, Poverty Mouth, the Sediment (Depocenter), and the Outer Shelf are also presented in Table 3-2, but not pictured here.

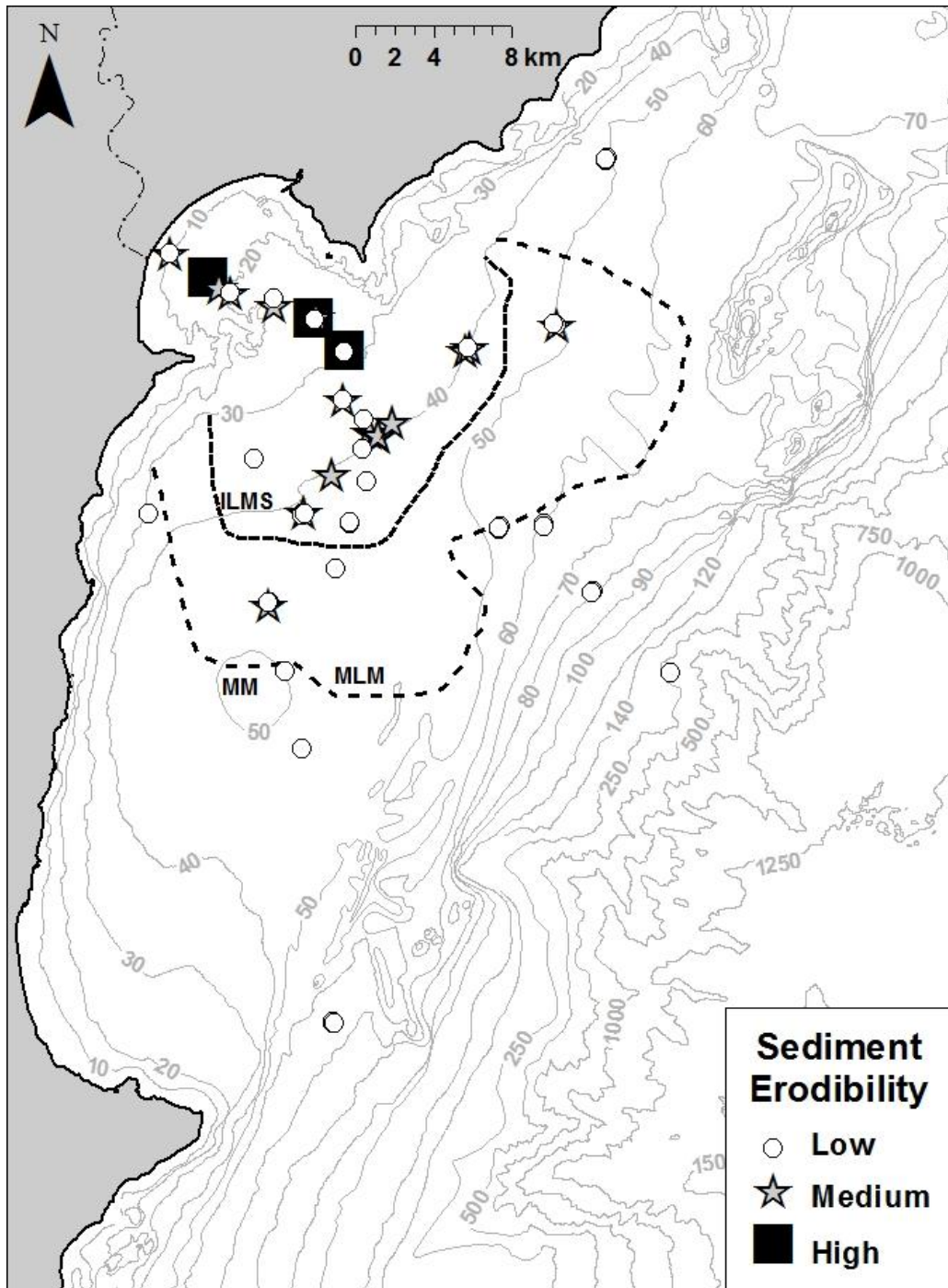


Figure 3-13 Spatial distributions of sediment erodibility for the 13-month period of observation. Gradational boundaries between sedimentary facies for the Waipaoa River margin are indicated with dotted lines, where ILMS = interbedded laminated muds and sands, MLM = mixed layers and mottles, and MM = mottled muds (from Miller and Kuehl, 2010; Rose and Kuehl, 2010).

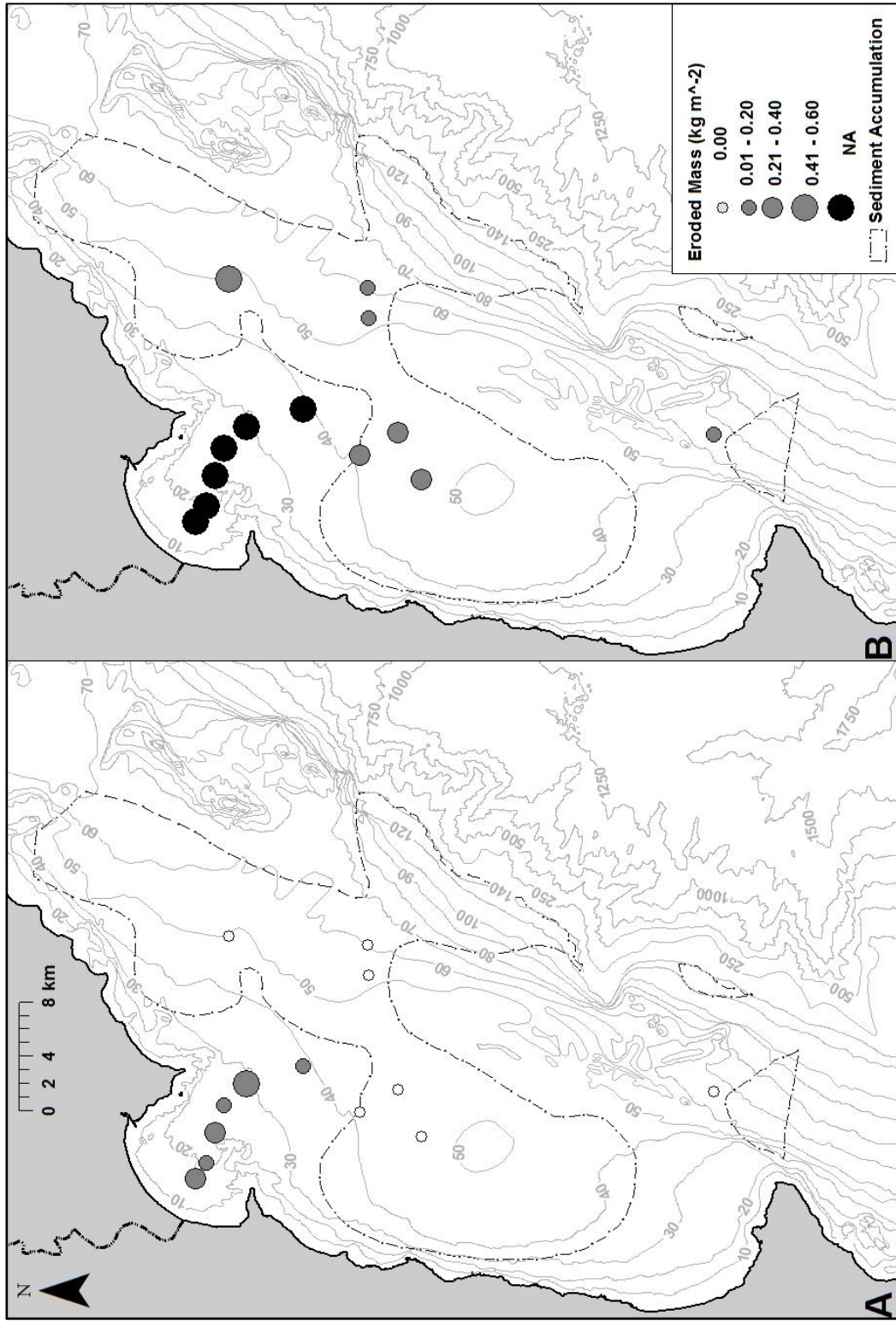


Figure 3-14 Potential sediment erodibility for non-event (A) and event (B) time periods. The eroded masses selected for each region are based on maximum measured bed shear stresses associated with model runs (J. Moriarty, personal communication). Sites deemed as NA are areas where observed bed shear stresses exceed the measurement capabilities of the Gust Microcosm.

Table 3-1 Power law fit parameters relating critical stress for erosion to eroded mass

Name	$a$	$b$	$\tau_{c0}$	$R^2$	# of samples
Sanford and Maa (2001)	0.833	0.790	0.115	0.89	6
Sanford (2006)	0.590	0.366	0.010	0.95	2
York River (low erodibility)	0.835	0.508	0.010	0.87	50
York River (transitional)	0.531	0.646	0.017	0.91	10
York River (high erodibility)	0.243	0.754	0.030	0.85	12
Waipaoa (low erodibility)	0.166	1.621	0.030	0.63	27
Waipaoa (medium erodibility)	0.523	1.684	0.027	0.71	27
Waipaoa (high erodibility)	2.827	1.604	-0.066	0.52	6

Fit was in the form  $\tau_c = am^b + \tau_{c0}$ , where  $\tau_c$ =critical shear stress for erosion (Pa),  $m$ =cumulative eroded mass ( $\text{kg m}^{-2}$ ) and  $\tau_{c0}$ =initial critical stress for erosion (Pa). For Sanford and Maa (2001), the # of samples represents erodibility measurements taken with the VIMS Sea Carousel. For the remaining data, # of samples represents the amount of individual cores eroded with a Gust erosion microcosm.

Table 3-2 Power law fit parameters relating erosion rate constant to eroded mass

Name	$a$	$b$	$R^2$	# of samples
Sanford and Maa (2001)	0.0027	0.54	0.69	4
Waipaoa (Poverty Bay)	0.0044	0.68	0.61	10
Waipaoa (Poverty Mouth)	0.0053	0.75	0.71	22
Waipaoa (Depocenter)	0.0092	1.03	0.63	20
Waipaoa (Outer Shelf)	0.0139	1.11	0.51	13
Waipaoa (All)	0.0053	0.76	0.69	65

Fit was in the form  $M = am^b$ , where  $M$ =erosion rate constant ( $\text{kg m}^{-2} \text{s}^{-1}$ ) and  $m$ =eroded mass ( $\text{kg m}^{-2}$ ).

## 4 CONCLUSIONS AND FUTURE WORK

Spatial and temporal patterns in sediment deposition and erodibility were determined via time-series sampling of the seabed. For the period of study, both sediment deposition and erodibility vary significantly through space and time.

The influences of sediment deposition on seabed character are shown to be spatially complex, especially when viewing the whole shelf. However, dividing the shelf into regions greatly simplified interpretation, showing that deposition resulted in changes to seabed character in the nearshore. Fluvial and oceanographic conditions prior to sampling were also related to the pattern of sediment deposition and therefore are partially responsible for observed variability in seabed character.

Ephemeral deposition in Poverty Bay and Poverty Mouth is related to river discharge and wave events and is responsible for grain-size variability in these regions. The high energy oceanic regime in these areas leads to the development of interbedded muds and sands on the shelf. Therefore the temporary emplacement of fine-grained flood layers introduces heterogeneity in seabed character. However, the opposite is true at more distal shelf locations. Although, deposition was punctuated through time in these regions, flood deposits have similar grain-size to the underlying seabed. Therefore, little variability in seabed character is associated with flood deposition in the mid- to outer shelf. Fluvial discharge and shelf wave events were related to depositional patterns, leading to the interpretation of different modes of sediment deposition. In summary, three proposed modes of sediment deposition indicate that waves are the dominant mechanism responsible for dispersing sediment to the mid- and outer shelf. This suggests that new sediment delivered by the Waipaoa River will be sequestered in Poverty Bay until a substantial wave event occurs (e.g., January 2010).

Patterns of sediment deposition and erodibility were also measured across the Waipaoa River margin. An attempt was made to compare spatial complexity in sediment erodibility with observed patterns of deposition. However, the spatial patterns of erodibility did not correlate well to patterns of sediment deposition. Post-depositional reworking of sediment (e.g., bioturbation) is most pronounced in deeper shelf regions and complicates the relationship between sediment deposition and erodibility. Erodiability was most variable in Poverty Bay and Poverty Mouth, where sediment deposition was ephemeral. Although, no quantitative relationship between sediment erodibility and deposition was determined, effort was made to qualitatively assess the impact of sediment deposition on seabed erodibility in this dynamic shelf setting. Erodiability was assessed at a site in Poverty Mouth displaying a drastic change in seabed character from May, 2010 to February, 2011. In May, the seabed was dominantly sand (>70 %), with little clay (~10 %), whereas in February there was deposition of a fine-grained flood layer. Erodiability measurements suggest that the fine-grained flood layer was less erodible, most likely a function of seabed cohesion. It was suspected that newly deposited sediments should be more erodible as this is what previous researchers have shown. Therefore, a site in the northern depocenter was chosen that was depositional over the course of this study. More importantly, excess  $^{234}\text{Th}$  suggests that there is a difference in how recently each flood layer was deposited in relation to sampling. Erodiability correlated well with surface  $^{234}\text{Th}$  activities suggesting that more recently deposited sedimentary layers are more erodible than those that have had longer to consolidate. The results of this study are important as they add to the erodibility literature on continental margins, which is not that extensive. This research shows the complexity associated with sediment erodibility, especially in such a dynamic system and over large spatial scales. The influence of post-depositional processes on observed patterns of sediment erodibility could be



reduced through rapid response sampling of a major sediment discharge event or with laboratory experiments that simulate sediment deposition and measure associated erodibility.

## References

- Alexander, C.R., Simoneau, A.M., 1999. Spatial variability in sedimentary processes on the Eel Continental slope. *Marine Geology* 154, 243-254.
- Alexander, C.R., Walsh, J.P., Orpin, A.R., 2010. Modern sediment dispersal and accumulation on the outer Poverty continental margin. *Marine Geology* 270, 213-226.
- Aller, R.C., Benninger, L.K., Cochran, J.K., 1980. Tracking particle-associated processes in nearshore environments by use of  $^{234}\text{Th}/^{238}\text{U}$  disequilibrium. *Earth and Planetary Science Letters* 47, 161-175.
- Aller, R.C., Cochran, J.K., 1976.  $^{234}\text{Th}/^{238}\text{U}$  disequilibrium in near-shore sediment: particle reworking and diagenetic time scales. *Earth and Planetary Science Letters* 29, 37-50.
- Allison, M.A., Sheremet, A., Gõni, M.A., Stone, G.W., 2005. Storm layer deposition on the Mississippi-Atchafalaya subaqueous delta generated by Hurricane Lili in 2002. *Continental Shelf Research* 25, 2213-2232.
- Amos, C.L., Bergamasco, A., Umgiesser, G. Cappucci, S., Cloutier, D., DeNat, L., Flindt, M., Bonardi, M., Cristante, S., 2004. The stability of tidal flats in Venice Lagoon – the results of in-situ measurements using two benthic, annular flumes. *Journal of Marine Systems* 51, 211-241.
- Andersen, T.J., Lund-Hansen, L.C., Pejrup, M., Jensen, K.T., Mouritsen, K.N., 2005. Biologically induced differences in erodibility and aggregation of subtidal and intertidal sediments: a possible cause for seasonal changes in sediment deposition. *Journal of Marine Systems* 55, 123-138.
- Bale, A.J., Stephens, J.A., Harris, C.B., 2007. Critical erosion profiles in macro-tidal estuary sediments: implications for the stability of intertidal mud and the slope of mud banks, *Continental Shelf Research* 27, 2303-2312.
- Bale, A.J., Widdows, J., Harris, C.B., Stephens, J.A., 2006. Measurements of the critical erosion threshold of surface sediments along the Tamar Estuary using a mini-annular flume. *Continental Shelf Research* 26, 1206-1216.
- Barrell, J., 1917. Rhythms and the measurement of geologic time: *Geological Society of America Bulletin* 28, 745-904.
- Bentley, S.J., Nittrouer, C.A., 2003. Emplacement, modification, and preservation of event strata on a flood-dominated continental shelf: Eel shelf, Northern California. *Continental Shelf Research* 23, 1465-1493.

- Bever, A.J., Harris, C.K., Sherwood, C.R., Signell, R.P., 2009. Deposition and flux of sediment from the Po River, Italy: An idealized and wintertime numerical modeling study. *Marine Geology* 260, 69-80.
- Bever, A.J., McNinch, J.E., Harris, C.K., 2011. Hydrodynamics and sediment-transport in the nearshore of Poverty Bay, New Zealand: Observations of nearshore sediment segregation and oceanic storms. *Continental Shelf Research* 31, 507-526.
- Bonniwell, E.C., Matisoff, G., and Whiting, P.J., 1999. Determining the times and distances of particle transit in a mountain stream using fallout radionuclides. *Geomorphology* 27, 75-92.
- Canuel, E., Martens, C., Benninger, L., 1990. Seasonal variations in Be-7 activity in the sediments of Cape Lookout Bight, North Carolina. *Geochemica et Cosmochimica Acta* 54, 237-245.
- Carter, L., Orpin, A.R., Kuehl, S.A., 2010. From mountain source to ocean sink – the passage of sediment across an active margin, Waipaoa Sedimentary System, New Zealand. *Marine Geology* 270, 1-10.
- Chen, J.H., Edwards, R.L., and Wasserburg, G.J., 1986.  $^{238}\text{U}$ ,  $^{234}\text{U}$  and  $^{232}\text{Th}$  in seawater. *Earth and Planetary Science Letters* 80, 241-251.
- Coakley, J.P., Syvitski, J.P.M., 1991. SediGraph technique In: *Principles, Methods, and Application of Particle Size Analysis* (Ed. By J.P.M. Syvitski), Cambridge University Press, Cambridge, 129-142.
- Corbett, D.R., Dail, M., McKee, B., 2007. High-frequency time-series of the dynamic sedimentation processes on the western shelf of the Mississippi River Delta. *Continental Shelf Research* 27, 1600-1615.
- Corbett, D.R., McKee, B., Duncan, D., 2004. An evaluation of mobile mud dynamics in the Mississippi River deltaic region. *Marine Geology* 209, 91-112.
- Crockett, J.S., Nittrouer, C.A., 2004. The sandy inner shelf as a repository for muddy sediment: an example from Northern California. *Continental Shelf Research* 24, 55-73.
- Cutshall, N.H., Larsen, I.L., Olsen, C.R., 1983. Direct analysis of  $^{210}\text{Pb}$  in sediment samples: self-absorption corrections. *Nuclear Instruments and Methods* 206, 309-312.
- Dail, M.B., Corbett, D.R., Walsh, J.P., 2007. Assessing the importance of tropical cyclones on continental margin sedimentation in the Mississippi delta region. *Continental Shelf Research* 27, 1857-1874.
- DeRose, R.C., Gomez, B., Marden, M., Trustrum, N.A., 1998. Gully erosion in Mangatu Forest, New Zealand, estimated from digital elevation models. *Earth Surface Processes and Landforms* 23, 1045-1053.

- Dean, W. E., 1974. Determination of carbonate and organic matter in calcareous sediments and sedimentary rocks by Loss on Ignition: comparison with other methods. *Journal of Sedimentary Petrology* 44, 242-248.
- Dickhudt, P.J., 2008. Controls on Erodibility in a Partially Mixed Estuary: York River, Virginia. M.S. thesis, Virginia Institute of Marine Science. 102 pp plus appendices.
- Dickhudt, P.J., Friedrichs, C.T., Sanford, L.P., 2011. Mud matrix solids fraction and bed erodibility in the York River estuary, USA, and other muddy environments. *Continental Shelf Research* 31, S3-S13.
- Dickhudt, P.J., Friedrichs, C.T., Schaffner, L.C., Sanford, L.P., 2009. Spatial and temporal variation in cohesive sediment erodibility in the York River estuary, eastern USA: A biologically influenced equilibrium modified by seasonal deposition. *Marine Geology* 267, 128-140.
- Eden, D.N., Page, M.J., 1998. Palaeoclimatic implications of a storm erosion record from late Holocene lake sediments, North Island, New Zealand. *Palaeogeography, Palaeoclimatology, Palaeoecology* 139, 37-58.
- Fanning, K.A., Breland, J.A., II, Byrne, H., 1982.  $^{226}\text{Ra}$  and  $^{222}\text{Rn}$  in the coastal waters of west Florida: high concentrations and atmospheric degassing. *Science* 215, 667-670.
- Feng H., Cochran, J.K., Hirschberg, D.J., 1999.  $^{234}\text{Th}$  and  $^7\text{Be}$  as tracers for the transport and dynamics of suspended particles in a partially mixed estuary. *Geochimica et Cosmochimica Acta* 63, 2487-2505.
- Fernandes, S., Sobral, P., Costa, M.H., 2006. *Nereis diversicolor* effect on the stability of cohesive intertidal sediments. *Aquatic Ecology* 40, 567-579.
- Foster, G., Carter, L., 1997. Mud sedimentation on the continental shelf at an accretionary margin – Poverty Bay, New Zealand. *New Zealand Journal of Geophysics* 40, 157-173.
- Friedrichs, C.T., Scully, M.E., 2007. Modeling deposition by wave-supported gravity flows on the Po River prodelta: From seasonal floods to prograding clinoforms. *Continental Shelf Research* 27, 322-337.
- Friend, P.L., Ciavola, P., Cappucci, S., Santos, R., 2003. Bio-dependent bed parameters as a proxy tool for sediment stability in mixed habitat intertidal areas. *Continental Shelf Research* 23, 1899-1917.
- Gage, M., Black, D., 1979. Slope-stability and geological investigations at Mangatu State Forest. New Zealand Forest Service Technical Paper No. 66, New Zealand Forest Service, Wellington, 37pp.

- Gerdol, V., Hughes, R.G., 1994. Effect of *Corophium volutator* on the abundance of benthic diatoms, bacteria and sediment stability in two estuaries in southeastern England. *Marine Ecology-Progress Series* 114, 109-115.
- Giffin, D., Corbett, D.R., 2003. Evaluation of sediment dynamics in coastal systems via short-lived radioisotopes. *Journal of Marine Systems* 42, 83-96.
- Goff, J.A., Wheatcroft, R.A., Lee, H., Drake, D.E., Swift, J.P., Fan, S. 2002. Spatial variability of shelf sediments in the STRATAFORM natural laboratory, Northern California. *Continental Shelf Research* 22, 1199-1223.
- Göni, M.A., Alleau, Y., Corbett, D.R., Walsh, J.P., Mallinson, D., Allison, M., Gordon, E.S., Petsch, S., Dellapenna, T.M., 2007. The effects of Hurricanes Katrina and Rita on the seabed of the Louisiana shelf. *Sedimentary Record* 5, 4-9.
- Grabowski, R.C., Droppo, I.G., Wharton, G., 2011. Erodibility of cohesive sediment: The importance of sediment properties. *Earth-Science Reviews* 105, 101-120.
- Green Eyes, LLC, 2010. U-GEMS Manual Version 1.1. 68 pp.
- Guillen, J., Bourrin, F., Palanques, A., Durrieu de Madron, X., Puig, P., Buscail, R., 2006. Sediment dynamics during wet and dry storm events on the Tet inner shelf (SW Gulf of Lions). *Marine Geology* 234, 129-142.
- Gust, G., Muller V., 1997. Interfacial hydrodynamics and entrainment functions of currently used erosion devices. In: N. Burt, R. Parker and J. Watts, Editors, *Cohesive Sediments*, Wallingford, UK, 149–174.
- Håkanson, L., 2006. *Suspended particulate matter in lakes, rivers and marine systems*. New Jersey: The Blackburn Press, 331 pp.
- Hicks, D. M., Gomez, B., Trustrum, N.A., 2000. Erosion thresholds and suspended sediment yields, Waipaoa River Basin, New Zealand. *Water Resource Research* 36, 1129-1142.
- Horowitz, A.Z., 1995. The use of suspended sediment and associated trace elements in water quality studies. *International Association of Hydrological Sciences Special Publication* 4, IAHS Press, Wallingford, Oxfordshire, U.K., 58 pp.
- Houwing, E.J., 1999. Determination of the critical erosion threshold of cohesive sediments on intertidal mudflats along the Dutch Wadden Sea Coast. *Estuarine, and Coastal Shelf Science* 49, 545-555.
- Jepsen, R., Roberts, J., Lick, W., 1997. Effects of bulk density on sediment erosion rates. *Water Air and Soil Pollution* 99, 21-31.

- Jones, K.E., Preston, N.J., 2012. Spatial and temporal patterns of off-slope sediment delivery for small catchments subject to shallow landslides within the Waipaoa catchment, New Zealand. *Geomorphology* 141-142, 150-159.
- Jones, K.P.N., McCave, I.N., Patel., P.D., 1988. A computer-interfaced sedigraph for modal size analysis of fine-grained sediment. *Sedimentology* 35, 163-172.
- Jumars, P.A., Nowell, A.R.M., 1984. Effects of benthos on sediment transport: difficulties with functional grouping. *Continental Shelf Research* 3, 115-130.
- Kandiah, A., 1974. Fundamental aspects of surface erosion of cohesive soils. PhD Thesis, University of California, Davis. Cited in Winterwerp and van Kesteren (2004).
- Kineke G.C., Sternberg, R.W., Trowbridge, J.H., Geyer, W.R. 1996. Fluid-mud processes on the Amazon continental shelf. *Continental Shelf Research*, 16, 667-696.
- Law, B.A., Hill, P.S., Milligan, T.G., Curran, K.J., Wiberg, P.L., Wheatcroft, R.A., 2008. Size sorting of fine-grained sediments during erosion: Results from the western Gulf of Lions. *Continental Shelf Research* 28, 1935-1946.
- Lawrence, D., Dagg, M.J., Liu, H., Cummings, S.R., Ortner, P.B., Kelble, C., 2004. Wind events and benthic-pelagic coupling in a shallow subtropical bay in Florida. *Marine Ecology Progress Series* 266, 1-13.
- Lick, W., McNeil, J., 2001. Effects of sediment bulk properties on erosion rates. *Science of the Total Environment* 266, 41-48.
- Lundkvist, M., Grue, M., Friend, P.L., Flindt, M.R., 2007. The relative contributions of physical and microbiological factors to cohesive sediment stability. *Continental Shelf Research* 27, 1143-1152.
- Ma, Y., Friedrichs, C.T., Harris, C.K., Wright, L.D., 2008. Deposition by seasonal wave- and current-supported sediment gravity flows interacting with spatially varying bathymetry: Waiapu shelf, New Zealand. *Marine Geology* 275, 199-211.
- Ma, Y., Wright, L.D., Friedrichs, C.T., 2010. Observations of sediment transport on the continental shelf off the mouth of the Waiapu River, New Zealand: Evidence for current-supported gravity flows. *Continental Shelf Research* 28, 516-532.
- Mazik, K., Elliot, M., 2000. The effects of chemical pollution on the bioturbation potential of estuarine intertidal mudflats. *Helgoland Marine Research* 54, 99-109.
- McKee, B.A., Aller, R.C., Allison, M.A., Bianchi, T.S. and Kineke, G.C., 2004. Transport and transformation of dissolved and particulate materials on continental margins influenced

- by major rivers: benthic boundary layer and seabed processes. *Continental Shelf Research*, 24, 899-926.
- McKee, B.A., Nittrouer, C.A., DeMaster, D.J., 1983. Concepts of sediment deposition and accumulation applied to the continental shelf near the mouth of the Yangtze River. *Geology* 11, 631-633.
- Miller, A.J., Kuehl, S.A., 2010, Shelf sedimentation on a tectonically active margin: A modern sediment budget for Poverty continental shelf, New Zealand, *Marine Geology*, 270, 175-187.
- Mitchener, H., Torfs, H., 1996. Erosion of mud/sand mixtures. *Coastal Engineering* 29, 1-25.
- Moore, J.W., 2006. Animal ecosystem engineers in streams. *Bioscience* 56, 237-246.
- Nittrouer, C.A., Austin, J.A., Field, M.E., Kravitz, J.H., Syvitski, J.M.P., Wiberg, P.I., 2007. Writing a Rosetta Stone: Insights into Continental-Margin Sedimentary Processes and Strata, Special Publication 37 of the International Association of Sedimentologists. Blackwell Publishing Ltd., Oxford 549 pp.
- Ogston, A.S., Cacchoine, D.A., Sternberg, R.W., Kineke, G.C., 2000. Observations of storm and river flood-driven sediment transport on the northern California continental shelf. *Continental Shelf Research* 20, 2141-2162.
- Ogston, A.S., Sternberg, R.W., 1999. Sediment-transport events on the northern California continental shelf. *Marine Geology* 154, 69-82.
- Ogston, A.S., Sternberg, R.W., Nittrouer, C.A., Martin, D.P., Göni, M.A., Crockett, J.S., 2008. Sediment delivery from the Fly River tidally dominated delta to the nearshore marine environment and the impact of El Nino. *Journal of Geophysical Research* 113, F01S11, doi:10.1029/2006JF000669.
- Olsen, C.R., Larsen, I.L., Lowry, P.D., Cutshall, N.H., Nichols, M.M., 1986. Geochemistry and deposition of <sup>7</sup>Be in river-estuarine and coastal waters. *Journal of Geophysical Research* 91, 896-908.
- Orpin, A.R., Alexander, C., Carter, L., Kuehl, S., Walsh, J.P., 2006. Temporal and spatial complexity in post-glacial sedimentation on the tectonically active, Poverty Bay continental margin of New Zealand. *Continental Shelf Research* 26, 2205-2224.
- Page, M.J., Trustrum, N.A., Gomez, B., 2000. Implications of a century of anthropogenic erosion for future land use in the Gisborne-East Coast region of New Zealand. *New Zealand Geographer* 56, 13-24.
- Panagiotopoulos, I., Voulgaris, G., Collins, M.B., 1997. The influence of clay on the threshold of movement of fine sandy beds. *Coastal Engineering* 32, 19-43.

- Puig, P., Ogston, B.L., Mullenbach, B.L., Nittrouer, C.A., Sternberg, R.W., 2003. Shelf-to-canyon sediment-transport processes on the Eel continental margin (northern California). *Marine Geology* 193, 129-149.
- Reyners, M., McGinty, P., 1999. Shallow subduction tectonics in the Raukumara Peninsula, New Zealand, as illuminated by earthquake focal mechanisms. *Journal of Geophysical Research* 104, 3025-3034.
- Righetti, M., Lucarelli, C., 2007. May the Shields theory be extended to cohesive and adhesive benthic sediments? *Journal of Geophysical Research-Oceans* 112, C05039.
- Roberts, J., Jepsen, R., Gotthard, D., Lick, W., 1998. Effects of particle size and bulk density on erosion of quartz particles. *Journal of Hydraulic Engineering-ASCE* 124, 1261-1267.
- Rose, L. E., Kuehl, S. A., 2010. Recent sedimentation patterns and facies distribution on the Poverty Shelf, New Zealand, *Marine Geology*, 270, 160-174.
- Ross, M.A., Mehta, A., 1989. On the Mechanics of lutoclines and fluid mud. *Journal of Coastal Research*, special issue 5, 51-61.
- Sanford, L.P. 2006. Uncertainties in sediment erodibility estimates due to a lack of standards for experimental protocols and data interpretations. *Integrated Environmental Assessment and Management* 2, 29-34.
- Sanford, L.P., Maa, J.P.Y., 2001. A unified erosion formulation for fine sediments. *Marine Geology* 179, 9-23.
- Sgro, L., Mistri, M., Widdows, J., 2005. Impact of the infaunal Manila clam, *Ruditapes philippinarum*, on sediment stability. *Hydrobiologia* 550, 175-182.
- Sommerfield, C.K., Nittrouer, C.A., Alexander, C.R., 1999. <sup>7</sup>Be as a tracer of flood sedimentation on the northern California continental margin. *Continental Shelf Research* 19, 335-361.
- Stevens, A.W., Wheatcroft, R.A., Wiberg, P.L., 2007. Seabed properties and sediment erodibility along the western Adriatic margin, Italy. *Continental Shelf Research* 27, 400-416.
- Sutherland, T.F., Amos, C.L., Grant, J., 1998. The effect of buoyant biofilms on the erodibility of sublittoral sediments of a temperate microtidal estuary. *Limnology and Oceanography* 43, 225-235.
- Syvitski, J.P.M., Vorosmarty, C.J., Kettner, A.J., Green, P., 2005. Impact of humans on the flux of terrestrial sediment to the global coastal ocean. *Science* 308, 376-380.
- Tate, K.R., Scott, N.A., Parshotam, A., Brown, L., Wilde, R.H., Giltrap, D.J., Trustrum, N.A., Gomez B., and Ross, D.J., 2000. A multi-scale analysis of a terrestrial carbon budget: Is



- New Zealand a source or sink of carbon? *Agriculture, Ecosystems & Environment* 82, 229-246.
- Thomsen, L., Gust, G., 2000. Sediment erosion thresholds and characteristics of resuspended aggregates on the western European continental margin. *Deep-Sea Research I* 47, 1881-1897.
- Tolhurst, T.J., Black, K.S., Paterson, D.M., Mitchener, H.J., Termaat, G.R., Shayler, S.A., 2000. A comparison and measurement standardisation of four in situ devices for determining the erosion shear stress of intertidal sediments. *Continental Shelf Research* 20, 1397-1418.
- Tolman, H.L., 2001. Improving propagation in ocean wave models. In B.L. Edge and J.M. Hemsley, editors, *Ocean Wave Measurement and Analysis*, pp. 507-516. ASCE.
- Traykovski, P., Geyer, W.R., Irish, J.D., Lynch, J.F., 2000. The role of wave-induced density-driven fluid mud flows for cross-shelf transport on the Eel River continental shelf. *Continental Shelf Research* 20, 2113-2140.
- Traykovski, P., Wiberg, P.L., Geyer, W.R., 2007. Observations and modeling of wave-supported gravity flows on the Po prodelta and comparison to prior observations from the Eel shelf. *Continental Shelf Research* 27, 375-399.
- Walling, D.E., Webb, B.W., 1996. Erosion and sediment yield: a global overview. *IAHS Publications* 236, 3-19.
- Walsh, J.P., Nittrouer, C.A., 1999. Observations of sediment flux to the Eel continental slope, northern California. *Marine Geology* 154, 55-68.
- Walsh, J.P., Nittrouer, C.A., 2009. Understanding fine-grained river-sediment dispersal on continental margins. *Marine Geology* 263, 34-45.
- Walsh, J.P., Alexander, C.A., Gerber, T., Orpin, A.R., Sumners, B.W., 2007. The demise of a submarine canyon? Evidence for highstand infilling on the Waipaoa River continental margin, New Zealand. *Geophysical Research Letters* 34, L20606. Doi:10.1029/2007GL031142.
- Waples, J.T., Benitez-Nelson, C., Savoye, N., Rutgers van der Loeff, M., Baskaran, M., Gustafsson, Ö., 2006. An introduction to the application and future use of  $^{234}\text{Th}$  in aquatic systems. *Marine Chemistry* 100, 166-189.
- Warner, J.C., Sherwood, C.R., Signell, R.P., Harris, C.K., Arango, H.G., 2008. Development of three-dimensional, regional, coupled wave, current, and sediment-transport model. *Computers & Geosciences* 34, 1284-1306.
- Wheatcroft, R.A., 2006. Time-series measurements of macrobenthos abundance and sediment bioturbation intensity on a flood-dominated shelf. *Progress in Oceanography* 71, 88-122.

- Wheatcroft, R.A., Drake, D.E., 2003. Post-depositional alteration and preservation of sedimentary event layers on continental margins, I. The role of episodic sedimentation. *Marine Geology* 199, 123-137.
- Widdows, J., Brinsley, M.D., Pope, N.D., 2009. Effects of *Nereis diversicolor* density on the erodability of estuarine sediment. *Marine Ecology-Progress Series* 378, 135-143.
- Wilmhurst, J.M., 1997. The impact of human settlement on vegetation and soil stability in Hawke's Bay New Zealand. *New Zealand Journal of Botany* 35, 97-111.
- Wilmhurst, J.M., McGlone, M.S., Partridge, T.R., 1997. A late Holocene history of natural disturbance in lowland podocarp/hardwood forest, Hawke's Bay, New Zealand. *New Zealand Journal of Botany* 35, 79-96.
- Wood, M.P., 2006. Sedimentation on a high input continental shelf at the active Hikurangi margin, Poverty Bay, New Zealand. Unpublished M.S. thesis, Victoria University of Wellington. 141 pp plus appendices.
- Wright, L.D., Nittrouer, C.A., 1995. Dispersal of river sediments in coastal seas: six contrasting cases. *Estuaries* 18, 494-508.
- Wright, L.D., Friedrichs, C.T., Kim, S.C., Scully, M.E., 2001. Effects of ambient currents and waves on gravity-driven sediment transport on continental shelves. *Marine Geology* 175, 25-45.

## **Appendix I Site Logs**

Site ID	New Site ID	Latitude (DD)	Longitude (DD)	Water Depth (m)	Shelf Environment
S101	C1-36	-38.824050	178.183993	60	Outer shelf
S102	C1-15	-38.787242	178.083450	39	Poverty Mouth
S103	C1-7	-38.735367	178.042517	29	Poverty Mouth
S104	C1-34	-38.811517	178.136267	49	Outer shelf
S105	NA	-38.880633	178.232217	115	Outer shelf
S107	C1-23	-38.898242	178.036367	55	S. Depocenter
S108	NA	-39.041175	177.936483	28	Other
S109	C1-22	-38.957758	177.983843	57	S. Depocenter
S111	NA	-38.762100	178.190400	52	N. Depocenter
S112	C1-31	-38.702100	178.206150	53	N. Depocenter
S113	C1-33	-38.650117	178.261933	62	N. Depocenter
S114	NA	-38.618000	178.350367	76	Other
S116	NA	-38.742083	178.384700	112	Outer shelf
S117	NA	-38.718933	178.269683	62	Outer shelf
S118	NA	-38.688067	178.144933	38	Other
S119	C1-12	-38.771850	178.062833	34	Poverty Mouth
S120	C1-28	-38.805142	178.110083	48	Mid-Shelf
S121	C1-24	-38.866150	178.053850	51	S. Depocenter
S123	C1-41	-39.043983	178.147550	102	Outer shelf
S124	NA	-39.024300	178.085867	62	Outer shelf
S125	NA	-39.001183	178.026283	44	Other
S126	NA	-38.933217	177.934900	40	Other
S127	C1-25	-38.849967	178.063400	54	S. Depocenter
S128	C1-26	-38.828367	178.069933	47	S. Depocenter
S129	C1-27	-38.808558	178.078050	44	Mid-Shelf
S130	NA	-38.938350	178.199217	133	Outer shelf
S131	NA	-38.990867	178.225933	889	Slope
S132	NA	-38.986200	178.166383	256	Canyon
S133	C1-44	-38.889000	178.263517	340	Canyon
S134	NA	-38.844867	178.275133	111	Outer shelf
S135	C1-39	-38.815150	178.238567	70	Outer shelf
S136	NA	-38.721033	178.139750	39	Poverty Mouth
S137	C1-18	-38.745050	178.133450	40	Poverty Mouth
S138	C1-17	-38.770050	178.117833	40	Poverty Mouth
S139	C1-3	-38.722867	177.984417	26	Poverty Bay
S140	C1-1	-38.708667	177.955733	16	Poverty Bay
S141	C1-4	-38.726033	177.992233	26	Poverty Bay
S146	C1-35	-38.825542	178.158700	54	Outer shelf
S147	C1-40	-38.853383	178.215267	82	Outer shelf
S148	NA	-38.982200	178.179567	358	Canyon
S149	NA	-38.905117	178.091450	41	Other
S150	C1-20	-38.825217	178.041517	44	S. Depocenter

Site ID	New Site ID	Latitude (DD)	Longitude (DD)	Water Depth (m)	Shelf Environment
S151	NA	-38.871083	177.974383	52	S. Depocenter
S152	C1-10	-38.829033	177.950983	34	Other
S155	C1-32	-38.654058	178.208500	48	Other
S157	C1-37	-38.713300	178.249783	62	Outer shelf
S159	C1-38	-38.771150	178.289017	62	Outer shelf
S160	C1-43	-38.823992	178.300567	125	Outer shelf
S161	NA	-38.812283	178.328983	339	Canyon
S162	NA	-38.824000	178.365233	884	Slope
S163	C1-42	-38.900933	178.215233	115	Outer shelf
S165	C1-30	-38.732367	178.184317	55	N. Depocenter
S166	NA	-38.745367	178.103367	34	Poverty Mouth
S167	C1-20	-38.825617	178.041083	45	S. Depocenter
S168	C1-11	-38.801033	178.011783	36	Poverty Mouth
S169	NA	-38.833600	178.017033	44	S. Depocenter
S170	C1-20	-38.825383	178.042117	44	S. Depocenter
S171	C1-21	-38.867083	178.024883	49	S. Depocenter
S172	C1-29	-38.933350	178.049033	53	Other
S176	C1-9	-38.990900	177.949117	39	Other
S178	NA	-39.058000	178.076450	67	Outer shelf
S179	NA	-39.087350	178.066300	71	Outer shelf
S201	C2-33	-38.649850	178.261683	64	N. Depocenter
S202	C2-32	-38.654050	178.208800	51	Other
S203	C2-31	-38.701717	178.206900	55	N. Depocenter
S204	C2-30	-38.732200	178.184700	52	N. Depocenter
S205	C2-25	-38.849950	178.063450	50	S. Depocenter
S206	C2-3	-38.722817	177.984233	23	Poverty Bay
S208	C2-12	-38.771700	178.061200	35	Poverty Mouth
S209	C2-15	-38.785983	178.078400	40	Poverty Mouth
S210	C2-18	-38.744733	178.134350	40	Poverty Mouth
S211	C2-10	-38.828900	177.951617	35	Other
S212	C2-22	-38.956600	177.984517	49	S. Depocenter
S213	C2-9	-38.990350	177.949233	42	Other
S214	C2-23	-38.897183	178.036483	53	S. Depocenter
S215	C2-24	-38.865783	178.054150	53	S. Depocenter
S216	C2-26	-38.828183	178.069517	48	S. Depocenter
S217	C2-27	-38.808383	178.077733	45	Mid-shelf
S218	C2-36	-38.824317	178.183950	61	Outer Shelf
S219	C2-40	-38.854133	178.214650	83	Outer Shelf
S220	C2-42	-38.901200	178.215567	110	Outer Shelf
S221	NA	-38.982550	178.179333	362	Canyon
S222	NA	-39.058450	178.076600	70	Outer Shelf
S223	C2-21	-38.867150	178.024750	51	S. Depocenter

Site ID	New Site ID	Latitude (DD)	Longitude (DD)	Water Depth (m)	Shelf Environment
S224	C2-20	-38.825583	178.041983	46	S. Depocenter
S225	C2-35	-38.826017	178.158417	56	Outer Shelf
S226	C2-4	-38.725817	177.992267	22	Poverty Bay
S230	C2-20	-38.825983	178.041850	46	S. Depocenter
S232	C2-7	-38.735467	178.041583	30	Poverty Mouth
S233	C2-6	-38.730433	178.018283	26	Poverty Bay
S234	NA	-38.708967	177.955800	14	Poverty Bay
S235	C2-2	-38.719100	177.978540		Poverty Bay
S236	C2-5	-38.726800	178.005467	25	Poverty Bay
S237	C2-8	-38.749067	178.060783	32	Poverty Mouth
S314	C3-21	-38.868000	178.024333	51	S. Depocenter
S315	C3-20	-38.825383	178.041683	45	S. Depocenter
S316	C3-3	-38.722733	177.984617	23	Poverty Bay
S317	C3-7	-38.734517	178.043067	29	Poverty Mouth
S318	C3-15	-38.787617	178.083850	40	Poverty Mouth
S319	C3-28	-38.805017	178.110167	47	Mid-shelf
S320	C3-27	-38.808100	178.078367	45	Mid-shelf
S321	C3-42	-38.900983	178.214633	105	Outer shelf
S322	NA	-38.982433	178.179267	355	Canyon
S323	C3-36	-38.823683	178.184033	63	Outer shelf
S324	C3-12	-38.771817	178.061650	35	Poverty Mouth
S325	C3-23	-38.898383	178.036317	52	S. Depocenter
S326	NA	-39.058000	178.076200	70	Outer shelf
S327	C3-25	-38.850033	178.062550	52	S. Depocenter
S328	C3-24	-38.865833	178.053700	53	S. Depocenter
S329	C3-18	-38.746000	178.131950	42	Poverty Mouth
S330	C3-32	-38.655150	178.208117	51	Other
S331	C3-33	-38.649750	178.258533	63	N. Depocenter
S332	C3-31	-38.702450	178.206550	55	N. Depocenter
S333	C3-30	-38.731767	178.182883	51	N. Depocenter
S334	C3-26	-38.830267	178.069850	47	S. Depocenter
S335	C3-22	-38.959833	177.981300	48	S. Depocenter
S336	C3-9	-38.990667	177.949583	41	Other
S337	C3-10	-38.828200	177.951733	35	Other
S338	C3-5	-38.725700	178.006500	25	Poverty Bay
S339	C3-2	-38.718483	177.977850	23	Poverty Bay
S340	NA	-38.708867	177.955533	13	Poverty Bay
S341	C3-4	-38.726267	177.993217	25	Poverty Bay
S342	C3-40	-38.854167	178.214417	83	Outer shelf
S343	C3-35	-38.827583	178.157450	56	Outer shelf
S344	NA	-38.771850	178.288933	65	Outer shelf
S345	C3-37	-38.713600	178.249083	63	Outer shelf

Site ID	New Site ID	Latitude (DD)	Longitude (DD)	Water Depth (m)	Shelf Environment
S346	C3-20	-38.825200	178.043217	46	S. Depocenter
S350	C3-29	-38.933717	178.048317	52	S. Depocenter
S351	C3-34	-38.812183	178.135717	51	Outer shelf
S352	C3-17	-38.770200	178.117217	41	Poverty Mouth
S353	C3-43	-38.823700	178.300350	125	Outer shelf
S354	C3-41	-39.045317	178.147900	99	Outer shelf
S402	C4-40	-38.853983	178.214567	82	Outer Shelf
S403	C4-4	-38.725967	177.992300	23	Poverty Bay
S404	C4-12	-38.771733	178.062000	35	Poverty Mouth
S405	C4-15	-38.786583	178.082450	40	Poverty Mouth
S406	C4-36	-38.823717	178.183867	61	Outer Shelf
S407	C4-33	-38.650017	178.262400	64	N. Depocenter
S408	C4-30	-38.732533	178.184533	52	N. Depocenter
S409	C4-37	-38.713283	178.249567	63	Outer Shelf
S410	NA	-38.770383	178.288933	65	Outer Shelf
S411	C4-43	-38.823267	178.300917	126	Outer Shelf
S412	C4-34	-38.811817	178.135633	51	Outer Shelf
S413	C4-35	-38.826767	178.157267	55	Outer Shelf
S414	C4-17	-38.769850	178.117533	41	Poverty Mouth
S415	C4-5	-38.726583	178.004467	25	Poverty Bay
S416	C4-25	-38.828217	178.069717	48	S. Depocenter
S417	C4-29	-38.932350	178.048550	51	Other
S418	NA	-39.058117	178.076967	70	Outer Shelf
S419	C4-41	-39.044183	178.147633	100	Outer Shelf
S420	NA	-38.980983	178.178850	359	Canyon
S421	C4-21	-38.867033	178.024517	51	S. Depocenter
S422	C4-10	-38.828783	177.949867	35	Other
S423	C4-27	-38.808733	178.078200	45	Mid-shelf
S424	NA	-38.736100	178.042583	28	Poverty Mouth
S425	NA	-38.736233	178.042650	28	Poverty Mouth
S426	C4-3	-38.723083	177.985667	22	Poverty Mouth
S427	C4-28	-38.805900	178.110717	47	Mid-shelf
S428	C4-26	-38.828733	178.069033	47	S. Depocenter
S429	C4-20	-38.824533	178.041983	45	S. Depocenter
S430	C4-9	-38.990867	177.949883	41	Other
S431	C4-22	-38.957367	177.983850	50	S. Depocenter
S432	NA	-38.708833	177.955667	13	Poverty Bay
S433	C4-18	-38.745050	178.134283	41	Poverty Mouth
S434	C4-31	-38.702033	178.207233	55	N. Depocenter
S435	C4-32	-38.654583	178.207550	50	Other
S436	NA	-38.786983	178.083400	40	Poverty Mouth
S437	C4-24	-38.865217	178.053817	51	S. Depocenter

Site ID	New Site ID	Latitude (DD)	Longitude (DD)	Water Depth (m)	Shelf Environment
S438	C4-8	-38.749717	178.061217	32	Poverty Mouth
S439	C4-2	-38.718967	177.977850	22	Poverty Bay
S440	C4-6	-38.727183	178.018200	26	Poverty Bay
S441	NA	-38.824833	178.183950	62	Outer Shelf
S442	C4-44	-38.889517	178.263183	343	Canyon
S443	C4-42	-38.900700	178.214900	108	Outer Shelf
S444	C4-23	-38.898417	178.036700	53	S. Depocenter
S445	NA	-38.786933	178.082933	40	Poverty Mouth
S446	NA	-38.793883	178.090467	43	Poverty Mouth
S447	C4-13	-38.780717	178.074517	38	Poverty Mouth
S448	C4-14	-38.781200	178.090983	40	Poverty Mouth
S449	C4-16	-38.793967	178.074683	40	Poverty Mouth
S450	NA	-38.800517	178.065833	40	Poverty Mouth
S451	NA	-38.806267	178.057733	41	Poverty Mouth
S452	C4-19	-38.812283	178.050783	40	Poverty Mouth
S453	NA	-38.715050	177.966100	19	Poverty Mouth
S454	NA	-38.760450	178.062083	33	Poverty Mouth
S456	NA	-38.938867	178.203950	123	Poverty Mouth



## **Appendix II Radioisotope Down-core Activities and Inventories**

Core ID	Mid-Depth (cm)	Fractional Porosity	<sup>7</sup> Be Activity (dpm g <sup>-1</sup> )	Error (+/-) (dpm g <sup>-1</sup> )	<sup>7</sup> Be Inventory (dpm cm <sup>-2</sup> )	Error (+/-) (dpm cm <sup>-2</sup> )	Excess <sup>234</sup> Th Activity (dpm g <sup>-1</sup> )	Error (+/-) (dpm g <sup>-1</sup> )	<sup>234</sup> Th Inventory (dpm cm <sup>-2</sup> )	Error (+/-) (dpm cm <sup>-2</sup> )	Date Collected
S101	0.5	0.75	0.70	0.29			11.76	1.04			
	1.5	0.77	1.09	0.35			9.27	0.94			
	2.5	0.72	0.76	0.35			1.92	0.69			
	3.5	0.71	0.45	0.30			0.91	0.55			
	4.5	0.70	BD	BD			1.36	0.62			
	5.5	0.70	0.64	0.31			1.85	0.55			
	6.5	0.68	BD	BD			*	*			
	7.5	0.67	BD	BD			1.12	0.64			
	8.5	0.66	BD	BD			2.84	0.71			
	9.5	0.66	BD	BD			0.35	0.69			
S102	11	0.68	BD	BD			*	*			
	13	0.63	BD	BD	2.06	0.65	0.42	0.67	18.07	1.96	1/14/2010
	0.5	0.61	0.35	0.38			2.93	0.51			
	1.5	0.60	0.48	0.36			0.25	0.47			
	2.5	0.56	0.43	0.36			1.03	0.41			
	3.5	0.54	BD	BD			0.83	0.47			
	4.5	0.64	BD	BD			*	*			
	5.5	0.67	0.59	0.47			*	*			
	6.5	0.68	BD	BD			1.29	0.52			
	7.5	0.71	0.72	0.46			1.62	0.58			
S103	8.5	0.65	BD	BD			*	*			
	9.5	0.46	0.67	0.34			*	*			
	11	0.48	BD	BD			1.09	0.49			
	13	0.48	BD	BD	1.39	0.64	0.00	0.41	5.56	1.03	1/14/2010
	0.5	NA	0.34	0.36			1.16	0.64			
	1.5	NA	1.10	0.42			*	*			
	2.5	NA	BD	BD			*	*			
	3.5	NA	BD	BD			*	*			
	5.5	NA	0.57	0.34	3.46	0.36	*	*	<2.00	NA	1/14/2010
	0.5	0.71	1.10	0.61			8.05	0.62			
S104	1.5	0.58	BD	BD			1.55	0.59			







	2.5	0.76	BD	BD	0.46	0.76	9.87	0.40	33.10	0.99	1/17/2010
S132	0.5	NA	0.68	0.45			95.19	2.23			
	1.5	NA	0.59	0.44			21.56	0.80			
	2.5	NA	BD	BD			1.68	0.48			
	3.5	NA	0.40	0.36			0.98	0.48			
	5.5	NA	BD	BD	3.23	0.72	*	*	304.16	2.54	1/17/2010
S133	0.5	0.83	1.05	0.51			29.76	0.76			
	1.5	0.83	BD	BD			20.81	0.63			
	2.5	0.81	0.99	0.46			6.15	0.47			
	3.5	0.79	0.37	0.45			4.83	0.46			
	5.5	0.76	0.50	0.43	NA	NA	2.83	0.45	29.64	1.49	1/17/2010
S134	0.5	0.78	BD	BD			3.67	0.30			
	1.5	0.79	BD	BD			5.30	0.30			
	2.5	0.79	BD	BD	0.00	0.00	4.24	0.33	<2.00	NA	1/17/2010
S135	0.5	0.75	0.70	0.48			9.35	0.39			
	1.5	0.76	1.47	0.52			13.43	0.38			
	2.5	0.66	BD	BD	1.41	0.71	*	*	14.86	0.84	1/17/2010
S136	0.5	0.62	0.59	0.60			*	*			
	1.5	0.60	BD	BD			*	*			
	2.5	0.63	BD	BD	0.60	0.60	*	*			1/17/2010
S137	0.5	0.62	0.58	0.49			5.94	0.35			
	1.5	0.56	BD	BD			2.66	0.34			
	2.5	0.55	BD	BD			1.38	0.30			
	3.5	0.46	BD	BD			*	*			
	5.5	0.52	BD	BD	0.58	0.49	1.71	0.31	<2.00	NA	1/17/2010
S138	0.5	0.61	0.43	0.69			*	*			
	1.5	0.60	1.31	0.72			0.71	0.30			
	2.5	0.14	BD	BD	1.83	1.00	4.38	0.30	X	X	1/17/2010
S139	0.5	NA	3.42	0.73			17.80	0.67			
	1.5	NA	1.56	0.49			7.52	0.42			
	2.5	NA	0.94	0.40			1.19	0.29			
	3.5	NA	BD	BD			0.83	0.29			
	4.5	NA	0.50	0.36			0.29	0.28			









	5.5	0.69	0.08	0.31						0.19	0.38								
	6.5	0.70	BD	BD						0.37	0.42								
	7.5	0.71	0.13	0.29						1.61	0.41								
	8.5	0.70	0.16	0.28						1.18	0.40								
	9.5	0.69	BD	BD						0.79	0.42								
	11	0.71	BD	BD						*	*								
	13	0.69	BD	BD	1.59	0.65				*	*	15.11	1.91	1/20/2010					
S171	0.5	0.75	0.99	0.60						11.17	0.43								
	1.5	0.75	1.27	0.59						*	*								
	2.5	0.69	0.43	0.53	1.85	1.00				1.03	0.38	<2.00	NA	1/20/2010					
S172	0.5	0.74	1.89	0.75						*	*								
	1.5	0.78	BD	BD						*	*								
	2.5	0.77	BD	BD	1.28	0.75				*	*	<2.00	NA	1/20/2010					
S176	0.5	0.66	0.34	0.75						2.32	0.32								
	1.5	0.56	BD	BD						1.39	0.32								
	2.5	0.60	0.62	0.75	0.30	0.75				*	*	<2.00	NA	1/20/2010					
S178	0.5	0.86	0.71	0.45						10.20	0.55								
	1.5	0.77	1.35	0.50						6.11	0.51								
	2.5	0.78	BD	BD						0.48	0.47								
	3.5	0.75	0.32	0.40						*	*								
	5.5	0.73	0.30	0.38	1.09	0.68				3.44	0.48	7.54	0.98	1/20/2010					
S179	0.5	0.81	1.27	0.62						2.13	0.53								
	1.5	0.79	0.84	0.66						*	*								
	2.5	0.77	BD	BD	1.10	0.91				*	*	<2.00	NA	1/20/2010					
S201	0.5	0.81	2.09	0.59						20.38	4.07								
	1.5	0.72	0.96	0.44						8.09	3.16								
	2.5	NA	NA	NA						NA	NA	NA	NA						
	3.5	0.75	BD	BD						3.22	3.13	18.47	1.27						
	4.5	0.74	BD	BD	1.77	0.74				0.26	3.16			5/19/2010					
S202	0.5	0.75	1.28	0.41						19.32	2.84								
	1.5	0.69	0.63	0.28						0.27	1.38								
	2.5	0.66	0.28	0.25						*	*								
	4.5	0.64	BD	BD	1.73	0.56				*	*	12.56	1.09	5/19/2010					







	1.5	0.77	0.64	0.39					4.93	1.40			
	2.5	0.75	0.34	0.36					1.96	0.97			
	3.5	0.74	0.33	0.44					2.69	1.55			
	4.5	0.72	0.44	0.42					2.44	1.46			
	5.5	0.71	BD	BD	1.46	0.89			2.14	1.44	16.86	1.58	5/22/2010
S220	0.5	0.83	BD	BD					0.73	1.69			
	1.5	0.79	BD	BD					1.99	1.83			
	2.5	0.77	BD	BD	0.00	0.00			1.25	1.88	2.21	1.01	5/22/2010
S221	0.5	0.86	1.07	0.51					54.15	5.07			
	1.5	0.83	0.86	0.51					29.35	3.46			
	2.5	0.79	BD	BD	0.79	0.72			7.11	2.16	37.55	1.93	5/22/2010
S222	0.5	0.79	1.52	0.47					13.58	2.23			
	1.5	0.78	0.48	0.40					6.50	2.01			
	2.5	0.75	0.41	0.43					1.81	2.27			
	3.5	0.74	0.41	0.38					0.06	1.84			
	4.5	0.74	BD	BD	1.68	0.85			*	*	12.56	1.45	5/22/2010
S223	0.5	0.82	1.43	0.55					16.41	2.50			
	1.5	0.77	0.00	0.00					2.51	1.72			
	2.5	0.74	0.73	0.60					0.38	2.47			
	3.5	0.72	0.51	0.42					*	*			
	4.5	0.72	0.68	0.57	NA	NA			2.20	2.44	9.20	1.12	5/22/2010
S224	0.5	0.74	BD	BD					*	*			
	1.5	0.53	BD	BD					*	*			
	2.5	0.72	0.38	0.44					*	*			
	3.5	0.73	0.74	0.39					*	*			
	4.5	0.71	BD	BD	0.00	0.00			*	*	0.00	1.33	5/23/2010
S225	0.5	0.67	0.36	0.25					10.21	0.87			
	1.5	0.60	0.00	0.00					*	*			
	2.5	0.56	BD	BD					0.75	0.63			
	3.5	0.55	BD	BD	0.31	0.25			*	*	8.88	0.85	5/23/2010
S226	0.5	0.82	1.99	0.55					17.72	2.78			
	1.5	0.86	2.06	0.56					15.16	2.70			
	2.5	0.80	1.16	0.44					12.34	2.57			

	3.5	0.68	0.67	0.32						1.81				
	4.5	0.68	0.23	0.28						*				
	5.5	0.68	BD	BD						0.29				
	6.5	0.70	BD	BD						0.76				
	7.5	0.71	BD	BD	3.07	1.00				2.08	22.08		1.86	5/23/2010
S230	0.5	0.75	1.49	0.52						16.51				
	1.5	0.69	BD	BD						2.71				
	2.5	0.73	0.49	0.52						5.06				
	3.5	0.71	BD	BD	1.00	0.52				3.51	19.57		1.28	5/23/2010
S232	0.5	0.60	0.56	0.28						1.49				
	1.5	0.53	0.28	0.25						0.46				
	2.5	0.45	0.17	0.22						*				
	3.5	0.46	0.06	0.29						*				
	4.5	0.50	0.39	0.29	1.28	0.52				*	2.17		1.21	5/23/2010
S233	0.5	0.54	0.52	0.30						0.09				
	1.5	0.57	0.40	0.29						*				
	2.5	0.58	0.95	0.33						2.10				
	3.5	0.63	0.75	0.34						0.37				
	4.5	0.60	0.58	0.33	3.50	0.71				1.93	<2.00		NA	5/23/2010
S234	0.5	0.97	0.57	0.38						0.10				
	1.5	0.61	0.57	0.31						*				
	2.5	0.44	0.65	0.31						*				
	3.5	0.45	0.49	0.31						*				
	4.5	0.46	BD	BD						*				
	5.5	0.45	0.62	0.51	2.30	0.66				2.51	<2.00		NA	5/24/2010
S235	0.5	0.64	0.19	0.41						*				
	1.5	0.48	BD	BD						*				
	2.5	0.47	BD	BD	0.18	0.41				*	0.00		0.92	5/24/2010
S236	0.5	0.49	BD	BD						*				
	1.5	0.44	BD	BD						*				
	2.5	0.46	0.72	0.42	0.00	0.00				*	0.00		0.78	5/24/2010
S237	0.5	0.49	0.33	0.30						0.27				
	1.5	0.50	0.44	0.27						3.20				





	1.5	0.71	0.41	0.41	0.41					*	*								
	2.5	0.74	0.41	0.44	0.44					0.30	0.35								
	3.5	0.71	BD	BD	BD	1.37	0.75			0.89	0.40	2.35	0.82						9/6/2010
S320	0.5	0.73	1.80	0.49	0.49					10.74	0.62								
	1.5	0.65	0.50	0.44	0.44					2.60	0.37								
	2.5	0.66	BD	BD	BD					0.86	0.28								
	3.5	0.66	BD	BD	BD	1.76	0.66			1.37	0.37	12.12	1.24						9/6/2010
S321	0.5	0.83	1.01	0.61	0.61					16.84	0.71								
	1.5	0.81	0.23	0.50	0.50					3.99	0.41								
	2.5	0.79	0.46	0.40	0.40					4.23	0.35								
	3.5	0.77	0.60	0.45	0.45					5.67	0.51								
	4.5	0.76	0.87	0.51	0.51					8.29	0.51								
	5.5	0.75	0.77	0.39	0.39					12.10	0.62								
	6.5	0.74	0.83	0.53	0.53					11.20	0.53								
	7.5	0.67	BD	BD	BD					4.66	0.47								
	8.5	0.70	BD	BD	BD	2.85	1.30			2.82	0.32	36.81	1.88						9/6/2010
S322	0.5	0.83	2.03	0.64	0.64					42.19	1.20								
	1.5	0.82	1.15	0.49	0.49					19.48	0.65								
	2.5	0.79	1.24	0.57	0.57					29.68	0.86								
	3.5	0.77	1.93	0.67	0.67					46.62	1.12								
	4.5	0.76	BD	BD	BD	3.28	1.19			12.01	0.57	79.94	2.28						9/7/2010
S323	0.5	0.75	1.62	0.38	0.38					15.55	0.82								
	1.5	0.72	BD	BD	BD					3.76	0.41								
	2.5	0.70	BD	BD	BD					3.04	0.37								
	3.5	0.69	0.16	0.34	0.34					4.62	0.50								
	4.5	0.66	0.00	0.00	0.00					1.48	0.38								
	5.5	0.65	0.49	0.32	0.32					0.74	0.34								
	6.5	0.64	BD	BD	BD					0.13	0.33								
	7.5	0.64	BD	BD	BD					2.97	0.39								
	8.5	0.65	BD	BD	BD					3.89	0.36								
	9.5	0.69	BD	BD	BD	1.08	0.38			*	*	19.17	1.87						9/7/2010
S324	0.5	0.61	BD	BD	BD					1.51	0.36								
	1.5	0.56	BD	BD	BD					2.33	0.37								





	3.5	0.62	BD	BD	BD	1.07			1.04	0.37				
	4.5	0.62	BD	BD	BD	4.62			*	*	8.13	0.86	9/8/2010	
S338	0.5	0.73	BD	BD	BD				*	*				
	1.5	0.69	BD	BD	BD				*	*				
	2.5	0.65	BD	BD	BD				*	*				
	3.5	0.45	BD	BD	BD				*	*				
	4.5	0.63	BD	BD	BD	0.00			*	*	BD	BD	9/9/2010	
S339	0.5	0.53	0.07	0.29					*	*				
	1.5	0.51	0.23	0.31					*	*				
	2.5	0.56	BD	BD					2.49	0.35				
	3.5	0.55	0.75	0.36					*	*				
	4.5	0.53	0.66	0.34					3.58	0.31				
	5.5	0.45	0.19	0.29					*	*				
	6.5	0.63	BD	BD	0.39	0.31			*	*	<2.00	NA	9/9/2010	
S340	0.5	0.79	0.33	0.33					1.21	0.43				
	1.5	0.82	0.78	0.43					1.30	0.48				
	2.5	0.80	BD	BD					1.85	0.47				
	3.5	0.80	0.35	0.43					2.71	0.51				
	4.5	0.75	0.52	0.39					*	*				
	5.5	0.45	0.68	0.47	0.55	0.54			*	*	<2.00	NA	9/9/2010	
S341	0.5	0.82	1.56	0.49					1.71	0.48				
	1.5	0.80	0.97	0.44					1.60	0.49				
	2.5	0.61	0.50	0.37					*	*				
	3.5	0.49	0.55	0.36					*	*				
	4.5	0.49	BD	BD	2.52	0.83			*	*	<2.00	NA	9/9/2010	
S342	0.5	0.87	1.95	0.69					38.34	1.04				
	1.5	0.81	1.29	0.76					20.77	0.80				
	2.5	0.78	0.83	0.59					8.24	0.55				
	3.5	0.77	1.65	0.65					9.09	0.56				
	4.5	0.75	0.53	0.63					6.31	0.53				
	5.5	0.73	BD	BD					4.95	0.47				
	6.5	0.72	BD	BD	3.14	1.49			5.52	0.51	38.05	1.89	9/9/2010	
S343	0.5	0.64	0.73	0.27					6.00	0.44				







	1.5	0.79	1.48	1.04					19.07	14.12			
	2.5	0.76	0.83	1.03					5.56	13.33			
	3.5	0.73	BD	BD					20.01	11.55			
	4.5	0.72	BD	BD					6.30	11.22			
	6	0.71	BD	BD					5.02	10.59			
	8	0.70	BD	BD	1.95	1.64			7.23	10.29	X	X	2/9/2011
S410	0.5	0.63	BD	BD					35.22	19.94			
	1.5	0.52	0.34	0.52					*	*			
	2.5	0.49	0.74	0.89					*	*			
	3.5	0.43	1.01	1.07					0.03	16.78			
	4.5	0.47	0.71	0.92					*	*			
	5.5	0.46	BD	BD	4.13	1.75			*	*	X	X	2/9/2011
S411	0.5	0.85	BD	BD					28.28	23.70			
	1.5	0.84	BD	BD					24.52	27.36			
	2.5	0.83	0.88	1.34					10.08	28.16			
	3.5	0.80	0.89	1.03					12.67	33.46			
	4.5	0.79	1.08	1.11					1.34	34.44			
	6	0.77	BD	BD					53.79	37.54			
	8	0.75	BD	BD	0.00	0.00			*	*	X	X	2/9/2011
S412	0.5	0.74	BD	BD					18.71	25.83			
	1.5	0.65	BD	BD					1.89	25.10			
	2.5	0.64	BD	BD					10.97	24.39			
	3.5	0.64	0.80	1.22					3.20	23.70			
	4.5	0.63	0.00	0.00					1.32	21.74			
	6	0.61	1.36	1.27					7.40	21.12			
	8	0.60	BD	BD	0.00	0.00			8.91	20.52	X	X	2/9/2011
S413	0.5	0.64	0.32	0.25					6.67	1.83			
	1.5	0.60	0.62	0.28					*	*			
	2.5	0.60	BD	BD					*	*			
	3.5	0.57	BD	BD					0.68	1.68			
	4.5	0.57	BD	BD	0.99	0.38			1.00	1.63	6.53	1.65	2/9/2011
S414	0.5	0.58	BD	BD					7.27	10.00			
	1.5	0.56	1.22	1.35					6.50	30.70			









	6.5	0.74	BD	BD					7.50				
	7.5	0.74	BD	BD				*	*				
	8.5	0.74	BD	BD	1.03	0.68		3.05	8.66	11.15	1.01	2/11/2011	
S429	0.5	0.78	0.63	0.31				14.26	2.44				
	1.5	0.77	0.23	0.35				2.25	2.37				
	2.5	0.72	0.30	0.32				3.27	2.31				
	3.5	0.72	0.56	0.36				1.26	2.59				
	4.5	0.69	0.28	0.40				0.12	2.66				
	5.5	0.67	0.28	0.42				2.48	4.10				
	6.5	0.68	0.60	0.48				2.61	4.22				
	7.5	0.69	BD	BD				*	*				
	8.5	0.70	BD	BD				0.61	7.50				
	9.5	0.71	BD	BD	2.21	1.01		1.69	8.66	13.59	1.36	2/11/2011	
S430	0.5	0.62	BD	BD				4.37	5.79				
	1.5	0.56	0.37	0.50				4.79	5.96				
	2.5	0.56	0.25	0.45				*	*				
	3.5	0.57	BD	BD				1.70	6.69				
	4.5	0.56	1.17	1.00	0.75	0.67		6.21	28.98	<2.00	NA	2/11/2011	
S431	0.5	0.78	1.15	0.34				7.87	1.30				
	1.5	0.72	0.93	0.32				2.58	1.34				
	2.5	0.69	0.34	0.29				0.59	1.37				
	3.5	0.69	0.00	0.00				1.20	1.68				
	4.5	0.67	0.32	0.58	1.71	0.55		*	*	7.31	1.32	2/11/2011	
S432	0.5	0.88	BD	BD				2.66	4.60				
	1.5	0.86	1.11	0.50				10.86	4.73				
	2.5	0.83	1.25	0.53				8.94	4.87				
	3.5	0.84	0.44	0.44				9.71	5.01				
	4.5	0.85	0.64	0.46				0.88	5.16				
	5.5	0.86	BD	BD				*	*				
	6.5	0.81	BD	BD	1.49	0.97		15.04	9.17	13.95	1.59	2/11/2011	
S433	0.5	0.73	1.86	0.55				16.17	1.41				
	1.5	0.67	0.88	0.40				4.79	1.46				
	2.5	0.62	0.38	0.34				2.75	1.50				

		3.5	0.60	0.61	0.39						1.63								
		4.5	0.56	0.90	0.40						*								
		5.5	0.53	BD	BD						*								
		6.5	0.54	BD	BD						*								
		7.5	0.53	BD	BD	4.34	0.94				3.31	19.23	1.50	2/12/2011					
S434		0.5	0.79	0.97	0.69						10.92								
		1.5	0.77	0.80	0.74						*								
		2.5	0.75	0.29	0.80						*								
		3.5	0.74	0.54	0.66						10.21	10.59							
		4.5	0.71	BD	BD						*								
		6	0.69	BD	BD						*								
		8	0.69	0.91	0.67	1.64	1.45				*	X	X	2/12/2011					
S435		0.5	0.74	0.80	0.40						8.68	2.74							
		1.5	0.69	0.81	0.38						3.23	2.82							
		2.5	0.67	BD	BD						2.15	2.90							
		3.5	0.67	0.37	0.41						0.47	3.76							
		4.5	0.64	BD	BD	1.25	0.55				*	10.81	1.17	2/12/2011					
S437		0.5	0.78	0.34	0.25						7.09	1.41							
		1.5	0.73	0.28	0.30						4.32	2.31							
		2.5	0.70	BD	BD						3.25	2.37							
		3.5	0.69	BD	BD						4.55	2.59							
		4.5	0.70	BD	BD	0.42	0.39				2.70	2.51	1.79	2/12/2011					
S438		0.5	0.68	1.05	0.35						7.09	1.54							
		1.5	0.75	0.80	0.42						0.58	2.74							
		2.5	0.75	0.38	0.42						3.75	2.82							
		3.5	0.75	0.65	0.46						*	*							
		4.5	0.74	0.36	0.39						0.45	2.99							
		5.5	0.74	0.25	0.46						0.36	4.10							
		6.5	0.60	0.66	0.45						*	*							
		7.5	0.55	0.69	0.46						*	*							
		8.5	0.57	BD	BD	4.20	1.21				*	9.16	1.47	2/12/2011					
S439		0.5	0.78	1.53	0.97						19.98	26.59							
		1.5	0.81	BD	BD						8.29	27.36							

	2.5	0.81	1.82	1.06						1.88	28.16			
	3.5	0.79	BD	BD						*	*			
	4.5	0.76	BD	BD						0.11	29.83			
	6	0.77	0.84	1.02						*	*			
	8	0.57	0.94	0.94	1.87	1.44				*	*	X	X	2/12/2011
S440	0.5	0.72	0.72	0.40						4.23	3.26			
	1.5	0.67	BD	BD						0.02	3.35			
	2.5	0.72	BD	BD						*	*			
	3.5	0.73	0.41	0.53						1.17	5.16			
	4.5	0.72	BD	BD						2.58	5.96			
	5.5	0.71	BD	BD						*	*			
	6.5	0.69	1.25	0.61						0.58	8.18			
	7.5	0.75	0.19	0.55						*	*			
	8.5	0.62	0.26	0.46						*	*			
	9.5	0.56	BD	BD	2.35	1.15				*	*	3.30	0.69	2/13/2011
S441	0.5	0.76	0.51	0.31						11.43	1.68			
	1.5	0.73	0.37	0.34						3.28	2.12			
	2.5	0.70	BD	BD						0.85	2.06			
	3.5	0.68	BD	BD						0.29	2.00			
	4.5	0.68	0.24	0.30						1.13	1.83			
	5.5	0.68	BD	BD						*	*			
	6.5	0.68	0.76	0.38						1.13	2.59			
	7.5	0.68	BD	BD						1.38	2.90			
	8.5	0.67	1.10	0.49						1.89	4.22			
	9.5	0.66	BD	BD	0.62	0.46				*	*	10.81	1.27	2/13/2011
S443	0.5	0.88	BD	BD						37.92	14.12			
	1.5	0.88	BD	BD						14.93	12.59			
	2.5	0.66	BD	BD						0.46	11.55			
	3.5	1.06	BD	BD						0.36	10.29			
	4.5	0.57	BD	BD						1.28	10.00			
	6	0.88	BD	BD						*	*			
	8	NA	BD	BD	0.00	0.00				6.12	9.17	X	X	2/13/2011
S444	0.5	0.78	0.59	0.34						6.46	1.16			

	1.5	0.74	0.42	0.40						3.82	1.19			
	2.5	0.73	BD	BD						3.74	1.23			
	3.5	0.77	0.30	0.46						3.33	1.26			
	4.5	0.79	1.36	0.51						1.48	1.63			
	5.5	0.78	BD	BD						3.47	1.78			
	6.5	0.79	1.14	0.47						4.74	1.73			
	7.5	0.76	BD	BD						1.53	1.83			
	8.5	0.74	0.78	0.43						2.62	1.89			
	9.5	0.75	BD	BD						0.94	2.00			
	11	0.71	BD	BD						2.37	5.31			
	13	0.70	BD	BD						*	*			
	15	0.68	BD	BD	2.32	0.99				1.58	5.63	20.77	2.41	2/13/2011
S445	0.5	0.69	1.05	0.37						4.42	1.63			
	1.5	0.69	0.29	0.33						2.10	1.68			
	2.5	0.62	BD	BD						1.12	2.31			
	3.5	0.58	BD	BD						1.23	2.12			
	4.5	0.62	0.11	0.32						1.38	2.44			
	5.5	0.61	BD	BD						0.17	2.51			
	6.5	0.59	BD	BD						0.26	2.59			
	7.5	0.48	0.18	0.38						*	*			
	8.5	0.50	BD	BD						*	*			
	9.5	0.53	0.57	0.43	1.16	0.49				*	*	9.63	1.52	2/13/2011
S446	1	0.70	BD	BD						0.18	22.37			
	3	0.59	BD	BD						*	*			
	5	0.55	BD	BD						*	*			
	7	0.57	BD	BD	0.00	0.00				*	*	X	X	2/13/2011
S447	0.5	0.52	BD	BD						3.80	2.99			
	1.5	0.67	BD	BD						0.80	3.08			
	2.5	0.64	0.84	0.44						0.79	3.45			
	3.5	0.59	BD	BD						*	*			
	4.5	0.53	0.57	0.41						*	*			
	5.5	0.50	BD	BD						2.45	7.72			
	6.5	0.50	0.56	0.69						2.45	7.72			

	7.5	0.51	BD	BD	BD	0.00	0.00	0.00	0.00	0.00	5.72	0.86	2/13/2011
S448	0.5	0.66	0.43	0.35	0.35			4.36	3.17				
	1.5	0.58	BD	BD	BD			0.45	3.26				
	2.5	0.54	BD	BD	BD			*	*				
	3.5	0.54	BD	BD	BD			*	*				
	4.5	0.54	BD	BD	BD	0.41	0.35	*	*	4.10	0.63	2/14/2011	
S449	0.5	0.64	0.29	0.49	0.49			7.55	3.17				
	1.5	0.63	0.68	0.50	0.50			3.09	3.26				
	2.5	0.60	0.82	0.48	0.48			2.47	3.35				
	3.5	0.63	1.49	0.60	0.60			0.01	3.55				
	4.5	0.63	BD	BD	BD			0.44	3.76				
	5.5	0.53	BD	BD	BD			1.03	7.29				
	6.5	0.50	0.50	0.64	0.64			*	*				
	7.5	0.51	BD	BD	BD	3.39	1.04	*	*	13.40	1.15	2/14/2011	
S450	0.5	0.69	0.59	0.53	0.53			3.12	5.16				
	1.5	0.64	0.23	0.53	0.53			1.69	5.31				
	2.5	0.60	BD	BD	BD			*	*				
	3.5	0.55	BD	BD	BD			0.71	5.63				
	4.5	0.57	0.45	0.56	0.56			44.93	6.13				
	5.5	0.58	BD	BD	BD			0.49	6.69				
	6.5	0.55	BD	BD	BD	0.73	0.75	*	*	<2.00	NA	2/14/2011	
S451	0.5	0.67	1.23	0.52	0.52			7.02	2.59				
	1.5	0.63	0.16	0.49	0.49			*	*				
	2.5	0.60	0.58	0.59	0.59			2.84	4.73				
	3.5	0.57	BD	BD	BD			*	*				
	4.5	0.57	1.40	0.69	0.69			2.18	5.31				
	5.5	0.56	0.73	0.67	0.67			*	*				
	6.5	0.55	0.08	0.74	0.74			*	*				
	7.5	0.56	BD	BD	BD			*	*				
	8.5	0.60	BD	BD	BD			*	*				
	9.5	0.60	0.30	0.81	0.81	4.58	1.53	3.82	8.41	6.40	0.94	2/14/2011	
S452	0.5	0.72	0.51	0.65	0.65			4.18	5.63				
	1.5	0.72	BD	BD	BD			3.76	5.79				



	2.5	0.74	BD	BD					*				
	3.5	0.69	BD	BD				6.95	6.13				
	4.5	0.70	0.31	0.71	0.39	0.65		11.09	6.31	<2.00	NA	2/14/2011	
S453	0.5	0.83	0.57	0.49				*	*				
	1.5	0.82	0.66	0.47				0.44	5.63				
	2.5	0.81	BD	BD				5.00	5.96				
	3.5	0.73	0.00	0.00				5.53	5.47				
	4.5	0.79	0.45	0.56				1.35	8.18				
	5.5	0.78	BD	BD				*	*				
	6.5	0.76	BD	BD				*	*				
	7.5	0.72	BD	BD	0.60	0.68		8.82	36.48	<2.00	NA	2/14/2011	
S454	1	0.65	0.95	0.98				*	*				
	3	0.63	1.76	0.92				*	*				
	5	0.50	1.02	0.89				*	*				
	7	0.51	BD	BD				*	*				
	9	0.49	BD	BD	8.23	1.61		*	*	X	X	2/14/2011	
S455	1	0.81	0.58	0.89				9.04	28.16				
	3	0.78	0.58	0.99				*	*				
	5	0.75	BD	BD				*	*				
	7	0.74	BD	BD	1.28	1.33		*	*	X	X	2/14/2011	

BD = Below Detection Level of Analytical Equipment. Activity was assumed to be zero.

\* = Instances where Supported  $^{234}\text{Th}$  > XS  $^{234}\text{Th}$ . Therefore, XS  $^{234}\text{Th}$  activity was assumed to be zero.

NA = Instances where  $^7\text{Be}$  inventory could not be calculated because depth of  $^7\text{Be}$  penetration was not determined, or measurements of porosity were not made.

X = Instances where XS  $^{234}\text{Th}$  inventories could not be calculated because samples were analyzed outside of the counting window.

### **Appendix III Grain Size and LOI Data**

Core ID	Mid-Depth (cm)	Sand %	Silt %	Clay %	LOI %	Core ID	Mid-Depth (cm)	Sand %	Silt %	Clay %	LOI %
S101	0.5	12.3	39.2	48.5	4.1	S139	0.5	8.2	29.6	62.3	6.1
	1.5	29.4	31.3	39.2	4.8		1.5	31.2	29.3	39.6	3.9
	2.5	34.4	31.8	33.9	4.3		2.5	54.1	23.6	22.3	2.2
	3.5	32.9	31.6	35.5	4.4		3.5	48.0	37.2	14.8	2.6
	4.5	34.2	31.9	33.9	4.3		4.5	47.3	38.0	14.7	2.4
S102	0.5	7.6	69.0	23.4	3.6	S140	0.5	43.9	47.4	8.7	2.2
	1.5	6.5	62.9	30.6	3.7		1.5	53.0	34.9	12.2	2.0
	2.5	18.7	60.5	20.8	3.2		2.5	83.4	12.3	4.3	2.3
	3.5	19.4	51.4	29.2	3.5		3.5	47.3	31.8	20.9	2.6
	4.5	10.6	46.2	43.2	5.0		4.5	51.7	24.5	23.8	2.6
S103	0.5	25.4	38.1	36.6	4.4	S141	0.5	NA	NA	NA	5.7
	1.5	9.3	43.4	47.2	4.5		1.5	64.5	24.2	11.3	3.9
	2.5	8.5	42.3	49.2	4.2		2.5	33.2	41.4	25.4	3.9
	3.5	48.7	29.7	21.7	2.5		3.5	12.0	37.0	51.1	6.3
	4.5	52.5	25.9	21.6	2.6		4.5	1.0	30.9	68.1	6.2
S107	0.5	7.3	46.6	46.0	5.1	S146	0.5	75.2	10.6	14.1	2.3
	1.5	6.4	48.8	44.8	4.7		1.5	75.6	9.7	14.7	2.2
	2.5	8.6	51.2	40.2	4.7		2.5	71.2	11.1	17.7	2.6
	3.5	6.9	51.7	41.4	5.1		3.5	67.0	13.1	19.9	2.6
	4.5	6.8	50.2	42.9	5.0		4.5	62.4	15.9	21.6	3.0
S119	0.5	41.0	39.6	19.4	3.0	S147	0.5	16.0	35.3	48.7	4.8
	1.5	34.4	45.9	19.7	3.7		1.5	16.7	36.6	46.8	5.1
	2.5	33.2	47.0	19.8	3.6		2.5	18.3	30.8	50.9	4.7
	3.5	32.2	27.7	40.1	3.8		3.5	21.4	33.9	44.7	4.8
	4.5	35.9	41.4	22.7	3.0		4.5	21.7	35.5	42.7	4.8
S127	0.5	9.9	52.3	37.7	4.9	S150	0.5	1.3	51.6	47.1	4.5
	1.5	12.1	48.2	39.6	4.5		1.5	1.8	49.0	49.2	5.4
	2.5	11.1	48.4	40.6	4.8		2.5	1.4	53.3	45.2	5.3
	3.5	9.3	47.6	43.1	4.8		3.5	1.5	49.1	49.3	5.2
	4.5	8.7	46.9	44.4	5.1		4.5	0.7	44.7	54.6	5.8
S137	0.5	42.0	38.5	19.6	2.5	S155	0.5	19.2	49.5	31.3	3.6
	1.5	26.6	50.6	22.7	3.2		1.5	19.1	44.2	36.6	3.9
	2.5	45.1	36.3	18.7	2.8		2.5	14.6	49.7	35.7	4.1
	3.5	37.7	44.1	18.2	2.7		3.5	10.8	50.7	38.5	4.2
	4.5	17.0	68.7	14.4	2.9		4.5	14.1	50.9	35.1	4.0

Core ID	Mid-Depth (cm)	Sand %	Silt %	Clay %	LOI %	Core ID	Mid-Depth (cm)	Sand %	Silt %	Clay %	LOI %
S165	0.5	9.1	56.1	34.8	4.8	S205	0.5	13.8	47.3	39.0	5.5
	1.5	11.9	55.2	33.0	3.9		1.5	16.3	45.9	37.8	5.3
	2.5	9.4	53.4	37.1	4.2		2.5	9.9	49.1	41.0	5.2
	3.5	6.8	56.3	36.9	4.1		3.5	10.1	50.5	39.4	5.9
	4.5	15.9	50.8	33.3	3.4		4.5	6.2	44.6	49.3	5.2
S167	0.5	4.1	53.2	42.7	5.1	S206	0.5	28.0	30.2	41.8	5.6
	1.5	2.3	48.8	49.0	5.7		1.5	9.4	35.6	55.0	6.8
	2.5	0.7	37.7	61.6	6.3		2.5	7.1	36.8	56.1	5.1
	3.5	2.7	52.0	45.4	4.6		3.5	5.2	45.9	48.9	5.4
	4.5	1.5	48.6	50.0	5.2		4.5	5.3	48.9	45.7	6.1
S170	0.5	4.3	45.8	50.0	5.0	S208	0.5	38.7	44.8	16.6	3.2
	1.5	1.7	50.8	47.5	5.7		1.5	40.2	41.7	18.1	2.6
	2.5	8.4	52.0	39.7	5.7		2.5	41.9	34.9	23.2	2.7
	3.5	1.4	55.2	43.4	5.5		3.5	42.0	37.9	20.1	3.3
	4.5	1.3	52.6	46.1	5.1		4.5	37.3	39.5	23.2	3.9
S171	0.5	1.4	53.0	45.6	5.6	S209	0.5	12.3	64.0	24.9	4.1
	1.5	1.3	52.6	46.1	5.8		1.5	3.8	59.2	39.1	5.8
	2.5	3.4	51.4	45.2	4.9		2.5	2.8	58.2	42.8	4.6
	3.5	3.7	51.8	44.5	5.3		3.5	2.3	57.4	41.5	4.3
	4.5	2.6	52.4	45.0	4.9		4.5	2.2	57.5	40.4	3.4
S178	0.5	10.4	38.9	50.7	5.7	S210	0.5	14.3	47.6	38.1	5.0
	1.5	8.5	42.9	48.6	5.5		1.5	6.3	56.1	37.6	5.0
	2.5	7.8	43.4	48.8	5.6		2.5	20.8	44.1	35.1	4.8
	3.5	7.9	41.3	50.7	5.5		3.5	24.5	47.8	27.7	2.5
	4.5	7.7	39.6	52.7	5.5		4.5	42.7	35.5	21.8	2.6
S202	0.5	15.4	31.9	52.7	4.4	S214	0.5	8.6	40.1	53.9	5.6
	1.5	19.0	39.1	41.9	4.2		1.5	6.8	42.9	53.2	7.5
	2.5	17.3	30.9	51.9	4.7		2.5	8.1	36.1	57.7	5.0
	3.5	20.2	29.2	50.6	4.6		3.5	9.1	36.2	56.2	3.6
	4.5	11.3	34.8	53.9	3.3		4.5	7.0	34.2	60.4	3.2
S204	0.5	5.7	49.5	44.8	6.3	S218	0.5	36.8	23.6	41.1	4.3
	1.5	7.2	43.6	49.2	5.9		1.5	31.3	25.4	45.8	7.2
	2.5	11.8	43.8	44.5	5.3		2.5	36.1	21.7	43.5	5.0
	3.5	11.8	51.3	37.0	6.2		3.5	34.7	28.6	51.9	7.6
	4.5	11.4	49.9	38.7	6.0		4.5	35.8	19.1	45.1	4.2

Core ID	Mid-Depth (cm)	Sand %	Silt %	Clay %	LOI %	Core ID	Mid-Depth (cm)	Sand %	Silt %	Clay %	LOI %
S219	0.5	25.6	31.0	43.4	6.0	S232	0.5	66.8	19.9	13.3	2.3
	1.5	23.0	31.9	45.1	4.8		1.5	74.1	15.3	10.6	2.6
	2.5	23.2	32.0	44.8	4.3		2.5	72.0	18.6	9.4	2.1
	3.5	25.2	30.6	44.2	6.3		3.5	72.6	17.7	9.7	2.0
	4.5	21.7	33.1	45.2	4.2		4.5	68.5	18.6	12.9	2.2
S222	0.5	7.1	42.9	50.0	5.7	S233	0.5	69.2	21.1	9.6	2.1
	1.5	7.4	45.1	47.5	3.3		1.5	61.7	23.3	15.0	2.8
	2.5	10.1	43.6	46.3	6.0		2.5	58.0	23.5	18.5	2.7
	3.5	10.2	42.3	47.5	4.9		3.5	50.8	24.2	24.9	2.1
	4.5	9.0	40.9	50.0	5.7		4.5	49.2	28.3	22.6	4.8
S223	0.5	4.2	48.8	47.0	7.8	S234	0.5	NA	NA	NA	NA
	1.5	3.6	52.7	43.7	6.7		1.5	61.8	20.3	17.9	2.6
	2.5	4.2	47.6	48.2	4.7		2.5	77.3	12.4	10.3	1.9
	3.5	2.5	48.4	49.1	5.0		3.5	69.7	15.9	14.4	2.0
	4.5	3.1	48.4	48.4	5.3		4.5	65.0	20.5	14.6	2.1
S224	0.5	1.5	48.3	50.2	5.1	S235	0.5	77.2	13.2	9.6	1.6
	1.5	1.6	46.5	51.9	4.5		1.5	81.0	9.8	9.2	2.3
	2.5	3.4	46.9	49.6	5.3		2.5	82.6	6.7	10.7	1.4
	3.5	4.6	46.7	48.6	3.5		3.5	81.7	6.6	11.6	1.0
	4.5	3.9	45.5	50.7	4.3		4.5	79.1	9.4	11.6	2.1
S225	0.5	67.8	13.2	19.0	4.6	S237	0.5	69.2	21.1	9.6	2.1
	1.5	73.3	11.1	15.6	1.9		1.5	61.7	23.3	15.0	2.8
	2.5	72.1	11.0	17.0	2.1		2.5	58.0	23.5	18.5	2.7
	3.5	69.4	12.6	17.9	3.1		3.5	50.8	24.2	24.9	2.1
	4.5	68.8	12.2	19.0	2.8		4.5	49.2	28.3	22.6	4.8
S226	0.5	0.0	33.2	66.8	6.8	S314	0.5	0.5	3.2	51.9	44.9
	1.5	0.0	42.0	58.0	6.6		1.5	1.5	3.1	67.4	29.4
	2.5	0.0	52.8	47.2	6.0		2.5	2.5	3.6	58.2	38.2
	3.5	1.7	52.0	46.3	5.0		3.5	3.5	3.4	52.1	44.4
	4.5	1.0	46.9	52.1	6.3		4.5	4.5	3.2	48.5	48.3
S230	0.5	5.7	50.7	43.6	4.9	S315	0.5	0.5	3.5	55.6	40.9
	1.5	3.6	49.4	46.9	3.5		1.5	1.5	2.9	57.9	39.2
	2.5	2.0	43.1	54.9	5.4		2.5	2.5	1.7	54.6	43.6
	3.5	1.6	46.9	51.6	5.7		3.5	3.5	1.8	57.2	41.1
	4.5	1.1	47.1	51.8	5.3		4.5	4.5	1.3	58.2	40.5

Core ID	Mid-Depth (cm)	Sand %	Silt %	Clay %	LOI %	Core ID	Mid-Depth (cm)	Sand %	Silt %	Clay %	LOI %
S316	0.5	0.8	45.6	53.6	7.7	S327	0.5	22.1	39.2	38.7	4.4
	1.5	0.4	26.0	73.6	7.1		1.5	17.5	51.2	31.4	4.0
	2.5	0.1	38.6	61.2	6.1		2.5	12.8	45.5	41.7	4.1
	3.5	0.0	38.3	61.7	6.2		3.5	9.5	46.5	44.0	4.9
	4.5	0.1	38.8	61.1	5.9		4.5	8.5	47.7	43.7	5.3
S317	0.5	15.1	39.3	45.6	5.6	S329	0.5	6.5	64.7	28.8	3.9
	1.5	24.5	54.9	20.6	3.0		1.5	7.1	50.5	42.4	3.8
	2.5	28.2	55.2	16.7	2.8		2.5	27.5	41.6	30.9	3.4
	3.5	46.3	42.8	11.0	2.3		3.5	53.6	17.8	28.6	2.6
	4.5	58.3	31.0	10.7	2.0		4.5	48.3	20.3	31.4	2.7
S318	0.5	1.6	73.5	24.9	4.9	S330	0.5	21.3	44.5	34.2	3.6
	1.5	2.0	68.2	29.8	5.3		1.5	23.0	43.1	33.9	3.5
	2.5	15.8	62.2	22.0	3.7		2.5	23.4	35.3	41.3	3.4
	3.5	27.5	47.4	25.1	3.1		3.5	26.0	40.6	33.4	3.5
	4.5	29.3	56.0	14.8	3.0		4.5	21.0	44.0	35.0	4.0
S323	0.5	43.7	16.5	39.7	3.2	S333	0.5	4.5	46.7	48.8	5.0
	1.5	36.7	19.5	43.7	3.3		1.5	5.6	58.8	35.6	4.2
	2.5	35.2	19.1	45.7	3.7		2.5	6.2	56.0	37.8	3.4
	3.5	35.4	28.0	36.6	2.3		3.5	9.6	46.6	43.7	3.4
	4.5	33.4	29.9	36.7	1.8		4.5	10.6	55.3	34.2	3.4
S324	0.5	9.8	62.6	27.6	2.9	S339	0.5	61.1	20.4	18.4	2.5
	1.5	7.6	64.6	27.8	2.8		1.5	58.6	21.0	20.4	2.4
	2.5	5.4	62.7	31.9	3.2		2.5	55.0	24.4	20.7	2.9
	3.5	5.8	73.2	21.0	2.7		3.5	56.8	22.5	20.7	2.6
	4.5	4.0	76.4	19.6	3.4		4.5	61.4	19.5	19.2	2.8
S325	0.5	9.8	44.8	45.4	4.8	S340	0.5	30.1	22.9	47.0	4.3
	1.5	8.7	38.5	52.8	4.7		1.5	19.3	27.9	52.8	4.3
	2.5	9.9	45.0	45.0	4.2		2.5	31.8	23.0	45.2	5.2
	3.5	9.2	65.4	25.4	2.2		3.5	23.2	25.0	51.8	4.5
	4.5	7.6	44.5	47.8	4.6		4.5	38.8	24.2	37.0	4.3
S326	0.5	8.6	44.3	47.2	5.3	S341	0.5	13.8	35.9	50.2	5.5
	1.5	7.0	45.4	47.6	5.2		1.5	7.7	40.7	51.6	5.9
	2.5	8.2	43.8	48.0	5.2		2.5	42.9	32.9	24.2	3.3
	3.5	8.3	44.2	47.5	4.9		3.5	55.3	28.9	15.8	2.3
	4.5	7.8	44.5	47.8	4.8		4.5	54.5	30.0	15.5	2.7

Core ID	Mid-Depth (cm)	Sand %	Silt %	Clay %	LOI %	Core ID	Mid-Depth (cm)	Sand %	Silt %	Clay %	LOI %
S342	0.5	14.3	37.5	48.2	5.5	S408	0.5	2.8	71.5	25.7	5.8
	1.5	17.1	38.0	44.8	5.5		1.5	4.1	55.5	40.4	5.4
	2.5	20.0	36.5	43.4	5.5		2.5	4.1	51.7	44.2	5.0
	3.5	20.1	35.9	44.0	5.0		3.5	6.6	54.1	39.3	4.7
	4.5	21.7	35.1	43.2	5.1		4.5	5.5	50.2	44.3	4.7
S343	0.5	60.2	16.7	23.0	3.0	S413	0.5	63.8	14.6	21.6	2.9
	1.5	68.2	12.9	18.9	2.6		1.5	60.5	10.8	28.7	2.9
	2.5	72.4	11.2	16.4	2.3		2.5	63.1	11.2	25.7	2.8
	3.5	67.1	13.4	19.5	2.5		3.5	68.0	8.2	23.8	2.5
	4.5	64.7	14.3	21.0	2.7		4.5	68.0	8.7	23.3	2.6
S346	0.5	2.0	55.0	43.0	5.9	S416	0.5	7.2	53.5	39.3	5.1
	1.5	2.0	55.6	42.4	5.4		1.5	5.0	53.9	41.1	4.9
	2.5	2.2	54.6	43.1	4.7		2.5	6.2	50.1	43.7	4.9
	3.5	3.4	55.4	41.3	4.7		3.5	3.2	50.2	46.5	4.9
	4.5	2.3	52.3	45.4	5.0		4.5	5.8	50.8	43.4	4.8
S402	0.5	21.5	33.3	45.1	5.1	S418	0.5	8.9	43.2	47.9	5.8
	1.5	22.5	34.3	43.1	4.6		1.5	9.5	41.4	49.2	5.8
	2.5	23.5	33.7	42.9	4.8		2.5	8.6	42.0	49.3	5.6
	3.5	29.8	31.2	39.0	4.6		3.5	7.5	43.0	49.5	5.5
	4.5	21.1	34.9	43.9	4.7		4.5	7.1	42.9	50.0	5.5
S403	0.5	2.3	53.8	43.9	4.6	S421	0.5	2.3	50.0	47.7	4.4
	1.5	1.3	60.6	38.1	4.0		1.5	2.7	39.0	58.3	4.4
	2.5	1.7	66.5	31.9	4.8		2.5	3.6	52.1	44.2	3.9
	3.5	1.7	64.5	33.8	5.4		3.5	2.7	50.0	47.3	4.5
	4.5	2.0	68.6	29.4	4.7		4.5	2.2	50.1	47.7	4.6
S404	0.5	3.2	54.9	41.9	6.2	S424	0.5	15.7	44.0	40.3	4.3
	1.5	4.4	44.5	51.0	6.6		1.5	7.5	37.1	55.4	5.4
	2.5	2.2	43.0	54.8	6.1		2.5	6.2	39.5	54.3	5.1
	3.5	4.7	59.4	35.9	4.3		3.5	2.1	37.9	60.0	5.3
	4.5	1.9	72.1	26.0	3.2		4.5	0.9	39.3	59.9	5.9
S405	0.5	19.9	55.4	24.7	3.6	S426	0.5	18.3	59.6	22.1	2.8
	1.5	13.1	55.6	31.3	4.3		1.5	10.7	67.2	22.1	3.3
	2.5	26.5	49.8	23.7	3.5		2.5	11.4	65.2	23.4	3.6
	3.5	21.2	55.0	23.7	3.2		3.5	19.0	60.8	20.2	2.6
	4.5	16.7	45.1	38.2	3.7		4.5	25.8	50.2	24.0	4.7

Core ID	Mid-Depth (cm)	Sand %	Silt %	Clay %	LOI %	Core ID	Mid-Depth (cm)	Sand %	Silt %	Clay %	LOI %
S429	0.5	2.6	53.8	43.5	5.2	S441	0.5	36.0	28.2	35.9	4.3
	1.5	2.8	54.5	42.7	4.4		1.5	36.6	31.0	32.5	3.8
	2.5	2.2	52.5	45.3	4.5		2.5	38.2	28.1	33.7	3.5
	3.5	2.0	52.4	45.6	4.6		3.5	33.9	29.0	37.1	4.3
	4.5	2.3	53.0	44.6	4.4		4.5	31.8	31.7	36.5	4.3
S432	0.5	0.1	51.5	48.5	6.0	S444	0.5	10.1	52.6	37.3	4.4
	1.5	0.1	54.2	45.8	5.5		1.5	7.3	44.9	47.8	3.2
	2.5	0.3	47.3	52.5	5.2		2.5	9.0	48.1	42.9	4.7
	3.5	0.3	39.7	60.0	5.8		3.5	3.2	36.8	60.0	5.0
	4.5	0.1	28.9	71.0	4.0		4.5	4.5	37.1	58.5	6.0
S433	0.5	16.7	54.9	28.4	3.3	S447	0.5	15.1	60.4	24.4	2.8
	1.5	27.8	48.6	23.6	4.7		1.5	4.8	57.9	37.3	3.8
	2.5	28.6	47.4	24.0	5.3		2.5	11.6	57.1	31.3	3.6
	3.5	41.3	37.6	21.1	4.5		3.5	16.2	56.6	27.1	3.0
	4.5	42.2	38.5	19.3	3.1		4.5	18.3	57.8	23.9	2.3
S435	0.5	22.3	30.1	47.6	4.7	S448	0.5	17.4	47.7	34.9	3.3
	1.5	22.1	31.0	46.9	3.9		1.5	26.9	56.4	17.6	2.7
	2.5	18.3	33.2	48.5	4.1		2.5	26.2	48.1	25.7	2.7
	3.5	16.6	41.5	41.8	4.3		3.5	23.2	52.1	24.7	2.6
	4.5	20.2	40.3	39.5	4.4		4.5	24.5	51.9	23.6	2.7
S436	0.5	9.6	57.5	32.9	4.5	S449	0.5	19.0	39.1	41.9	2.9
	1.5	10.4	57.9	31.7	4.2		1.5	23.6	33.6	42.8	2.7
	2.5	17.6	56.5	26.0	3.9		2.5	21.4	50.9	27.7	2.7
	3.5	20.4	51.3	28.3	3.7		3.5	14.2	45.2	40.6	3.7
	4.5	12.5	49.8	37.7	4.1		4.5	7.2	48.2	44.7	3.6
S438	0.5	14.2	52.4	33.4	4.3	S451	0.5	17.3	52.8	29.9	2.7
	1.5	6.4	43.6	50.0	5.4		1.5	13.7	53.2	33.0	2.6
	2.5	3.1	39.8	57.1	6.0		2.5	13.8	56.3	29.9	3.3
	3.5	1.9	40.5	57.6	6.3		3.5	16.5	50.9	32.6	3.1
	4.5	0.4	40.4	59.1	6.1		4.5	11.8	55.1	33.1	2.7
S440	0.5	18.1	46.5	35.4	4.1						
	1.5	12.7	53.3	34.1	4.5						
	2.5	5.1	44.6	50.3	5.8						
	3.5	1.8	41.5	56.6	6.0						
	4.5	1.1	42.6	56.3	5.8						



**Appendix IV Site X-radiographs and Other Physical Data**

